THE ROLE OF ALTERED GAIT MECHANICS ON STRESS CONCENTRATIONS IN TIBIOFEMORAL JOINT CARTILAGE AFTER ANTERIOR CRUCIATE LIGAMENT RECONSTRUCTION: A FINITE ELEMENT STUDY

by

Kelsey A. Neal

A dissertation submitted to the Faculty of the University of Delaware in partial fulfillment of the requirements for the degree of Doctor of Philosophy in Mechanical Engineering

Summer 2023

THE ROLE OF ALTERED GAIT MECHANICS ON STRESS CONCENTRATIONS IN TIBIOFEMORAL JOINT CARTILAGE AFTER ANTERIOR CRUCIATE LIGAMENT RECONSTRUCTION: A FINITE ELEMENT STUDY

by

Kelsey A. Neal

Approved: _____
Ajay Prasad, Ph.D.
Chair of the Department of Mechanical Engineering

Approved: _____
Levi T. Thompson, Ph.D.
Dean of the College of Engineering

Approved: _____
Louis F. Rossi, Ph.D.
Vice Provost for Graduate and Professional Education and
Dean of the Graduate College

I certify that I have read this dissertation and that in my opinion it meets the academic and professional standard required by the University as a dissertation for the degree of Doctor of Philosophy.

Signed: _____

Thomas S. Buchanan, Ph.D.
Professor in charge of dissertation

I certify that I have read this dissertation and that in my opinion it meets the academic and professional standard required by the University as a dissertation for the degree of Doctor of Philosophy.

Signed: _____

Lynn Snyder-Mackler, Sc.D.
Member of dissertation committee

I certify that I have read this dissertation and that in my opinion it meets the academic and professional standard required by the University as a dissertation for the degree of Doctor of Philosophy.

Signed: _____

Jill S. Higginson, Ph.D.
Member of dissertation committee

I certify that I have read this dissertation and that in my opinion it meets the academic and professional standard required by the University as a dissertation for the degree of Doctor of Philosophy.

Signed: _____

Michael Santare, Ph.D.
Member of dissertation committee

ACKNOWLEDGMENTS

First and foremost, I would like to thank my advisor Dr. Thomas S. Buchanan and Dr. Lynn Snyder-Mackler. Without their continued support, guidance, and encouragement none of this work would have been possible. I would also like to thank Dr. Jill S. Higginson who has been an incredible mentor to me over this journey as well as a part of my dissertation committee. I would also like to thank Dr. Michael Santare for serving on my dissertation committee and teaching me the true versatility of the term capiche. During the early days of my doctoral work Dr. Ashutosh Khandha, Dr. Jacob J. Capin, and Dr. Kurt Manal all played a critical part in helping me develop my research project and have played a pivotal role helping me to develop into the researcher I am today. There are several people that I would like to thank who assisted with the project from which this dissertation was based. This includes Marlo, Lisa, Martha, Jenn, Megan, Kendra, and Leah. There is a long list of people who I had the extreme luck to get to work along side during my time at the University of Delaware who have become far more to me than work colleagues. This includes: Kayla, Nao, Majeed, Kaleb, Margo, Ana, Nicole, Rósa, Luke, Kaleb, Kleio and Jan. I would like to give a special thanks to Dr. Jack R. Williams who has been through every step of this process with me and without his encouragement, support, and friendship I am certain none of this work would have been possible.

I would also like to thank the Perry Initiative (Laurie, Hannah, Jenni, and all the fellows) for being the light that I needed throughout this difficult process. Without

Perry I would have never realized my true life's calling and for that I will be forever thankful.

Thank you to my direct family (mom, dad, Dot, Avery, Amy, Cruiser, Ralle, and Scout) and to the family I have made (Mia, AJ, Victor, Isabel, Dana, Steve, Link, Susan, Annie, and Oak) you have always been there no matter what and have always taught me to chase after my dreams. I could not have asked for a better group of people to get to do life with. Finally, I would like to thank my husband Jack, you are the best human I have ever met, and you are the reason I have been able to make it through both the good and hard times of this doctoral work. Thank you for giving me the courage to step into the unknown and to push out of my comfort zone.

Funding for this work was provided by the Eunice Kennedy Shriver National Institute of Child Health and Human Development (R01-HD087459), the University of Delaware's Mechanical Engineering Helwig Fellowship, and the University of Delawares Doctoral Fellowship Award.

TABLE OF CONTENTS

LIST OF TABLES x
LIST OF FIGURES xi
ABSTRACT xvii

Chapter

1 INTRODUCTION 1

ACL Injuries, Reconstruction, and Osteoarthritis 1
Knee Joint Structures 1
Post-traumatic Osteoarthritis and Early Detection 4
Mechanisms for OA Development after ACLR 5
Biomechanical Computational Modeling 8

Musculoskeletal modeling 9
Finite Element Models 10

The Aims of this Dissertation 11
Aim 1 (Chapter 2) 13

Goal 13
Hypotheses 13
Why is this important? 13

Aim 2 (Chapter 3) 14

Goal 14
Why is this Important? 14

Aim 3 (Chapter 4) 14

Goal 14
Hypotheses 15
Why is this important? 15

Aim 4 (Chapter 5) 15

Goal 15
Hypotheses 16
Why is this important? 16

2 KNEE JOINT BIOMECHANICS DURING GAIT IMPROVE FROM 3 TO 6 MONTHS AFTER ANTERIOR CRUCIATE LIGAMENT RECONSTRUCTION 17

Introduction 17
Methods 21

Participants 21
Gait Analysis 22
Statistical Analyses 24

Results 25

Knee Flexion Angle 25
Knee Flexion Moment 27
Knee Adduction Moment 30
Knee Extensor Forces 31
Medial Compartment Force 33

Discussion 35

Knee Flexion Angle 37
Knee Flexion Moment 38
Knee Adduction Moment 39
Knee Extensor Forces 40
Medial Compartment Force 41
Limitations and Future work 42
Conclusion 43

3 A PROTOCOL FOR THE DEVELOPMENT OF SUBJECT-SPECIFIC FINITE ELEMENT MODELS OF THE KNEE FOR ANALYSIS OF CARTILAGE STRESS AFTER ACLR 45

Introduction 45
Methods 46

Gait analysis and EMG Driven Musculoskeletal Model 47
Geometry Acquisition 50
Mesh Development 52
Material Constitutive Models 56

Contact Interactions 58
Model Assembly and Boundary Conditions 59
Model input variables and simulation 61
Mesh Scaling 62
Model Validation Analysis 65

Validation Results 66

Discussion 68

4 LONGITUDINAL CHANGES IN MEDIAL TIBIOFEMORAL CARTILAGE STRESSES AFTER ACLR AND THEIR ASSOCIATION TO CHANGES IN KNEE FLEXION ANGLE 70

Introduction 70
Methods 72

Participants 72
Motion Analysis 73
Finite Element Analysis 74
Statistical Analyses 76

Results 77

Model Inputs: Gait Mechanics 77
Tibial Cartilage Stress 77
Femoral Cartilage Stress 79
Knee Flexion Angle vs. Tibial Cartilage Stress 81
Femoral Cartilage Stress vs. Knee Flexion Angle 83

Discussion 85

5 MEDIAL TIBIOFEMORAL CARTILAGE STRESSES 3 AND 6 MONTHS AFTER ACLR AND THEIR ASSOCIATION WITH QUANTITATIVE MRI 90

Introduction 90
Methods 93

Participants 93
Quantitative Magnetic Resonance Imaging (qMRI) 93
Finite Element Analysis 94
Statistical Analyses 95

Results 96

Tibial Cartilage 96
Femoral Cartilage 100

Discussion 102

6 CONCLUSIONS AND FUTURE WORK 108

Aim 1 108

Conclusions 108
Future Work 109

Aim 2 110

Conclusions 110
Future Work 110

Aim 3 112

Conclusions 112
Future Work 113

Aim 4 114

Conclusions 114
Future Work 115

REFERENCES 117

Appendix

A INSTITUTIONAL REVIEW BOARD APPROVAL LETTER 133
B INSTITUTIONAL REVIEW BOARD INFORMED CONSENT 134
C AIM 1 (CHAPTER 2) PERMISSION 144

LIST OF TABLES

Table 1 Participant Demographic Characteristics (n = 35) 21

Table 2 Element types for each mesh and number of elements 55

Table 3 Material properties applied to the finite element model..... 57

Table 4 Scaling run times by parts and total run times. 65

Table 5 Model inputs for validation simulations..... 66

Table 6 Statistical results for validation between our model (FE) and the experimental and FE model results from Mootanah et al..... 67

Table 7 Demographic Characteristics of Participants 3 Months after ACLR (n = 15)..... 73

Table 8 Medial tibial stress at pMCF by region at 3, 6, and 24 months after ACLR statistical analysis. Significant results are bolded..... 79

Table 9 Medial femoral cartilage stress at pMCF by region at 3, 6, and 24 months after ACLR statistical analysis. Significant results are bolded. 81

Table 10 Involved and uninvolved limbs association between KFA and average regional stress for all three time points. Significant associations are bolded. 83

Table 11 Involved and uninvolved limbs association between KFA and average regional stress for all three time points. Significant associations are bolded. 85

LIST OF FIGURES

Figure 1 (A: top) 3 (blue) and 6 (orange) month KFA for the involved (dashed line) and uninvolved (solid line) limbs throughout stance. Interlimb differences were present at both time points during weight acceptance and parts of midstance and terminal stance. (A: bottom) SPM Limb x Time repeated measures ANOVA F statistic over 100% of stance. The red dashed line indicates the critical F-value (F = 7.99) where results are considered significant ($\alpha \leq 0.05$). A significant limb-by-time interaction was seen from 56%-66% of stance. (B: top) Interlimb differences at 3 and 6 months. ILD significantly decreased over 56%-66% of stance. (B: bottom) Two-tailed paired Student's t-test using SPM for ILD at 3 and 6 months. The red dashed line indicates the critical t-value ($\alpha = 0.05$)..... 26

Figure 2 The top graph of each subfigure shows KFA through 100% of stance ± one standard deviation (shaded regions). The lower graph displays a two-tailed paired Student's t-test using SPM. The red dashed line indicates the critical t-value ($\alpha = 0.05$). (A) Involved (dashed line) vs uninvolved (solid line) KFA 3 months after ACLR; significant differences were present from 11%-33% and 52%-85% of stance. (B) Involved (dashed line) vs uninvolved (solid line) KFA 6 months after ACLR; significant differences were seen from 8%-30% and 60%-80% of stance. (C) Involved 3 months (blue) vs 6 months (orange); no significant differences were present. (D) Uninvolved 3 months (blue) vs 6 months (orange); significant differences were seen from 0%-7% of stance. 27

Figure 3 (A: top) 3 (blue) and 6 (orange) month KFM for the involved (dashed line) and uninvolved (solid line) limbs throughout stance. Interlimb differences were present at both time points during weight acceptance into midstance and terminal stance. These differences decreased from 3 to 6 months during weight acceptance into midstance. (A: bottom) SPM Limb x Time repeated measures ANOVA F-statistic over 100% of stance. The red dashed line indicates the critical F-value (F = 10.37) where results are considered significant ($\alpha \leq 0.05$). A significant limb-by-time interaction was seen from 16%-23% of stance. (B: top) Interlimb differences at 3 and 6 months. ILD significantly decreased from 3 to 6 months between 15%-23% of stance. (B: bottom) Two-tailed paired Student's t-test using SPM for ILD at 3 and 6 months. The red dashed line indicates the critical t-value ($\alpha = 0.05$)..... 29

Figure 4 The top part of each subfigure shows KFM through 100% of stance ± one standard deviation (shaded regions). The lower portion displays a two-tailed paired Student's t-test using SPM. The red dashed line indicates the critical t-value (α = 0.05). (A) Involved (dashed line) vs uninvolved (solid line) KFM 3 months after ACLR; significant differences were present from 5%-36%, 64%-71%, and 86-96% of stance. (B) Involved (dashed line) vs uninvolved (solid line) KFM 6 months after ACLR; significant differences were seen from 5%-31% of stance. (C) Involved 3 months (blue) vs 6 months (orange); significant differences were seen from 13%-29% of stance. (D) Uninvolved 3 months (blue) vs 6 months (orange); no significant differences were present. 29

Figure 5: (A: top) 3 (blue) and 6 (orange) month KAM for the involved (dashed line) and uninvolved (solid line) limbs throughout stance. (A: bottom) SPM Limb x Time repeated measures ANOVA F-statistic over 100% of stance. The red dashed line indicates the critical F-value (F = 9.94) where results are considered significant. No significant limb-by-time interaction was present. (B: top) Interlimb differences at 3 and 6 months. No significant differences were present. (B: bottom) Two-tailed paired Student's t-test using SPM for ILD at 3 and 6 months. The red dashed line indicates the critical t-value (α = 0.05). 30

Figure 6 The top part of each subfigure shows KAM through 100% of stance ± one standard deviation (shaded regions). The lower portion displays a two-tailed paired Student's t-test using SPM. The red dashed line indicates the critical t-value (α = 0.05). (A) Involved (dashed line) vs uninvolved (solid line) KAM 3 months after ACLR; no significant differences were present. (B) Involved (dashed line) vs uninvolved (solid line) KAM 6 months after ACLR; no significant differences were present. (C) Involved 3 months (blue) vs 6 months (orange); no significant differences were present. (D) Uninvolved 3 months (blue) vs 6 months (orange); no significant differences were present. 31

Figure 7 (A: top) 3 (blue) and 6 (orange) month knee extensor forces for the involved (dashed line) and uninvolved (solid line) limbs throughout stance. (A: bottom) SPM Limb x Time repeated measures ANOVA F-statistic over 100% of stance. The red dashed line indicates the critical F-value (F = 9.80). No limb-by-time interaction was seen. (B: top) Interlimb differences at 3 and 6 months. These differences decreased from 3 to 6 months but were not significant. (B: bottom) Two-tailed paired Student's t-test using SPM for ILD at 3 and 6 months. The red dashed line indicates the critical t-value (α = 0.05). 32

Figure 8: The top part of each subfigure shows the knee extensor forces through 100% of stance ± one standard deviation (shaded regions). The lower portion displays a two-tailed paired Student's t-test using SPM. The red dashed line indicates the critical t-value (α = 0.05). (A) Involved (dashed line) vs uninvolved (solid line) knee extensor forces 3 months after ACLR; significant differences were present from 3%-34% and 89%-100% of stance. (B) Involved (dashed line) vs uninvolved (solid line) knee extensor forces 6 months after ACLR; no significant differences were seen. (C) Involved 3 months (blue) vs 6 months (orange); significant differences were seen from 9%-25% and 95%-100% of stance. (D) Uninvolved 3 months (blue) vs 6 months (orange); no significant differences were present. 33

Figure 9: (A) 3 (blue) and 6 (orange) month medial compartment forces for the involved (dashed line) and uninvolved (solid line) limbs throughout stance. Participants underloaded the involved limb at both time points during weight acceptance (vs. uninvolved limb), however involved limb loading did increase from 3 to 6 months. (A: bottom) SPM Limb x Time repeated measures ANOVA F-statistic over 100% of stance. The red dashed line indicates the critical F-value (F = 9.91). No limb-by-time interaction was seen. (B: top) Interlimb differences at 3 and 6 months, no significant differences were present. (B: bottom) Two-tailed paired Student's t-test using SPM for ILD at 3 and 6 months. The red dashed line indicates the critical t-value (α = 0.05). 34

Figure 10: The top part of each subfigure shows the medial compartment force through 100% of stance ± one standard deviation (shaded regions). The lower portion displays a two-tailed paired Student's t-test using SPM. The red dashed line indicates the critical t-value (α = 0.05). (A) Involved (dashed line) vs uninvolved (solid line) medial compartment forces 3 months after ACLR; significant differences were present from 12%-20% of stance. (B) Involved (dashed line) vs uninvolved (solid line) medial compartment forces 6 months after ACLR; no significant differences were seen. (C) Involved 3 months (blue) vs 6 months (orange); no significant differences were seen. (D) Uninvolved 3 months (blue) vs 6 months (orange); no significant differences were present. 35

Figure 11 Segmentation workflow. Left: raw proton density image slice. Center: Example of a single segmented image, that includes segmented muscles, bones, cartilage, ligaments, and tendons. Right: Combined 2D segmentations to form a 3D geometry volume for each..... 52

Figure 12 Visuals of the different element types used to develop meshes from segmented geometries. Black dots in each figure represent the element nodes. 53

Figure 13 Meshed geometries and meshed parts. (A) Model assembly including bones, ligaments, cartilage, and menisci (B) Medial (left) and lateral (left) tibial cartilage (C) medial (left) and lateral (right) menisci (D) Femoral cartilage. 56

Figure 14 The local axis for the model was placed at the center of the transepicondylar axis. A reference point (RP-F) was placed at the center of the local axis. Compartmental reference points were place in the center of the lateral (RP-L) and medial (RP-M) compartments. RP-L and RP-M were tied to RP-F. Joint rotations were applied around the x-axis at RP-F and joint loads were applied to their respective compartmental reference point in the z direction. 60

Figure 15 Workflow for simulating knee joint mechanics during walking using an FE model. FE model inputs include KFA (°), MCF (N), and LCF (N) throughout gait are applied to the model using amplitudes. Model outputs were von Mises stress maps of the femoral and tibial cartilage. 62

Figure 16 (A) Measurements from frontal plane: mediolateral (ML) femoral bone and cartilage width, medial (M) and lateral (L) tibiofemoral joint space, thickness of M and L menisci, and ML tibial bone and cartilage width. (B) Measurements from sagittal plane: anteroposterior (AP) width of M and L femoral condyles, AP width of M and L menisci, AP tibial bone width. 64

Figure 17 Top: example of scaling the lateral tibial cartilage mesh and translating it to align with the scaled tibia bone. Bottom: sagittal and frontal views of the original model (left) and a scaled model (right). 65

Figure 18 Medial and lateral tibial cartilage pressure over the valgus (0 to 15 Nm) and varus (0 to -15 Nm) y-axis rotation. Model validation comparing experimental data and FEM results from Mootanah et al. and our FE model. 67

Figure 19 Peña contact pressure (top) compared to our FE Model (bottom) for each loading condition displayed on left. 68

Figure 20 Flow chart depicting steps involved in obtaining model inputs for the FE model and how model inputs are applied to simulations gait. 76

Figure 21 Mean involved (solid) and uninvolved (striped) model input data at 3 (Blue), 6 (green), and 24 months (yellow). (* = significantly different p<0.05) 77

Figure 22 Medial tibial cartilage regions of interest for mean stress values. Mean stresses for the involved (solid) and uninvolved (striped) taken at pMCF in the anterior, central, and posterior regions of the medial tibial cartilage. Data is shown for the 3 (Blue), 6 (green), and 24 months (yellow). (* = significantly different p<0.016) 79

Figure 23 Medial Femoral cartilage regions of interest for mean stress values. Mean stresses for the involved (solid) and uninvolved (striped) taken at pMCF in the anterior, central, and posterior regions of the medial tibial cartilage. Data is shown for the 3 (Blue), 6 (green), and 24 months (yellow). (* = significantly different p<0.016) 80

Figure 24 Association between KFA and average Von Mises Stress in the anterior, central, and posterior regions of the medial tibial cartilage at the 3 (Blue), 6 (green), and 24 months (yellow) for the involved and uninvolved limbs. 82

Figure 25 Association between KFA and average Von Mises Stress in the anterior, central, and posterior regions of the medial femoral cartilage at the 3 (Blue), 6 (green), and 24 months (yellow) for the involved and uninvolved limbs. 84

Figure 26 Medial femoral and tibial cartilage regions of interest for FE model results. 95

Figure 27 Workflow for simulating gait during walking using an FE model. FE model inputs include KFA (°), MCF (N), and LCF (N) throughout gait are applied to the model. Model outputs were von Mises stress maps of the femoral and tibial cartilage. 95

Figure 28 Medial tibial cartilage mean stress values taken at pMCF (top) and mean T_2 (bottom) for the involved (solid) and uninvolved (striped) in the anterior, central, and posterior regions of the medial tibial cartilage. Data is shown for the 3 (Blue), 6 (green), and 24 months (yellow). (* = significantly different p<0.016) 98

Figure 29 Changes in the involved limbs stress from 3 to 6 months compared to changes in T_2 relaxation time from values 3 to 6 months after ACLR for the anterior (blue), central (green), and posterior (yellow) regions of the medial tibial cartilage 100

Figure 30 Medial Femoral cartilage mean stress values taken at pMCF (top) and mean T_2 (bottom) for the involved (solid) and uninvolved (striped) in the anterior, central, and posterior regions of the medial tibial cartilage. Data is shown for the 3 (Blue), 6 (green), and 24 months (yellow). (* = significantly different $p<0.016$) 101

Figure 31 Changes in the involved limbs stress from 3 to 6 months compared to changes in T_2 relaxation time from values 3 to 6 months after ACLR for the anterior (blue), central (green), and posterior (yellow) regions of the medial femoral cartilage 102

ABSTRACT

Gait alterations after ACL reconstruction (ACLR) are commonly reported and have been linked to post-traumatic osteoarthritis development. It is hypothesized that these biomechanical alterations are impacting the way cartilage is stressed within the knee joint, however the acquisition of stress data is difficult/impossible from an *in vivo* approach limiting our understanding on this process in a clinical population. With improvements in computational abilities over the past 40 years some have begun to utilize an approach called finite element analysis to study stresses within the knee joint. The aim of this dissertation was to assess alterations in gait during the early stages of recovery after ACLR and to understand how these alterations impact the way in which cartilage is stressed between limbs and overtime using finite element models. Additionally, we sought to investigate if alterations in stress are associated with early signs of knee cartilage degeneration (assessed via advanced quantitative magnetic resonance imaging techniques).

Aim 1 of this dissertation focused on examining knee gait biomechanical variables over the entire stance phase of gait at both 3 and 6 months after ACLR and studied the progression of interlimb asymmetry between the two post-operative time points. We found that there were large asymmetries between limbs in several biomechanical variables of interest (e.g., knee flexion angles, medial compartment

forces, …) and that most progressed toward a more symmetrical gait pattern by 6 months. Aim 2 focused on the development of subject-specific finite element models of the knee joint that uses subject-specific joint mechanics and loading from the gait analysis and musculoskeletal modeling performed in Aim 1. Subject-specific model geometries were obtained through segmentation of MRIs. A single finite element model was then used in Aim 3 to better understand the relationship between joint biomechanics and joint contact stresses after ACLR. We found interlimb asymmetries in stress magnitude within select regions of interest and observed associations between stress magnitude and knee flexion angles; indicating a coupling between alterations in early knee mechanics and changes in stress environment within the knee. In the fourth, exploratory aim, we examined whether or not alterations in stress early after ACLR are associated with markers for knee cartilage biochemical composition. We found that there was an association between changes in stress and changes in knee cartilage biochemistry during the 3- to 6-month time period; where those who saw increases in involved limb stress magnitude during this time period saw improvements in knee cartilage health. This is among the first studies to explore how alterations in gait after ACLR affect how cartilage within the tibiofemoral joint is being stressed, and how these stress distributions affect cartilage at the biochemical level. This work demonstrates a link between altered gait mechanics after ACLR and changes in stress distributions within the medial cartilage. These findings help expand our understanding of how alterations at a macro-level impact the cartilage within the knee joint at a tissue level. Further investigation using the tools developed in this study

could help inform clinicians on which mechanical alterations are causing the most potential damage to cartilage and may ultimately help lead to the development of rehabilitative procedures to prevent long-term disease development.

Chapter 1

INTRODUCTION

ACL Injuries, Reconstruction, and Osteoarthritis

Knee joint stability is vital to maintaining an active lifestyle. For many, this becomes apparent when stability is lost following a traumatic injury such as an anterior cruciate ligament (ACL) tear. The ACL is often torn by a non-contact cutting or pivoting executed during dynamic activities and is a common injury in young active populations[1]. While some individuals can continue daily activities and athletics despite instability due to ACL loss, many need to undergo ACL reconstruction (ACLR) to help stabilize the joint and to protect the remaining knee structures[2]. While ACLR has proven to help restore stability within the joint, it fails to prevent the development of post-traumatic knee osteoarthritis (OA). In fact, 50% of the individuals who undergo an ACLR develop radiographic knee OA within 10 years of surgery[3]. While the onset of OA at such a young age may not immediately affect an individual's life, there is currently no cure for this disease[4]. This has led researchers to investigate the mechanisms behind the early degeneration of the cartilage and what clinical treatments can be developed to help prevent or slow disease onset.[5–10]

Knee Joint Structures

The knee is classified as a synovium joint and is composed of the proximal tibia, distal femur, and patella. The tibiofemoral joint includes the interface between the tibia and the femur and is divided into medial and lateral compartments. The

patellofemoral joint exists between the posterior aspect of the patella and the trochlear groove of the femur. The patella is a sesamoid bone that is integrated with the patellar ligament and the quadriceps tendon. Often referred to as a modified hinge joint, the knee allows for six degrees of freedom (flexion/extension in the sagittal plane, internal/external rotation in the transverse plane, and varus/valgus movement in the frontal plane, and anterior/posterior translations, medial/lateral translation, and super/inferior translation).[11]

Articular cartilage is a specialized tissue that coats the end of each bone in the joint, allowing for nearly frictionless movement while simultaneously assisting with the absorption and distribution of joint loads[12]. Articular cartilage has a highly organized structure composed of an extracellular matrix, specialized mechanosensitive cells called chondrocytes, and water. The extracellular matrix is further broken down into its components which include proteoglycans, a collagen matrix, and water. Together, these components work together in a delicate balance to maintain a healthy joint. Tissue organization and composition vary throughout different regions of the knee, which allows cartilage to withstand the wide variety of loads and stresses that occur within the joint[13,14]. With the help of chondrocytes, cartilage can adapt to the repetitive loading patterns of gait and other daily activities. Areas that see higher load and stresses adapt to become thicker than regions with comparatively lower mechanical burdens. Despite the mechanoadaptive nature of cartilage, sudden changes in the mechanical environment, such as those that occur following traumatic injury, can have devastating consequences for the health of this tissue[4].

Other tissues that play an important role in modulating knee joint stresses are the medial and lateral menisci. These crescent shaped structures sit on the tibial

plateau and are held in place through meniscal horns that insert into the bone. The primary function of these tissues is to increase the area of contact between the bone interfaces to help distribute load and provide shock absorption[15]. The meniscus is made of a transversely isotropic fibrocartilaginous tissue that can handle high hoop stresses and is split into two distinct regions. The vascular region lies on the peripheral portion of the meniscus and the avascular region corresponds to the central regions of the crescent[16].

Ligaments and soft tissues play a critical role in joint stability, with ligaments being responsible for preventing excessive motion of the joint[11]. Within the center of the joint, the anterior cruciate ligament (ACL) and the posterior cruciate ligament (PCL) connect the tibia and the femur and prevent extreme translations of the femur relative to the femur in the anterior/posterior directions. The ACL connects to the anterior aspect of the tibial plateau and the medial aspect of the lateral femoral condyle in the intercondylar notch. This ligament prevents excessive anterior translation of the tibia with respect to the femur. The PCL originates at the medial femoral condyle in the intercondylar notch and inserts on the posterior tibia and adds stability to the joint by preventing the posterior translation of the tibia with respect to the femur. Medial and lateral translations are constrained by the medial and lateral collateral ligaments (MCL and LCL), respectively. The MCL connects to the medial epicondyle of the femur and tibia and stabilizes the joint when valgus forces are applied. The LCL connects the lateral epicondyle of the femur to the head of the fibula and resists varus forces. Other connective tissues include the multiple muscles and tendons that span the joint, and a fibrous capsule. The totality of these structures allows the knee joint to remain stable while maintaining 6 degrees of freedom.

However, in the event of injury and damage to one or more of these structures, joint stability can be compromised and alterations in joint biomechanics can occur. These, in turn, can alter the loading environment of the knee and elevate the risk for further injury and osteoarthritic disease development. Articular cartilage is especially impacted by this change in the knee joint environment as it is avascular, which limits its ability to heal and repair damage.

Post-traumatic Osteoarthritis and Early Detection

Osteoarthritis occurs when the articular cartilage within a joint begins to degrade. Often OA is diagnosed using a combination of radiographs, where clinicians look to identify the presence of osteophytes and the occurrence of joint space narrowing, and patient-reported symptomology. These radiographically identifiable features, however, only occur in the late stages of the disease [17,18]. Allowing OA to progress to its later stages before diagnosis minimizes opportunity for preventative measures, often leaving individuals with little choice but to eventually undergo a total knee replacement (TKR) in order to restore function and alleviate pain. TKRs are a very invasive procedure with a shelf life which, if received at a young age, will require multiple revision surgeries[19,20]. For age-related OA, this is a reasonable approach to clinical management, the median age of ACLR patients, however, is 27 years old, which is a problematically young age to begin secondary OA development[21,22]. Since the effects of OA are currently irreversible, there is a critical need to identify new techniques for the early detection of its onset and to develop preventative treatments for those who are at risk of developing OA. Thus, it is essential to identify the mechanisms behind the onset of this disease. Some mechanisms that are thought to

play a role include trauma from an injury, inflammatory factors, and changes in biomechanics[23,24].

The early stages of OA do not often present with physical pain or morphometric changes that are radiographically identifiable[25,26]. The silent onset of this disease makes it clinically difficult to identify OA in its early stages. However, advancements in the medical imaging techniques enable the non-invasive assessment of cartilage during the early stages of OA. For example, quantitative magnetic resonance imaging (qMRI) can be used to monitor both the structural and biochemical composition of cartilage. T_2 Mapping is a qMRI scanning technique that has been extensively validated for its utility in monitoring the collagen matrix structure and water content within the cartilage [14,27]. Prolonged T_2 times are indicative of collagen matrix degradation and increased water content, both of which are signs of early knee OA. This can be particularly helpful when following subjects longitudinally to assess how their cartilage composition is changing or when comparing against their uninjured knee, as doing so may provide early glimpses into the initiation of disease development.

Mechanisms for OA Development after ACLR

One mechanism that is thought to initiate cartilage degradation is alterations to joint biomechanics and muscle activity during gait, both of which can lead to changes in joint loading[28–31]. Interlimb (involved vs. uninvolved) asymmetries in gait mechanics are commonly reported after surgery and tend to persist even after full return to activity[2,32]. Frequently reported alterations include changes in involved limb peak knee flexion angles (KFA)[2,33–37], peak knee extension angles (KEA)[38–40], peak knee flexion moments (KFM)[41–47], peak knee adduction moments (KAM)[42,43,45,48,49],

quadriceps strength[44,50,51], and peak medial compartment contact forces (MCF)[42] (when compared against the uninvolved limb and healthy controls). The continuation of these asymmetries is concerning as they increase an individual's risk of reinjury[52] and are thought to have enduring effects on joint health[29,42,53–57]. These changes in joint biomechanics can lead to a shift in location of load application on cartilage which could change how and when cartilage is stressed during the gait cycle[58–60]. This, in turn, could lead to alterations in the biochemical composition of knee cartilage.

The ability to understand how changes in gait mechanics effects cartilage health over time represents a major milestone on the road to translating basic science into clinical outcomes. One widely accepted framework for the initiation and progression of OA was proposed by Andriacchi et. al.[4,55]. Within this framework, they theorize that changes in load and kinematics following trauma, such as ACL rupture and subsequent ACLR, may be the primary driver for the early onset of OA. Of particular interest is the portion of the framework described as the "initiation phase." This stage begins when a traumatic event, such as ACLR, occurs and the motion in the knee joint changes, leading to a shift in the load-bearing cartilage contact location from a region that is conditioned for frequent high loads, to one that is not. This shift is of concern because cartilage composition and mechanical properties vary throughout the tissue to account for functional load bearing. Regions that experience higher loads tend to be thicker and have superior mechanical properties, when compared to regions that are infrequently loaded [58,60]. A study using magnetic resonance imaging (MRI) and fluoroscopy found that cartilage thickness in regions of contact on average were 1.4 times as thick in the medial tibial and femoral cartilage for healthy knees when compared to non-contact regions[61]. This suggests that regions

that normally experience higher contact stresses may have adapted over time to these stressors. While young healthy cartilage does have the ability to adapt to changes in load, adaptation is not instantaneous. When shifts in loading regions occur rapidly from a load-bearing region to a non-load-bearing region, the articular tissue may not be able to support the applied loads, which leads to a degradation of essential cartilage structures such as the collagen matrix and proteoglycans. Eventually these changes in cartilage structure may lead to an increase in friction, which increases the mechanical stresses applied to the cartilage, which in turn accelerates cartilage degradation.

Even with reduced total joint load after ACLR, specific regions of cartilage may experience a relative overload due to the alterations in knee joint kinematics that occur post-operatively. The cartilage experiencing load may shift between regions that are adapted for high loads to ones that are infrequently loaded. Even though the total joint load has decreased, the stresses applied to the new load-bearing region may exceed those seen prior to injury/surgery. Over time, many individuals return to symmetric kinematics and loading. While achieving post-operative symmetry is a universal rehabilitation goal, it is often confounded by a shift in cartilage loading sites. For example, cartilage that was once adapted to maintain higher loads will typically experience a reduction in loading in a post-operative setting. In some individuals, this could persist to the degree that tissue properties in this area shift to those seen in infrequently loaded regions, which then causes the same string of events to unfold on the once load bearing region [24,59].

Little is known about how changes in kinematics and joint load effect where and how cartilage is stressed after ACLR. The acquisition of *in vivo* stress distributions is no menial task, as to obtain *in vivo* stress distributions on living

subjects through experimental approaches is not ethical, which restricts researchers to investigating this problem through animal models or cadaveric studies[5,62–65]. These approaches lack the ability to track longitudinal changes in gait and tissue health over time in the human joint[66].

Biomechanical Computational Modeling

Computational modeling has become a powerful tool for researchers and clinicians to explore areas of biomechanics that were once elusive due to the near impossible nature of collecting *in vivo* measurements[67–72]. The use of these models can provide insights across the span of human body mechanics including full body mechanics, joint loads, muscle forces, and tissue deformation. Due to the complexity of the human body, no one model can perfectly capture every biological phenomenon. For this reason, it is essential to build a model to answer a specific question. This approach allows for assumptions to be made to simplify the model, leading to improvements in model convergence and decreased run times[73]. For questions focused on full body mechanics, tools designed for macroscale analysis, such as musculoskeletal models (MSM), are typically used. When trying to assess the body at a tissue level, a mesoscale modeling approach, such as finite element (FE) models should be used. While often used separately, the combined use of both macroscale and mesoscale modeling approaches has immense potential to answer unique research questions while providing a more holistic picture of the mechanism being investigated[74–77].

Musculoskeletal modeling

The *in vivo* measurement of joint reaction forces and individual muscle forces requires invasive testing techniques that are either expensive, unethical to perform, or very difficult to measure experimentally. Musculoskeletal modeling is used within the biomechanical community to study macroscale biomechanics at the whole-body level. This approach allows for the prediction of parameters *in silico*, through dynamic simulations of human movement; enabling studies focused on gait dynamics, rehabilitation, sports performance, the assessment of medical devices, and/or surgical procedures. Platforms for MSM are available through commercial and open-source avenues, including AnyBody[78], SIMM[79], and OpenSim[80].

Musculoskeletal modeling dynamic simulations utilize the classical equations of motion to study muscle recruitment[78,80]. There are two main approaches implemented for solving these equations known as forward and inverse dynamics. The main difference between these approaches lies in the available inputs. Forward dynamics requires muscle excitations or joint torques to produce movement and estimations of muscle forces. A study that has collected electromyography (EMG) data would utilize a forward dynamics MSM. Conversely, a study using motion capture would use inverse dynamics to known motion to predict joint torques and muscle forces. In cases where both motion capture data and EMG are available, both approaches may be implemented[71].

Finite Element Models

While MSM is a powerful tool for predicting kinematics, muscle forces, and joint loads it is limited to the macroscale. If the goal of the work is to investigate the impact of these parameters on the tissues within the joint, it is necessary to employ a modeling technique that can model the mesoscale. Finite element modeling and simulation is one such technique that allows for the prediction of tissue-level stress, strains, and deformations. The FE method is a numerical technique that is used when assessing boundary value problems characterized by partial differential equations to approximate the solution[81]. This method allows for the analysis of complex geometrical systems by discretizing the problem domain into finite elements and nodes, leading to a system of equations that can be computationally solved using commercial and open-source software including Abaqus [82], ANSYS[83], LS-DYNA[84], and FEbio[81].

The past twenty years of research has seen an exponential increase in FE models to explore knee biomechanics[85–87]. Finite element models of the knee joint allow for the implementation of joint anatomy, tissue material properties, and the application of joint loads and mechanics to study both the healthy and diseased knee. The complexity of human anatomy ranging from structures, material properties, and mechanics can make the task of developing a universal model highly difficult. The more complex a model design the more mathematically intensive each simulation becomes, which increases run times and the occurrence of convergence issues. Recently there has been a push to implement universal procedures for model development and validation[86]. Often research papers give a brief overview of the model being used, but they rarely go into detail on the model development and why

certain design choices were made. This process has been coined the "art" of modeling due to the modelers personal control over the model design which will have an impact on simulation results and conclusions[73]. The implementation of a standardized procedure is meant to give the modeling community confidence and to make model reproducibility possible. While open-source models are available, these tend to be generic models and are not necessarily appropriate for the research question at hand. Therefore, documentation of model development is essential, and allows the modeling community to understand the assumptions and limitations of each model.

The Aims of this Dissertation

Gait alterations after ACLR are commonly reported and have been linked to post-traumatic osteoarthritis development. While knee gait alterations have been studied at several time points after ACLR, little is known about how these biomechanical variables change within the early months after surgery, similarly little is known about how they differ over the entire stance phase of gait. Aim 1 of this dissertation focused on examining knee gait biomechanical variables over the entire stance phase of gait at both three and six months after ACLR and studied the progression of interlimb asymmetry between the two post-operative time points. The gait variables and musculoskeletal model used in Aim 1 allows for the assessment of changes in gait mechanics at the macroscale at these early post-operative time points; they fail, however, to provide insights into how these changes impact the knee joint at the mesoscale. Abnormal tibiofemoral kinematics, kinetics, and joint loading can lead to aberrant contact stresses within the knee joint that may spur the progression of osteoarthritis in the ACLR limb. Therefore, it is essential to employ a model aimed at

gaining a better understanding of how changes in gait kinematics and kinetics early after ACLR affect the knee joint at the mesoscale over time.

With the advancement in computational power over the past 40 years we can use FE modeling to predict how changes in full body biomechanical variables impact the underlying tissues. Aim 2 will focus on the development of a finite element model of the knee joint that uses subject-specific joint mechanics and loading from the gait analysis and the MSM performed in Aim 1. Documentation on model development procedures and scaling protocol will be provided to allow for replication of the model. This model will be used in Aims 3 and 4 to better understand the relationship between joint biomechanics and joint contact stresses after ACLR. The overall goal of this work is to gain a deeper understanding of how alterations in gait after ACLR affect how cartilage within the tibiofemoral joint is being stressed, and how these stress distributions affect cartilage at the biochemical level.

Aim 3 specifically looks at how alterations in gait mechanics can impact the way knee joint cartilage is stressed at 3, 6, and 24 months after ACLR and studies the progression of interlimb asymmetry between the two post-operative time points. We will also assess how asymmetries in knee flexion angle (KFA) after ACLR relate to contact stress magnitude and location within the femoral and tibial cartilage. Aim 4 used quantitative MRI, thought to provide insights into joint health, to assess if changes in cartilage stress between 3 to 6 months after ACLR correspond with worsening cartilage health from 3 to 6 months and at 24 months. The overall goal of this dissertation is to assess how changes in gait biomechanics evolve early after surgery and understand how these alterations impact the knee joint at a tissue level.

Aim 1 (Chapter 2)

Goal

Examine knee gait variables (flexion angle, flexion moment, adduction moment, extensor forces, and medial compartment force) between limbs at three and six months after ACLR and assess how these variables change from three to six months after ACLR.

Hypotheses

We hypothesized that 1) interlimb asymmetries in knee gait variables would be present at 3- and 6- months after ACLR and 2) these asymmetries would be greater at 3 months than at 6 months, with the involved limb changing over time.

Why is this important?

While knee gait alterations have been studied at several time points after ACLR, little is known about how these biomechanical variables change within the first six months after surgery, similarly little is known about how they differ over the entire stance phase of gait. Gaining insights into how biomechanical alterations are changing during these early time periods, when rehabilitation interventions may be more viable, may provide important insights into the mechanisms for long-term osteoarthritis development and could help inform the development of future rehab strategies.

Aim 2 (Chapter 3)

Goal

Develop a protocol for the construction of subject-specific finite element models that use the results of a validated EMG driven musculoskeletal model.

Why is this Important?

Diversity between individuals poses a unique challenge when using computer models to assess stresses within a joint. FE models that implement subject-specific geometry, joint loads, and kinematics can increase confidence in predictions of how stresses are being distributed within the joint. Understanding how joint loads are distributed throughout articular cartilage could significantly improve our understanding of why OA develops and may provide insight into what biomechanical behaviors are leading to abnormal stress distributions. This information can help inform the development of interventions aimed at restoring healthy joint biomechanics to a level that enables an active lifestyle.

Aim 3 (Chapter 4)

Goal

Assess stress patterns in the involved and uninvolved limb at 3, 6, and 24 months after ACLR and determine how changes in knee flexion angle (KFA) after ACLR relate to contact stress magnitude and location within the tibiofemoral joint.

Hypotheses

We hypothesize that the involved limb will experience lower stresses than the uninvolved limb, and that this asymmetry between limbs will decrease over time mostly due to the involved limb increasing to match the stresses in the uninvolved limb. We also hypothesize that stress location will be correlated with KFA in the femoral cartilage, with smaller knee flexion angles resulting in an anterior shift in stress.

Why is this important?

Very little is known about how changes in gait kinematics after ACLR affect the location and magnitude of cartilage contact stress within the tibiofemoral joint. The purpose of this aim is to identify if alterations in KFA shift the region of cartilage that is stressed during gait. We hypothesize that individuals who experience lower KFA in their involved knee will apply stress to different regions of cartilage compared to the stress distribution of their uninvolved limbs. The understanding of how this commonly seen alteration effects the distribution of stress in the joint can give insight into the mechanisms spurring the onset of OA and can be used to help inform new clinical interventions.

Aim 4 (Chapter 5)

Goal

The goal of this aim is to assess if alterations in cartilage stress after ACLR are associated with changes to cartilage's biochemical composition.

Hypotheses

We hypothesize that regions of cartilage with a limb-by-time interaction in stresses at peak medial compartment force (pMCF) will also have a limb-by-time interaction in T_2 relaxation times. Our second hypothesis is that regions of cartilage within the involved limb that experience larger changes in stress between 3 months and 6 months will experience larger changes in T_2 from 3 to 6 months and higher T_2 values at 24 months.

Why is this important?

Few studies have looked at the relationship between stresses within cartilage and the biochemical composition of cartilage. This aim will focus on gaining an understanding of this relationship. Studies have hypothesized that when the stress environment is rapidly increased the cartilage in that area is not able to withstand the stresses and starts to degrade. However, this has only been predicted by looking at cartilage thickness in these regions and has not considered the biochemical composition of the tissue. This comparison using qMRI variables and changes in stress distributions within the articular cartilage of the joint will provide further insights into the accuracy of this theory, which in turn will help with the identification of mechanisms that lead to the early onset of OA.

Chapter 2

KNEE JOINT BIOMECHANICS DURING GAIT IMPROVE FROM 3 TO 6 MONTHS AFTER ANTERIOR CRUCIATE LIGAMENT RECONSTRUCTION

NB: A version of this chapter has been published:

Neal K, Williams JR, Alfayyadh A, Capin JJ, Khandha A, Manal K, Snyder-Mackler L, Buchanan TS: Knee joint biomechanics during gait improve from 3 to 6 months after anterior cruciate ligament reconstruction. *J Orthop Research* 40(9): 2025-2038, 2022 [PMCID: PMC8976762]

Introduction

Anterior cruciate ligament (ACL) tears are one of the most common knee injuries among young, active populations[88]. Over the past few decades the number of individuals who have opted to undergo ACL reconstructive surgery (ACLR) after tearing their ACL has increased[89,90]. Many of these individuals undergo this procedure with the hope of restoring stability to their knee and returning to their pre-injury level of activity. While this procedure is successful at restoring knee stability it often fails to resolve alterations in gait mechanics.

Interlimb (involved vs. uninvolved) asymmetries in gait mechanics are commonly reported after surgery and tend to persist even after being cleared to return to sport[2,32]. Frequently reported alterations include changes in involved limb peak knee flexion angles (KFA)[2,33–37], peak knee extension angles (KEA)[38–40], peak knee flexion moments (KFM)[41–47], peak knee adduction moments (KAM)[42,43,45,48,49],

quadriceps strength[44,50,51], and peak medial compartment contact forces (MCF)[42] (vs. uninvolved and healthy controls). The continuation of these asymmetries are concerning as they leave individuals at risk of reinjury[52] and are thought to have long lasting effects on joint health[29,42,53–57]. While gait abnormalities tend to normalize around 2 years after surgery[44,91], changes in the loading environment that occur during these time periods may contribute to the premature development of post-traumatic knee osteoarthritis (OA)[3,29,42,55,57]. Understanding how gait aberrations progress during the early months after surgery, when interventions may be most feasible, can help inform new rehabilitative strategies to mitigate asymmetries and preserve long term joint health.

Three months after ACLR, Lin et al.[37] found an association between reduced involved limb knee flexion range of motion and lower knee extensor moments. Similarly, Sigward et al.[36] found that asymmetries in knee moments, work, and flexion angles 1 month after surgery that persisted to when individuals were cleared for running (~ 4 months). Likewise, Di Stasi et al.[2] found that regardless of return-to-sport status, at 6 months the involved limb demonstrates smaller knee extensor moments, suggesting that current rehabilitation protocols are not meeting their desired goals. These findings could be associated with quadriceps weakness. Lewek et al.[51] found that individuals with quadriceps weakness 4 months after ACLR exhibited reduced knee angles and moments. However, regaining quadriceps strength may not be enough to regain symmetry in gait mechanics. Roewer et al.[44] found that even after quadriceps strength symmetry was regained, asymmetries in knee flexion angles, moments, and

power persisted up to 6 months. Similarly, Arhos et. al.[92] found that restoration of quadriceps strength symmetry was not associated with symmetry in gait mechanics among individuals who were well rehabilitated. While gait mechanics have been assessed prior to 6 months after surgery, they have relied on surrogate measures for knee loading and have only assessed discrete points in the movement pattern (often peaks).

Many groups rely on surrogate measures for knee loading such as sagittal and frontal plane knee moments, due to the difficulty of obtaining *in vivo* joint loads[36,93]. Knee flexion moment (KFM) is used as a surrogate for total joint load and knee adduction moment (KAM) is thought to represent the distribution of load between the medial and lateral compartments of the knee[94–96]. In older populations higher knee moments have been correlated to the occurrence and severity of knee OA[96–98]. Early after ACLR, however, peak KFM[32,36,44] is lower and peak KAM is reported to be lower[42,43,45,48] or no different[42,49] in the involved limb compared to the uninvolved limb and healthy controls. While these measures play a role in knee joint loading, neither account for muscle co-contraction, which is heightened in the ACLR population and can also play a major role in joint load[99,100]. Thus, an EMG informed neuromusculoskeletal model, accounting for relative co-contraction of the muscles, may give a more accurate estimate of joint loads[101,102]. A study performed by Wellsandt et al.[42] utilized this approach and found that individuals who developed radiographic OA five years after ACLR displayed significantly lower peak medial compartment contact forces (MCF) in their involved limb six months after surgery,

compared to those who do not develop OA. These individuals also tended to underload their involved limb (vs. uninvolved).

Many have examined gait mechanics in the months and years following ACLR[35,54], mostly focusing on peak values of knee biomechanical variables during gait. While this approach may be traditional, the reduction of continuous *n* dimensional (*n*D) data to discrete values (0D) can lead to biasing of statistical results[103] and does not provide the full picture of how the variable of interest is progressing throughout stance, which may result in missing regions where alterations occur[103–105]. Since many biomechanical variables are time varying (1D) data, employing a continuous analysis technique may give a more accurate and comprehensive view of how these variables are affected after surgery[103,104]. Statistical parametric mapping (SPM), the applied form of Random Field Theory[106,107], allows for the statistical analysis of continuous data. SPM was originally developed for neuroimaging[108,109], but recently has been utilized within the biomechanics community[40,110,111]. By using SPM techniques for continuous data analysis, we seek to gain a more accurate and holistic view of how limb asymmetries evolve throughout the stance phase of gait, and over early post-surgery time points when interventions may be most effective.

Therefore, the purpose of this study was to 1) examine knee gait variables (flexion angle, flexion moment, adduction moment, extensor forces, and medial compartment force) between limbs at 3 and 6 months after ACLR and 2) assess how these variables change from 3 to 6 months after ACLR. We hypothesized that 1) interlimb asymmetries in knee gait variables would be present at 3 and 6 months after

ACLR and 2) these asymmetries would be greater at 3 months than at 6 months, with the involved limb changing over time.

Methods

Participants

Thirty-five individuals (**Table 1**) from a cohort study (R01-HD087459) were included in this study. Inclusion criteria were: no previous history of lower leg injury, no concomitant grade III ligament sprains, between the ages of 16 and 45, no meniscus repair, and unilateral primary ACLR. All data were collected at one institution following approval from an Institutional Review Board. All participants provided informed consent prior to participation in the study. For individuals under the age of 18, both minor assent and parental consent was obtained before enrolment.

Table 1 Participant Demographic Characteristics (n = 35)

Variable	**Mean ± Standard Deviation or Number (%)**
Age	22 ± 6 years
Sex	18 women (51%), 17 men (49%)
Height	1.7 ± 0.1 meters
Weight	72.7 ± 14.0 kilograms
BMI	24.7 ± 3.7 kilograms/meter^2
Graft Type	6 soft-tissue allograft (17%), 11 hamstring autograft (32%), 18 bone-patellar tendon-bone autograft (51%)

Meniscal Treatment	7 partial lateral meniscectomy (20%), 5 partial medial meniscectomy (14%), 2 partial medial and lateral meniscectomy (6%), 21 no meniscectomy (60%)
Walking Speed	1.6 ± 0.2 meters/second

Gait Analysis

All participants completed gait analysis during overground walking 3 (3.2 ± 0.5) and 6 (6.4 ± 0.7) months after ACLR using previously described methodologies[71,112].

Retroreflective markers were placed bilaterally on bony landmarks (iliac crests, greater trochanters, femoral epicondyles, malleoli, first and fifth metatarsal heads, and 2 markers on each calcaneus) and rigid shells containing multi-marker groupings were placed on the shanks, thighs, and pelvis[112]. Participants were directed to walk down a 6-meter walkway at a self-selected speed that was maintained across time points (± 5%). Walking speed was monitored using two photoelectric beams (Brower Timing Systems, Draper, UT). Once self-selected speed was established through practice trials, eight walking trials were collected for each limb. Kinematic (120Hz) and kinetic (1080 Hz) data were recorded using an 8-camera Vicon system (Oxford Metrics Limited, London UK) and an embedded force platform (Bertec Corporation, Worthington, OH), respectively. Kinematic data were filtered at 6 Hz using a zero-lag, fourth order Butterworth filter, while kinetic data were filtered at 25 Hz. Stance phase joint angles and moments were calculated using inverse dynamics in

Visual3D using a 6 DOF approach (C-motion, Germantown, MD) and were normalized to 100% of stance. All joint moments were normalized to body weight and height (%BW*HT) and reported as external moments in the tibial coordinate system.

Surface electromyography (EMG) electrodes (MA-300 EMG System, Motion Lab Systems, Baton Rouge, LA) were placed over seven muscles on each leg (rectus femoris, medial and lateral vasti, semimembranosus, long head of biceps femoris, medial and lateral gastrocnemius). EMG data were collected at 1080 Hz. Prior to walking, participants performed maximum voluntary isometric muscle contractions that were used to normalize the EMG signal obtained during overground walking. EMG data were high-passed filtered (30 Hz), rectified, and then low-passed filtered (6 Hz) using a second order Butterworth filter to create linear envelopes for the seven muscles. Additionally, the semitendinosus was set equal to the linear envelope of the semimembranosus, the short head of the biceps femoris to the long head of the biceps femoris, and the vasus intermedius was calculated by averaging the linear envelopes of the medial and lateral vasti.

The EMG and gait analysis data were used as inputs to a previously validated EMG-informed neuromusculoskeletal model to compute muscle forces and joint contact forces[71,101]. Validation was performed using *in vivo* contact force data recorded from an instrumented knee prosthesis and was found to produce accurate predictions of joint forces[71]. This model consisted of three components: an anatomical model, an activation dynamics model, and a contractions dynamics model. The anatomical model included a pelvis and femur, tibia, and foot segments that were

scaled using subject anthropomorphic measurements and was actuated by 10 muscle-tendon units. The activation dynamics model transformed the EMG data into muscle activations and the contraction dynamics model subsequently transformed muscle activations to muscle forces[112]. The medial compartment force was then estimated using a frontal plane moment balance between the external and internal frontal plane knee moments[102].

The variables of interest in this study were chosen based on previous evidence associating them with OA after ACLR[42,53,54]. These variables of interest included: knee flexion angle (KFA), knee flexion moment (KFM), knee adduction moment (KAM), knee extensor muscle forces (KEF), and knee medial compartment force (MCF). Extensor muscle forces were estimated by summing the forces of the rectus femoris, vastus medialis, vastus lateralis, and vastus intermedius[10]. Both the KEF and the MCF were normalized by bodyweight (BW).

Statistical Analyses

Statistical analyses were performed using SPM1D[113] in MATLAB (MathWorks, Natick, MA, USA). For each variable of interest, normality was assessed using D'Agostino-Pearson K2 tests[114]. Statistical parametric mapping (SPM) was used to conduct a 2x2 (Limb x Time) repeated measures ANOVA ($\alpha = 0.05$). Additionally, two-tailed students t-tests were conducted to assess limb asymmetry at each time point and to assess change in interlimb differences from 3 to 6 months. For both tests,

parametric or non-parametric approaches, depending on normality[115], were used (SPM1D supports both) to evaluate the data.

Results

Significant differences between limbs were observed at both 3- and 6-months for many of the kinematic and kinetic variables of interest. Generally, interlimb differences decreased from 3 to 6 months.

Knee Flexion Angle

A significant limb-by-time interaction for KFA was present during terminal stance (56%-66% of stance, $p = 0.038$; **Figure 1A**) as the knee was extending. During this portion of stance, the ILD significantly decreased from 3 to 6 months ($p = 0.010$; **Figure 1B**). At 3 months, significant differences were present between limbs during weight acceptance through midstance (11%-33% of stance, $p = 0.011$) and during terminal stance (52%-85% of stance, $p = 0.002$; **Figure 2A**). While the magnitude of interlimb differences decreased at 6 months, the differences were still significant during weight acceptance and part of midstance (8%-30% of stance, $p = 0.014$) and terminal stance (60%-80% of stance, $p = 0.019$; **Figure 2B**).

No significant differences were seen when comparing the involved limb across time points (**Figure 2C**). The uninvolved limb showed significant differences between time points during heel strike (0%-7%, p = 0.042; **Figure 2D**).

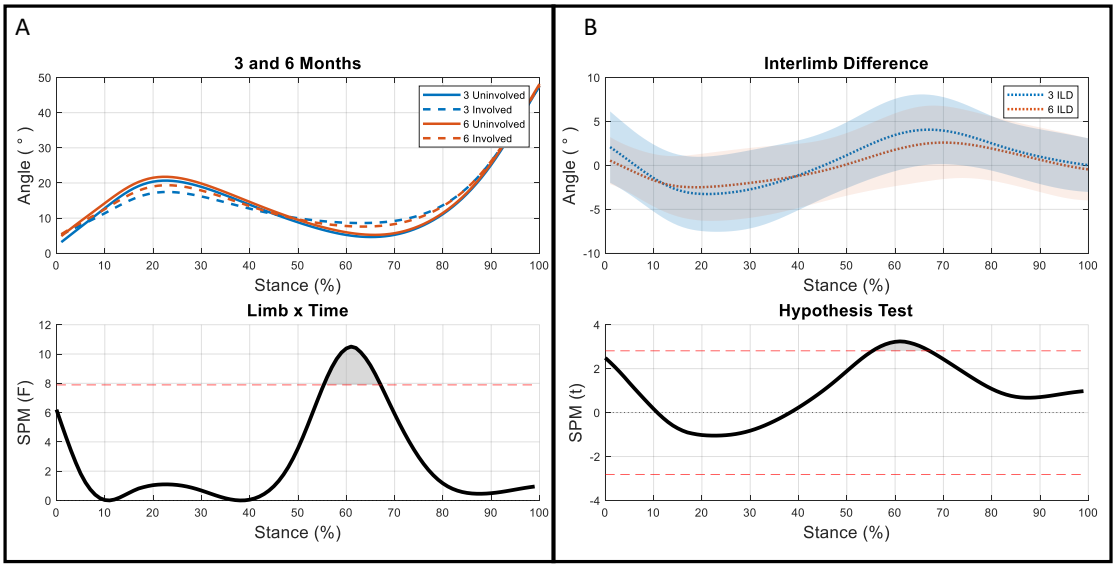

Figure 1 (A: top) 3 (blue) and 6 (orange) month KFA for the involved (dashed line) and uninvolved (solid line) limbs throughout stance. Interlimb differences were present at both time points during weight acceptance and parts of midstance and terminal stance. (A: bottom) SPM Limb x Time repeated measures ANOVA F statistic over 100% of stance. The red dashed line indicates the critical F-value (F = 7.99) where results are considered significant ($\alpha \leq 0.05$). A significant limb-by-time interaction was seen from 56%-66% of stance. (B: top) Interlimb differences at 3 and 6 months. ILD significantly decreased over 56%-66% of stance. (B: bottom) Two-tailed paired Student's t-test using SPM for ILD at 3 and 6 months. The red dashed line indicates the critical t-value ($\alpha = 0.05$).

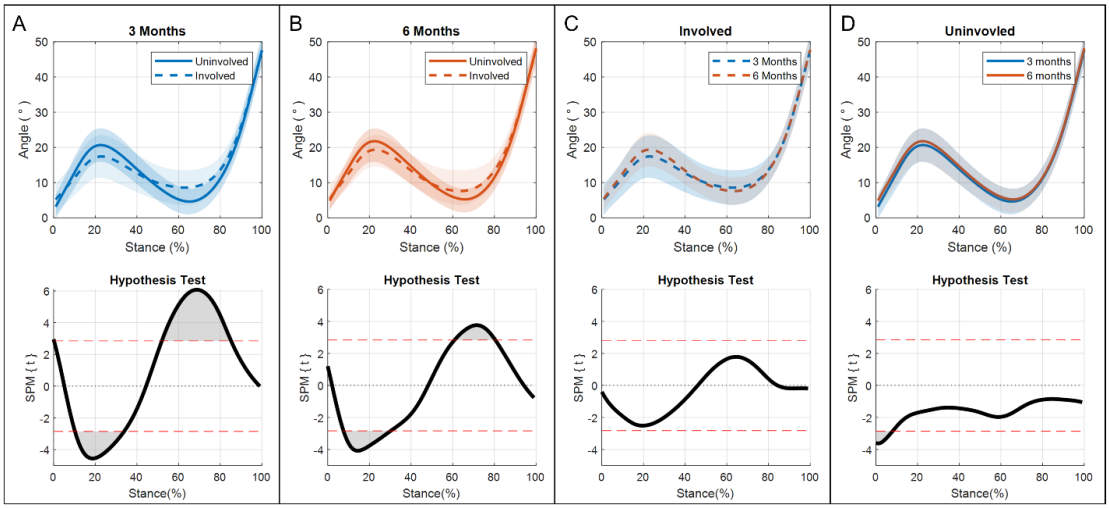

Figure 2 The top graph of each subfigure shows KFA through 100% of stance ± one standard deviation (shaded regions). The lower graph displays a two-tailed paired Student's t-test using SPM. The red dashed line indicates the critical t-value ($\alpha = 0.05$). (A) Involved (dashed line) vs uninvolved (solid line) KFA 3 months after ACLR; significant differences were present from 11%-33% and 52%-85% of stance. (B) Involved (dashed line) vs uninvolved (solid line) KFA 6 months after ACLR; significant differences were seen from 8%-30% and 60%-80% of stance. (C) Involved 3 months (blue) vs 6 months (orange); no significant differences were present. (D) Uninvolved 3 months (blue) vs 6 months (orange); significant differences were seen from 0%-7% of stance.

Knee Flexion Moment

A significant limb-by-time interaction for KFM was present during the end of weight acceptance and the start of midstance (15%-24% of stance, p=0.009; **Figure 3A**). The ILD significantly decreased from 3 to 6 months during this part of stance (p = 0.007; **Figure 3B**). T-tests showed significant differences between limbs at 3 months during weight acceptance and part of midstance (5%-36% of stance, p<0.001),

terminal stance (64%-71% of stance, p = 0.014), and pre-swing (86%-96% of stance, p = 0.005; **Figure 4A**). Interlimb differences decreased from 3 to 6 months with significant differences seen only during weight acceptance through midstance at 6 months (5%-31% of stance, p <0.001; **Figure 4B**). During the transition from weight acceptance to midstance, KFM in the involved limb increased from 3 to 6 months (13%-29%, p <0.001; **Figure 4C**). No differences were found for the uninvolved limb between time points (**Figure 4D**).

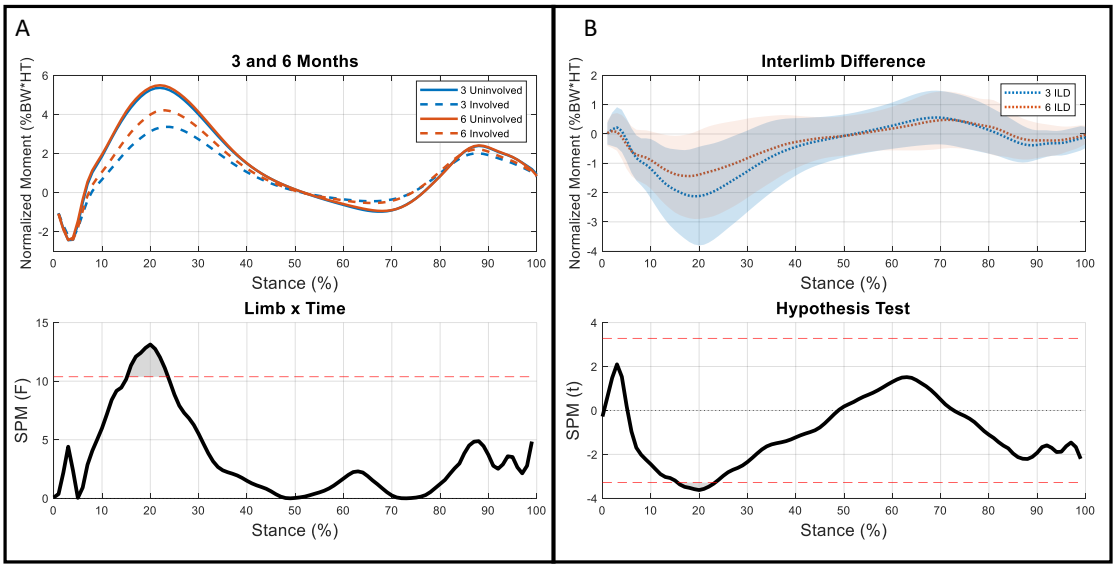

Figure 3 (A: top) 3 (blue) and 6 (orange) month KFM for the involved (dashed line) and uninvolved (solid line) limbs throughout stance. Interlimb differences were present at both time points during weight acceptance into midstance and terminal stance. These differences decreased from 3 to 6 months during weight acceptance into midstance. (A: bottom) SPM Limb x Time repeated measures ANOVA F-statistic over 100% of stance. The red dashed line indicates the critical F-value (F = 10.37) where results are considered significant ($\alpha \leq 0.05$). A significant limb-by-time interaction was seen from 16%-23% of stance. (B: top) Interlimb differences at 3 and 6 months. ILD significantly decreased from 3 to 6 months between 15%-23% of stance. (B: bottom) Two-tailed paired Student's t-test using SPM for ILD at 3 and 6 months. The red dashed line indicates the critical t-value ($\alpha = 0.05$).

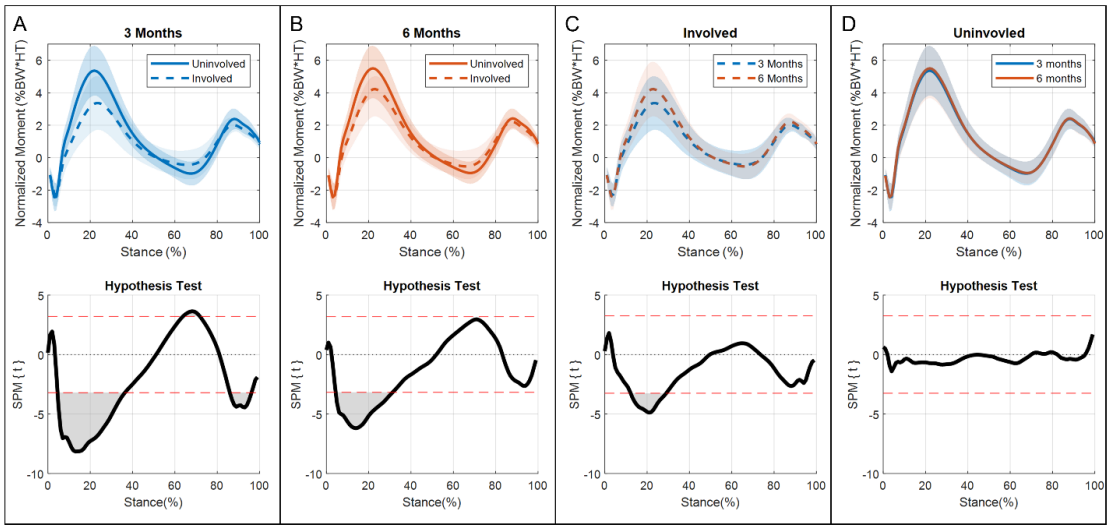

Figure 4 The top part of each subfigure shows KFM through 100% of stance ± one standard deviation (shaded regions). The lower portion displays a two-tailed paired Student's t-test using SPM. The red dashed line indicates the critical t-value ($\alpha = 0.05$). (A) Involved (dashed line) vs uninvolved (solid line) KFM 3 months after ACLR; significant differences were present from 5%-36%, 64%-71%, and 86-96% of stance. (B) Involved (dashed line) vs uninvolved (solid line) KFM 6 months after ACLR; significant differences were seen from 5%-31% of stance. (C) Involved 3 months (blue) vs 6 months (orange); significant differences were seen from 13%-29% of stance. (D) Uninvolved 3 months (blue) vs 6 months (orange); no significant differences were present.

Knee Adduction Moment

No significant differences were seen between limbs at either time point when assessing KAM (**Figures 5 and 6**).

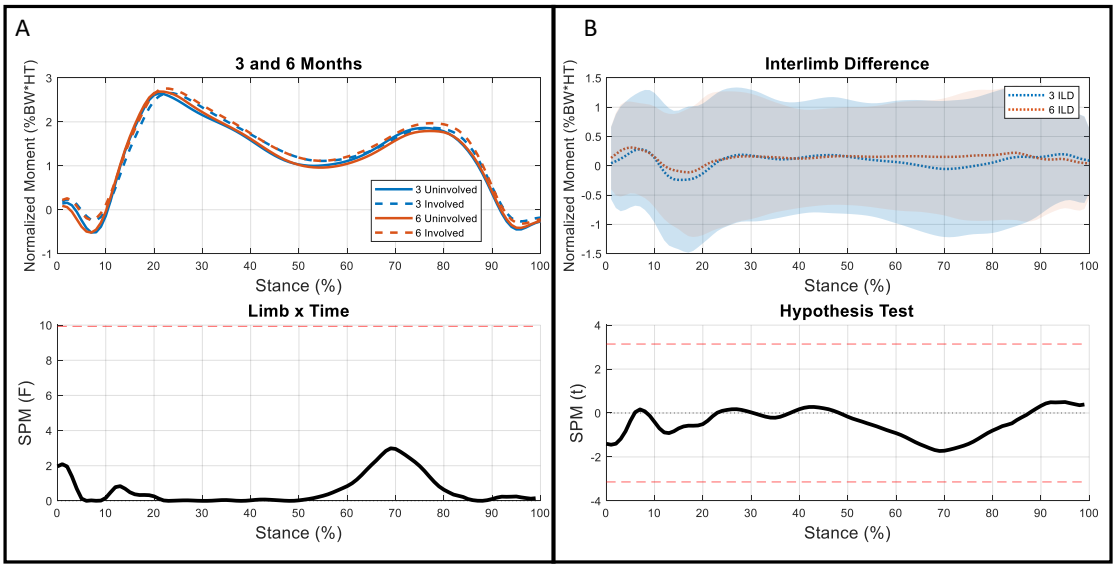

Figure 5: (A: top) 3 (blue) and 6 (orange) month KAM for the involved (dashed line) and uninvolved (solid line) limbs throughout stance. (A: bottom) SPM Limb x Time repeated measures ANOVA F-statistic over 100% of stance. The red dashed line indicates the critical F-value (F = 9.94) where results are considered significant. No significant limb-by-time interaction was present. (B: top) Interlimb differences at 3 and 6 months. No significant differences were present. (B: bottom) Two-tailed paired Student's t-test using SPM for ILD at 3 and 6 months. The red dashed line indicates the critical t-value ($\alpha = 0.05$).

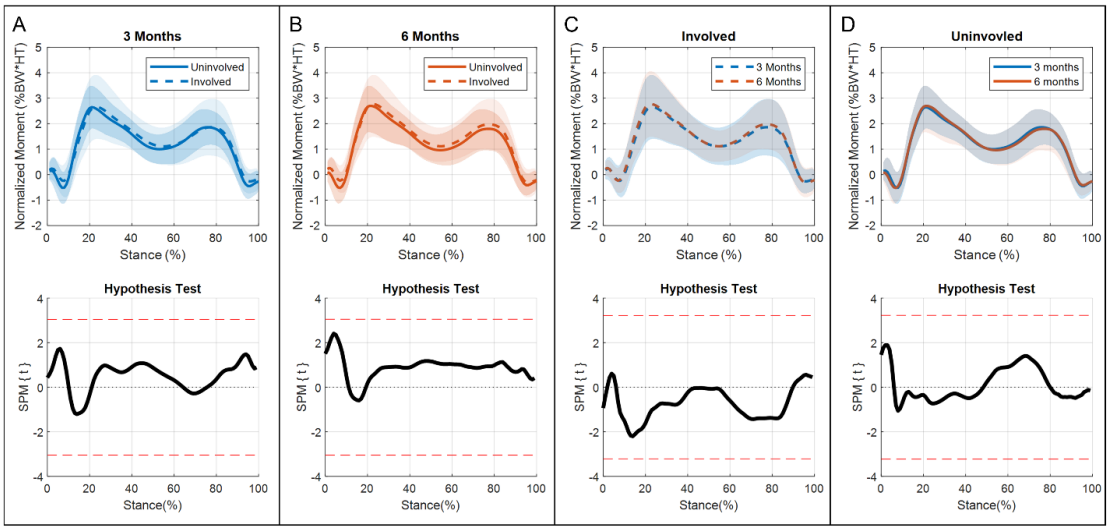

Figure 6 The top part of each subfigure shows KAM through 100% of stance ± one standard deviation (shaded regions). The lower portion displays a two-tailed paired Student's t-test using SPM. The red dashed line indicates the critical t-value ($\alpha = 0.05$). (A) Involved (dashed line) vs uninvolved (solid line) KAM 3 months after ACLR; no significant differences were present. (B) Involved (dashed line) vs uninvolved (solid line) KAM 6 months after ACLR; no significant differences were present. (C) Involved 3 months (blue) vs 6 months (orange); no significant differences were present. (D) Uninvolved 3 months (blue) vs 6 months (orange); no significant differences were present.

Knee Extensor Forces

Interlimb differences were not significantly different between time points and no limb-by-time interaction occurred (**Figure 7**). Significant differences were present between limbs at 3 months (3%-34%, $p < 0.001$; 89-100%, $p = 0.01$; **Figure 8A**), and approached significance at 6 months (**Figure 8B**). The involved limb's knee extensor

muscle forces significantly increased from 3 to 6 months (9%-25%, p =0.001; 95%-100%, p = 0.038; **Figure 8C**). There were no statistical differences between the uninvolved limb at 3 and 6 months (**Figure 8D**).

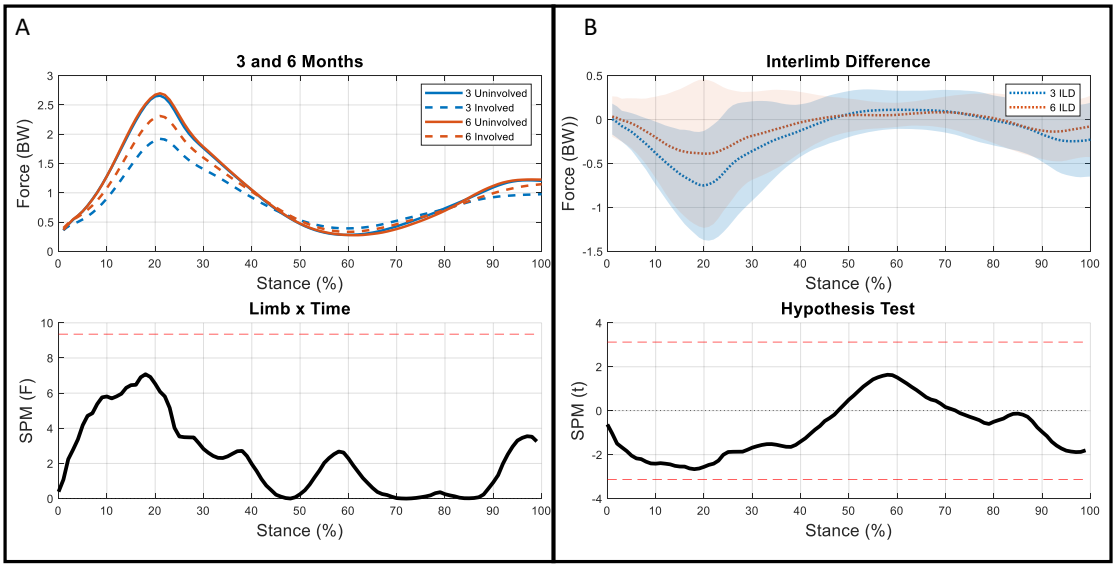

Figure 7 (A: top) 3 (blue) and 6 (orange) month knee extensor forces for the involved (dashed line) and uninvolved (solid line) limbs throughout stance. (A: bottom) SPM Limb x Time repeated measures ANOVA F-statistic over 100% of stance. The red dashed line indicates the critical F-value (F = 9.80). No limb-by-time interaction was seen. (B: top) Interlimb differences at 3 and 6 months. These differences decreased from 3 to 6 months but were not significant. (B: bottom) Two-tailed paired Student's t-test using SPM for ILD at 3 and 6 months. The red dashed line indicates the critical t-value ($\alpha = 0.05$).

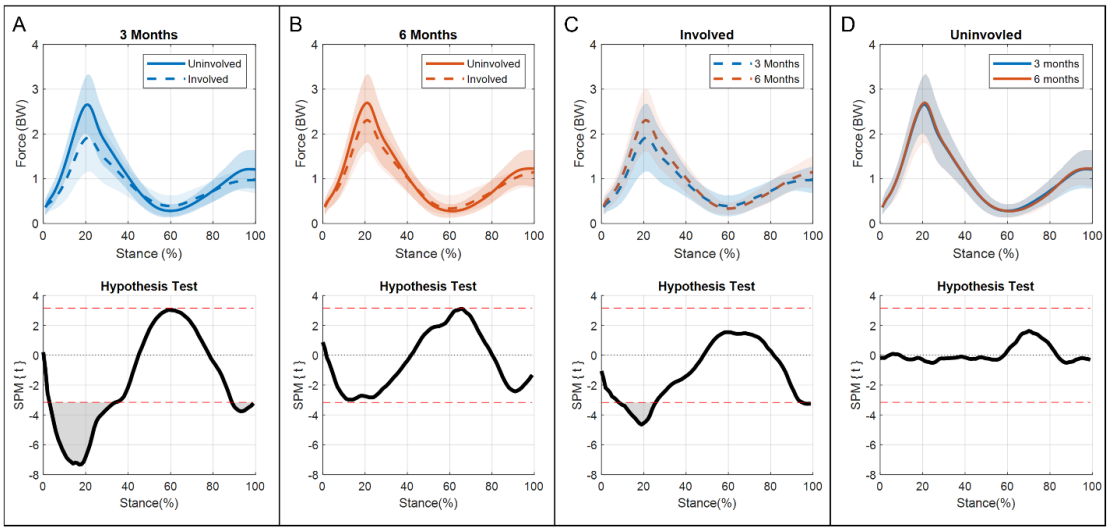

Figure 8: The top part of each subfigure shows the knee extensor forces through 100% of stance ± one standard deviation (shaded regions). The lower portion displays a two-tailed paired Student's t-test using SPM. The red dashed line indicates the critical t-value ($\alpha = 0.05$). (A) Involved (dashed line) vs uninvolved (solid line) knee extensor forces 3 months after ACLR; significant differences were present from 3%-34% and 89%-100% of stance. (B) Involved (dashed line) vs uninvolved (solid line) knee extensor forces 6 months after ACLR; no significant differences were seen. (C) Involved 3 months (blue) vs 6 months (orange); significant differences were seen from 9%-25% and 95%-100% of stance. (D) Uninvolved 3 months (blue) vs 6 months (orange); no significant differences were present.

Medial Compartment Force

There was no limb-by-time interaction for MCF, nor was there a significant change in ILD over time (**Figure 9**). The medial compartment of the involved limb was significantly underloaded compared to the uninvolved limb at 3 months (12%-20%, $p = 0.019$; **Figure 10A**). While underloading was still present at 6 months, it was no longer statistically significant (**Figure 10B**). The reduction in MCF interlimb

difference from 3 to 6 months appears to be driven by changes in the involved limb over time, as the involved limb's MCF increased from 3 to 6 months (**Figure 10C**) while the uninvolved limb's MCF stayed relativity consistent (**Figure 10D**).

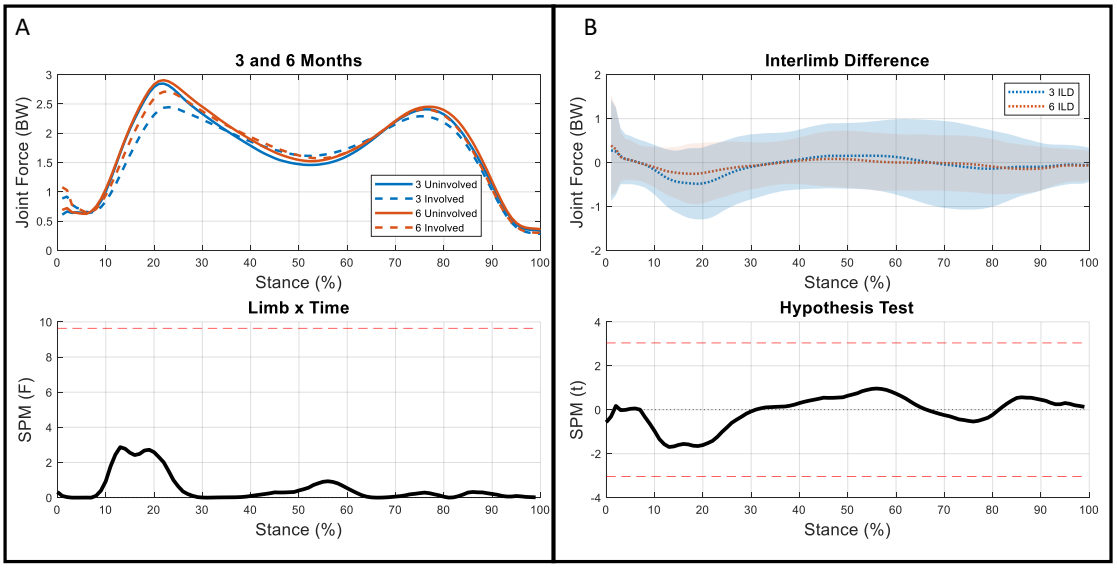

Figure 9: (A) 3 (blue) and 6 (orange) month medial compartment forces for the involved (dashed line) and uninvolved (solid line) limbs throughout stance. Participants underloaded the involved limb at both time points during weight acceptance (vs. uninvolved limb), however involved limb loading did increase from 3 to 6 months. (A: bottom) SPM Limb x Time repeated measures ANOVA F-statistic over 100% of stance. The red dashed line indicates the critical F-value (F = 9.91). No limb-by-time interaction was seen. (B: top) Interlimb differences at 3 and 6 months, no significant differences were present. (B: bottom) Two-tailed paired Student's t-test using SPM for ILD at 3 and 6 months. The red dashed line indicates the critical t-value ($\alpha = 0.05$).

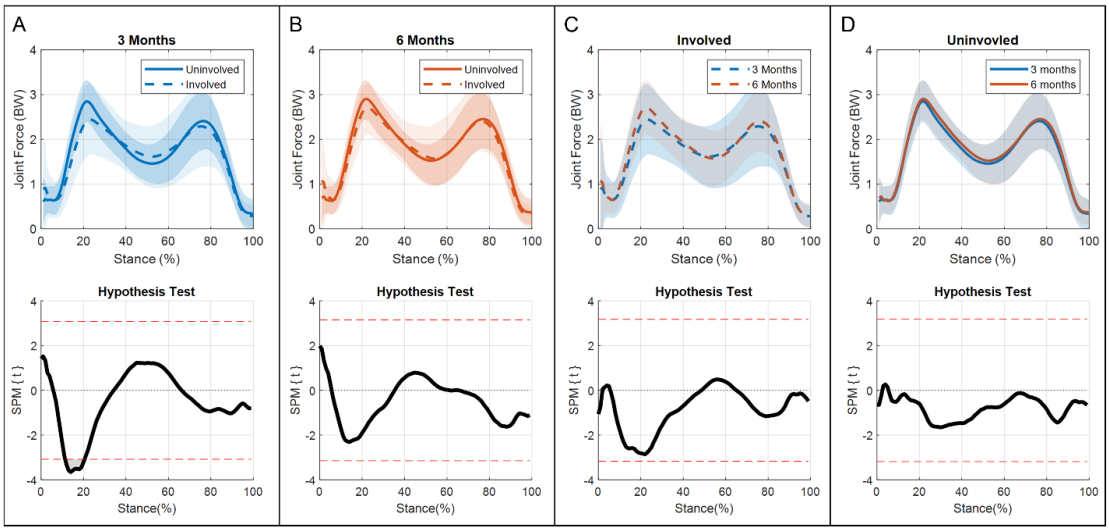

Figure 10: The top part of each subfigure shows the medial compartment force through 100% of stance ± one standard deviation (shaded regions). The lower portion displays a two-tailed paired Student's t-test using SPM. The red dashed line indicates the critical t-value ($\alpha = 0.05$). (A) Involved (dashed line) vs uninvolved (solid line) medial compartment forces 3 months after ACLR; significant differences were present from 12%-20% of stance. (B) Involved (dashed line) vs uninvolved (solid line) medial compartment forces 6 months after ACLR; no significant differences were seen. (C) Involved 3 months (blue) vs 6 months (orange); no significant differences were seen. (D) Uninvolved 3 months (blue) vs 6 months (orange); no significant differences were present.

Discussion

Our first hypothesis was partially supported; asymmetries in KFA and KFM were present at both time points. Asymmetries in KEF and MCF were present only at 3 months, while no asymmetries were found for KAM regardless of time point. Our second hypothesis, that asymmetries would be greater at three months than six months, was also partially supported. Descriptively, interlimb asymmetries were greater at 3 months (vs. 6 months) for all our variables of interest except for KAM.

However, this was only statistically supported in KFA and KFM, in which interlimb differences improved over time but were still present at the 6-month timepoint. Gait mechanics in the uninvolved limb stayed relatively consistent between 3 and 6 months, while the involved limb's mechanics trended towards that of the uninvolved limb over time. This pattern indicates that changes in mechanics early after ACLR primarily occur within the involved limb. The data presented here add to the timeline of how gait adapts early after ACLR. Understanding how gait alterations progress in the early months after surgery, when interventions may be most effective, may help inform the design of post-operative treatments aimed at mitigating altered biomechanics that are associated with the early onset of osteoarthritis.

One of the most unique aspects of this study was the use of SPM to assess biomechanical asymmetries, and their changes, over stance phase. Recent work using SPM has highlighted the importance of considering the entire time dependent data set rather than using discrete points. A study performed by Pataky et al.[104] compared SPM to scalar extraction by re-analyzing biomechanical datasets that had been published using traditional 0D statistical analyses. These two analysis techniques produced conflicting statistical conclusions. Pataky concluded that discrete analyses may suffer from type I and type II error as they fail to consider the entire measurement domain and ignore covariance amongst vector components. The utilization of SPM reduces the chance of these two sources of biases by performing hypothesis tests that consider the whole time series[103,104]. Thus, the use of SPM in this study, rather than traditionally used discrete values, reduces the likelihood of producing biased results.

Knee Flexion Angle

Previous studies have reported smaller peak KFAs and peak KEAs in the involved limb (vs. uninvolved and healthy controls) 3 and 6 months after ACLR[2,33–36,39]. Our data align well with these findings showing significant differences between limbs at 3 and 6 months around the peaks of KFA during stance. ILDs were present during weight acceptance into midstance and terminal stance at both time points. While the magnitude of interlimb difference decreased from 3 to 6 months during both these phases of stance, they only significantly decreased during terminal stance. Individuals who demonstrate smaller KFAs typically exhibit quadriceps weakness[51]. While quadriceps strength was not collected in this study, we did see an increase in the involved limb's knee extensor forces during weight acceptance into midstance from 3 to 6 months. However, it is unclear if this is driven by changes in neuromuscular activation patterns or increases in strength. Regardless, these increase in knee extensor forces may explain the increases in knee flexion angle between these time points.

A reduced KFA after ACLR is of concern as this may result in load being applied to regions of cartilage that are ill-suited to the new loading environment[56]. From 0°-30° of flexion, the point of contact within the medial compartment shifts posteriorly as KFA increases[116–118]. This means that individuals who exhibit a reduction in KFA may load more anterior regions of cartilage, which are normally thinner and less capable of load bearing[24,118,119]. Stress alterations in these newly loaded areas could be initiating irreversible cartilage damage[24]. The involved limb's

peak knee flexion angle tends to increase up to one year following ACLR, after which no differences between limbs have been reported[35,53]. A new concern arises when the point of contact within the joint now moves posteriorly as these flexion angles increase, as this region of cartilage may have experienced lower loads and stresses since ACLR[56,59,118]. During this period of relative unloading, the cartilage is at risk of being altered to resemble non-weight bearing cartilage, potentially leaving the tissue unable to withstand the return to pre-injury loads[24,59]. Therefore, it may not only be the reduction of knee flexion angle after ACLR that leads to irreversible cartilage damage but also the recovery of range of motion over this one-year timeline. Further studies are warranted to explore this hypothesis and to identify what is considered a clinically meaningful change in KFA over the entire stance phase.

Knee Flexion Moment

KFM showed ILDs at both 3 and 6 months however these ILD significantly decreased by the 6-month time point. The decrease in interlimb difference from 3 to 6 months is driven by a significant increase in the involved limb's KFM. Asymmetries have been reported to persist in peak KFM up to two years after surgery[41,44,47] and are partly attributed to insufficient quadriceps strength[33,51,120]. Experiencing lower KFM after ACLR may also be attributed to lack of confidence, as assessed by patient reported outcomes, in the individual's knee[121]. Future work looking at patient reported outcomes could help clarify if kinesiophobia is playing a role in these changes.

While decreases in interlimb difference are seen in these data, the involved limb is still experiencing significantly lower KFMs during weight acceptance into midstance at 6 months. A recently published study by our group using the same cohort found an association between lower involved limb (vs. uninvolved) KFMs and quantitative MRI values indicative of cartilage degradation 3 months after ACLR[31]. This agrees with reports that healthy individuals who walked with higher peak KFM had thicker (and thus healthier) cartilage[122]. However, conflicting evidence does exist as Teng et. al.[123] found that higher KFMs 6 months after ACLR were associated with worsening of joint cartilage (as assessed via quantitative MRI measures)[123]. It remains unclear if regaining symmetry in KFM from 3 to 6 months after ACLR will help preserve healthy knee cartilage, or if these adaptations may actually spur changes in the cartilage's biochemical health.

Knee Adduction Moment

Knee adduction moment did not show any significant differences between limbs at either time point. These data align well with previous studies that have found no difference in peak knee adduction moment between limbs at 6 months[49] and 1 year[42] after ACLR. However conflicting evidence suggesting lower peak KAM during this time also exists[42,47,124]. In individuals with medial compartment knee OA, increases in peak KAM have been associated with increases in OA severity[53,125]. This association, in conjunction with the results seen here, may suggest that altered KAM is a result of OA rather than an initiating factor; however, it is still an area of active

research of how the full spectrum of gait changes from healthy to post ACLR to OA and future work is needed to explore this idea.

Knee Extensor Forces

There were significant differences between limbs in knee extensor forces during weight acceptance into midstance at 3 months. These differences decreased from 3 to 6 months as the involved limb's knee extensor forces significantly increased. While there were no statistical differences between limbs at 6 months it should be noted that no significant changes in interlimb differences occurred from 3 to 6 months. This is not necessarily surprising as there is a high degree of variability in knee extensor forces at 6 months; likely reflective of the large variability in ability to regain quadriceps strength early after surgery[126]. A previous study from our lab assessing a different cohort reported KEF between 2 and 3 BW at peak MCF which align well with the results of the current study[10].

Quadriceps weakness after ACLR is common in the involved limb and has been linked to alterations in gait [127,128]. Individuals who were classified as having weak quadriceps were shown to have similar gait patterns to individuals who were ACL deficient, while those classified as having strong quadriceps were similar to healthy controls[51]. While it cannot be determined if differences in extensor forces reported here are due to muscle strength or how the muscle is being activated, these data suggest that regaining symmetric quadriceps forces could be essential to returning to pre-injury gait patterns. However, recent evidence from a separate cohort indicates

that improving quadriceps strength alone is not sufficient to restore symmetrical gait mechanics[92].

Medial Compartment Force

The magnitude, peak values (~2-3 BW), and shape of MCF curves in this study align well with previous studies utilizing the same model[42,102,129] and a study that reported values from instrumented knee implants[130]. We found significant asymmetries in medial compartment forces at 3 months, but not 6 months. These results contradict previous findings from our lab that reported lesser loading in the involved limb at 6 months after ACLR[42]. These findings highlight the importance of using EMG-driven models to assess joint loading as we saw different "loading" patterns when assessing KAM (no differences between limbs) and KFM (differences at 3 and 6 months) when compared to the medial compartment force.

It is still unclear how changes in loading magnitude and distribution effect the health of the cartilage over time. Since cartilage is conditioned for specific loading environments[56], the combination of changes in load and altered gait patterns may cause excessive loading in regions of cartilage that were once considered non-loadbearing[118]. A study by Kaiser et al.[131] provided evidence of this by using a combination of dynamic and quantitative MRI to assess joint contact and cartilage biochemical health. They found that reconstructed knees exhibited increased contact areas along the medial spine of the medial tibial plateau and exhibited quantitative

MRI values that are indicative of early cartilage degeneration in this area when compared to the contralateral limb and healthy controls.

Limitations and Future work

There are several limitations that should be considered when interpreting the results of this study. First, no strength measurements were performed. While we can estimate the muscle forces exerted throughout gait, no conclusions can be drawn about how muscular strength deficits progressed in the early months after surgery and how they relate to changes in knee mechanics. Another limitation is that we were not able to control for participants' post-operative rehabilitation and graft types used during surgery. Participants were recruited from multiple clinics from the surrounding area and therefore may have undergone different rehabilitation protocols. Similarly, participants underwent their ACL reconstructive surgery from a variety of surgeons who used different graft types and surgical techniques. While controlling these measures would be ideal, this would limit the generalizability of this study to the broader ACLR population. This study excluded individuals who required a meniscal repair due to the extended non-weight bearing period that is required after this procedure; however, individuals who received a meniscectomy are not required to remain non-weight bearing for an extended time due to the procedure and therefore were eligible for this study. It is unlikely that all the participants included in this study

will develop OA. Future work will examine the effect early changes in gait mechanics have on long term cartilage health.

While SPM has been shown to be a useful tool for analyzing biomechanical data it is not without limitations as a statistical analysis technique. Biomechanical curves may require registration due to data misalignment. For this study we normalized our curves to 100% of stance, which helped with data alignment. However, applying nonlinear registration may also be a helpful approach to mitigating misalignment of data and should be investigated. Another limitation is that significance does not necessarily indicate meaningful differences. Previous studies have reported clinically meaningful differences at discrete points during gait[53,132], but none currently exist for continuous data analysis. Future work should establish these thresholds for SPM. Finally, no power analysis was performed for the current study. Since the data for this study is a subset of data from a larger cohort, if a power analysis were performed it would be classified as a post-experimental power analysis, which has been shown to be an inappropriate test for power[133,134].

Conclusion

In this study we utilized SPM to assess how gait adapts from 3 to 6 months after ACLR. We found significant asymmetries between limbs in KFA, KFM, KEF and MCF 3 months after ACLR but by 6 months KEF and MCF were no longer significantly different. While differences between limbs were still present for KFA and KFM, these asymmetries had significantly decreased by 6 months. These early

time points after surgery may be the ideal period for interventions to develop a healthy gait pattern, since abnormal gait biomechanics as early as 6 months after ACLR are linked to the development of post-traumatic OA[42,57,93,135].

The use of discrete values to analyze gait after ACLR underutilizes the wealth of data that is collected during gait analyses. Through the use of SPM to assess the entire gait cycle we can paint a more holistic picture of alterations in gait after ACLR. This study expands upon the existing literature which has focused on discrete values to understand aberrations in gait mechanics. Altogether, this work adds to our understanding of how biomechanical alterations are changing over stance phase during the early months after surgery. These results may be used to help inform the design of future studies investigating the pathogenesis of osteoarthritis and may ultimately be useful in the design of early gait interventions aimed at mitigating the development of the disease.

Chapter 3

A PROTOCOL FOR THE DEVELOPMENT OF SUBJECT-SPECIFIC FINITE ELEMENT MODELS OF THE KNEE FOR ANALYSIS OF CARTILAGE STRESS AFTER ACLR

Introduction

The development of subject-specific knee models is a time consuming and intricate process. There is a well-established outline on the steps needed to design a finite element model, however the details to the process are often vaguely reported, leaving the modeler to make assumptions and development decisions that, while valid, can limit the model's accuracy and predicative capabilities. Without clear reporting on how a model is developed, many researchers are forced to develop their own approaches and tools which can limit reproducibility of the results. Open-source models help alleviate this burden but limits the research questions to those the model was designed to answer[136–139]. Due to the complexity of the human body most in-silico models are made as simple as possible and with the goal of answering a specific research question. Researchers must fully understand the assumptions and the limitations of the model before applying it to their specific research, making it even more essential to have access to the entire development process. While some have pushed for a standardized method for reporting the modeling process[73,86,87], there is still no universally accepted practice for this process. By having a standardized

reporting format, it will be easier to compare models and understand its limitations[73,87].

This chapter is a detailed protocol of the development of FE models of the knee joint for the assessment of cartilage stress during gait over multiple time points. The protocol utilizes a combination of open-source, commercial software, and self-developed tools. The goal of this chapter is to provide an understanding of the entire process needed for the development of these specific models, and to help provide others the opportunity to build their own models by utilizing the available tools and codes. It should be noted that this model protocol was developed to assist in the understanding of how stress is altered throughout gait following anterior cruciate ligament reconstruction (ACLR). This protocol will layout the exact process for development of this model as well as the steps taken for partial model validation.

Methods

A protocol for the development of a FE model of the knee, using a combination of open-source and commercial software, was developed to assess cartilage stress during gait for a large cohort of subjects. The following section describes, in detail, the acquisition of model inputs (gait analysis and musculoskeletal modeling), the FE model development, model validation and limitations and scaling protocol for model meshes. The current model will be used to assess cartilage stresses within the tibiofemoral joint stemming from changes in joint loads and other knee mechanics at multiple time points following ACLR.

Gait analysis and EMG Driven Musculoskeletal Model

Motion and load data were acquired via overground walking motion analysis and the use of a validated EMG-driven musculoskeletal model. Subjects were equipped with retroreflective markers placed on bony landmarks and rigid shells on their shanks, thighs, and pelvis for tracking. Walking trials were collected at a self-selected walking speed (±5%) that was replicated across data collections. Kinematic data were recorded using an 8 camera setup (Vicon, Oxford Metrics Limited, London UK) at a sampling rate of 120 Hz. Kinetic data were collected via a force plate (Bertec Corporation, Worthington, OH) at a sampling rate of 1080 Hz. Stance phase joint angles and moments were calculated using inverse dynamics in Visual 3D (C-motion, Germantown, MD) and were normalized to 100% of stance. For comparison purposes, moments were normalize to body weight and height (%BW*H) and were reported as external moments in the tibial coordinate system.

A patient-specific validated EMG-driven musculoskeletal model of the knee was used to estimate muscle forces [140–143]. These forces were then used for the estimation of joint contact forces. EMG data were collected for seven muscles on each leg and were used to estimate muscle forces throughout gait. Flexor muscles of interest included the semimembranosus, longhead of the biceps femoris, and the medial and lateral gastrocnemii. Extensor muscles included the rectus femoris and the medial and lateral vasti. Signals were band-pass filtered (20-500 Hz) prior to sampling

and were sampled at 1080 Hz using a MA-300 EMG system (MotionLab Systems, Baton Rouge, LA).

Each muscle signal was high-pass filtered using a 2nd order Butterworth filter with a cutoff of 30 Hz. The signals were then rectified and low-passed filtered using a cutoff of 6 Hz to create linear envelopes. Prior to collecting walking data, subjects performed maximum voluntary isometric contractions (MVICs) which were used for the normalization of each muscle signal.

The vastus intermedius EMG was calculated as the average of the vastus medialis and vastus lateralis. While the semitendinosus and the short head of the biceps femoris were set equal to the linear envelopes of the semimembranosus and the long head of the biceps femoris, respectively.

The linear envelopes obtained from these 10 muscles were used as inputs for the previously validated EMG model [140,141]. Subject-specific anatomical models were scaled using a standing calibration, which allow for muscle-tendon length and moment arms to be estimated during stance phase kinematics (SIMM 6.0, Musculographics INC, Chicago, IL).

Model calibration was performed to estimate tendon slack length and optimal muscle fiber length. During calibration, muscle activation and muscle contraction sub-components were iteratively adjusted to produce a flexion extension muscle moment that matches the knee moment derived from inverse-dynamics based gait analysis. Muscle activation was characterized by four parameters (two recursive filter coefficients, one electromechanical delay term, and one non-linear shape factor) and

was used for transforming the EMG signal to muscle activation measures. The muscle activation measures were then transformed to muscle forces using equations that estimate muscle contraction. Muscle contractile properties (force-length and force-velocity relationships) were represented using a modified Hill-type model of a muscle fiber in series with a tendon as shown in the equation below. The time varying parameters are based on the kinematics during gait, while the time invariant parameters are derived from literature [144].

$$F^m(t) = f\{a(t), l^m(t), v^m(t), \theta(t), l_o^m, l_s^t, F_o^m\}$$

Time varying parameters	Time invariant parameters
$a(t) = muscle\ activation$	$l_o^m = optimal\ fiber\ length$
$l^m(t) = fiber\ length$	$l_s^t = tendon\ slack\ length$145
$v^m(t) = fiber\ velocity$	$F_o^m = \max isometric\ muscle\ force$
$\theta(t) = pennation\ angle$	

Once calibration was completed, joint kinematics and EMG were used to estimate muscle forces for each gait trial. The medial compartment, lateral compartment, and total joint loads were then obtained by balancing the external frontal plane knee moments for each time step during gait using the muscle forces and frontal plane moment arms about a point that was ±25% of the tibial plateau width from the knee joint center[71].

Our unique ability to predict compartmental joint loads from validated EMG-driven musculoskeletal models creates the opportunity for the input variables of the

FE model to be limited to medial and lateral joint loads and knee flexion angle. This method considers muscle forces, co-contraction, and joint moments without having to apply excess moments and loads to the FE model simultaneously, which helps reduce model complexity[146].

Geometry Acquisition

Model geometry was segmented from a magnetic resonance imaging (MRI) scan of the healthy knee of a 19-year-old female from our cohort. Specifically, a sagittal proton density weighted sequence (Repetition time/echo time = 5100/30 ms, slice thickness = 2 mm with no gap, field of view = 14 cm, matrix = 800 x 800) from the subject's 6-month time point was used to obtain an image of the uninjured knee using a clinical 3.0 T MRI unit and a 16-channel knee coil (Siemens 3T Magnetom Prisma). Following the scan, MRI images in the DICOM format were imported into a segmentation software, Simpleware ScanIP (Synopsys, Inc., Mountain View, USA) and manually segmented. There are a variety of segmentation software that can be utilized for this step including commercial software like Mimics (materialise.com) and Simpleware ScanIP (www.synopsys.com) [147] as well as opensource options like ITK-Snap (www.itksnap.org)[148] and 3D Slicer (www.slicer.org)[147]. Segmented regions included the femur, tibia, and fibula, joint cartilage (femoral, medial and lateral tibia), the menisci, meniscal horns, and internal knee ligaments (ACL and PCL). Since sagittal scans were used it was not possible to segment the MCL and LCL. This was an acceptable limitation for the current model's purpose since ligament 3D geometries

were not included in this model and segmentation was performed to gain approximate insertion point locations. If ligaments are a focus of the simulation, axial MRI images should also be obtained. The segmented region of cartilage, menisci, and bones were then exported as .stl files that were used as the base geometry when developing the geometry's mesh (Figure 13).

The process of manual segmentation is a time-consuming task and accuracy can vary greatly between individuals. For the purpose of our study one model was built and scaled based on a ratio of measurements (Figure 16) taken of the segmented MRI and those of the subject of interest's MRIs, this processes is discussed in detail later on in this chapter. This approach helps limit the impact that manual segmentation has on results. Automated segmentation processes have been developed, and commercial software have options for partially automated segmentations which considerably speed up segmentation time but are also costly and still require time and expertise from the individual segmenting. Other segmentation pipelines are currently being developed by a variety of different groups using approaches such as artificial intelligence which require large training sets; at this time, however, none are publicly available[149–152].

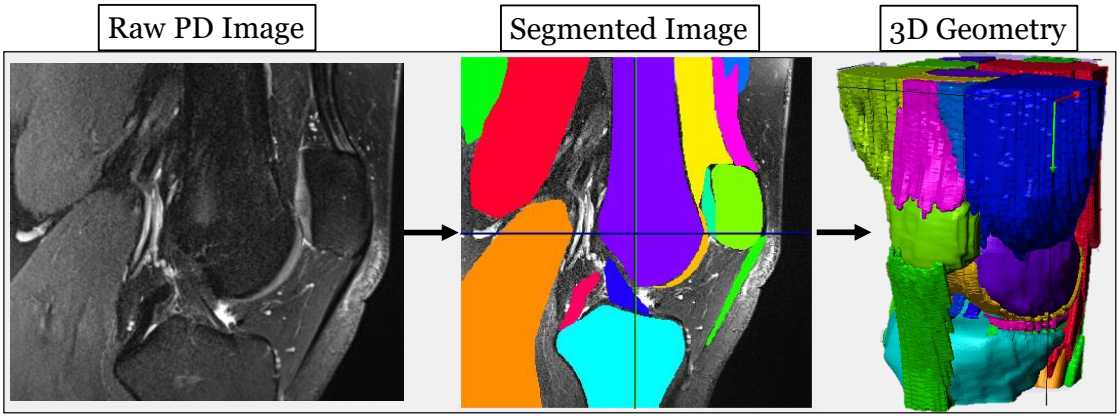

Figure 11 Segmentation workflow. Left: raw proton density image slice. Center: Example of a single segmented image, that includes segmented muscles, bones, cartilage, ligaments, and tendons. Right: Combined 2D segmentations to form a 3D geometry volume for each

Mesh Development

FE analysis requires the discretization of the complex geometries into small simple units called elements. This process is called mesh development and is a critical step during the development of a finite element model. The accuracy of the numerical results is highly related to the quality of the mesh. Elements can be described as 1D, 2D, or 3D and are composed of a collection of connected points called nodes. Within each element dimension there are a variety of different types of elements which are defined by the number of nodes and integration points. Choosing an element type for your model is an important step and is dependent on the research question. For our model a combination of 1D, 2D, and 3D elements were implemented, which helped reduce model complexity and minimized model run time. This model will be specifically used to analyze stress within the cartilage; therefore, the cartilage, the

menisci and the meniscal horns were modeled using 3D hexahedral elements, bones were modeled using 2D triangular shell elements, and ligaments were modeled as 1D linear elements (**Figure 1**2).

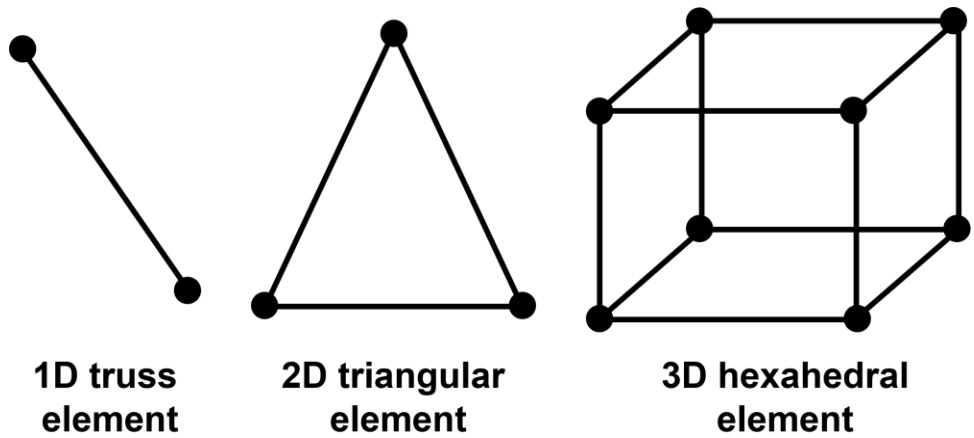

Figure 12 Visuals of the different element types used to develop meshes from segmented geometries. Black dots in each figure represent the element nodes.

Femoral cartilage, tibial cartilage, and the menisci were meshed using an open-source software developed by Rodriguez-Vila et al. 2017[153] that is specifically designed for the automated hexahedral meshing of knee cartilage structures and has been validated to produce high quality meshes. The decision to use hexahedral elements instead of tetrahedral elements was made because tetrahedral elements tend to overestimate stiffness during large deformations, while hexahedral elements are more suited for large deformations in nonlinear problems[153–155]. This approach allowed for reliable discretization of the soft tissues of our model while reducing the time needed to produce these meshes. The average element size was 1 mm for the femoral cartilage, 0.75 mm for the tibial cartilage, and 0.25 for the menisci. A

previous study performed a mesh sensitivity analysis on element size for knee cartilage and menisci and found that mesh sizes of 1 mm and below produce reliable stress results. When comparing the results of a model with an average mesh size of 1mm to the results from a reference model with average element sizes of 0.75 mm for the femoral mesh, 0.5 mm for tibial elements, and 0.5 mm for meniscal element, less than a 5% error between the two sets of results was found. These findings make us confident that our mesh density is adequate to produce accurate results[156]. The 3D meshes were then checked for poorly meshed elements and were cleaned manually by modifying the mesh in Hypermesh (HyperWorks, Altair Engineering, Inc, Troy, MI). Meniscal horns were manually meshed using the 3D mesh toolbox in Hypermesh. Meniscal horns can also be modeled as spring elements, but we found that a 3D representation allowed for more natural movements and helped with model convergence.

Bone geometries were imported into Hypermesh and meshed with triangular shell elements using the shrinkwrap tool. Mesh quality was tested and edited using the automated meshing tool. The bone cartilage interface and the meniscal horn insertion points were modified to match the bottom surface of the 3D mesh. This was done by creating a duplicate face of the bottom surface of the 3D mesh, renumbering the nodes and assigning them to the bone part. The original region of bone mesh was then removed, and the edges of the new region were manually connected. **Table 2** lists the number of elements for each part and the element type.

Table 2 Element types for each mesh and number of elements

Structure	Element Type	Number of Elements
Femur	Shell	8,141
Tibia		4,685
Fibula		922
Femoral cartilage	Hexahedral	22,143
Medial tibial cartilage		5,916
Lateral tibial cartilage		7,200
Medial meniscus		8,010
Lateral meniscus		7,200
Medial meniscal horns		4,779
Lateral meniscus meniscal horns		3,420
ACL	Truss	3
PCL		3
MCL		3
LCL		3

Ligaments were modeled using 1D elements. A review on different ligament modeling approaches found that a simplified ligament model produces similar results to more complex geometries[85]. Ligament insertion points were placed based off the segmented 3D MRI images for the ACL and PCL and were based on locations reported in literature for the MCL and LCL[157]. **Figure 13** shows the meshed components of the model. The meshed components were aligned in Hypermesh and exported as .inp files and imported as individual parts and assembled using Abaqus CAE and a python script.

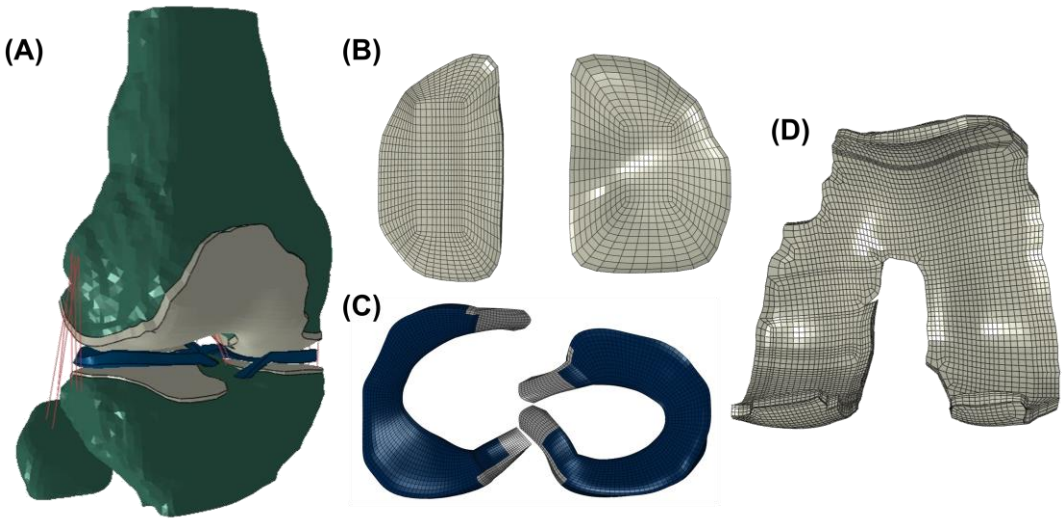

Figure 13 Meshed geometries and meshed parts. (A) Model assembly including bones, ligaments, cartilage, and menisci (B) Medial (left) and lateral (left) tibial cartilage (C) medial (left) and lateral (right) menisci (D) Femoral cartilage.

Material Constitutive Models

The proximal femur, distal tibia, and fibula were modeled as rigid bodies, helping reduce model runtimes while not having an impact on model results. The distal femur and proximal tibia material models were defined as isotropic elastic material models. Due to the large differences in stiffness between bone and the other tissues in the model, modeling the bones partially as rigid bodies is an acceptable assumption [158]. Articular cartilage was modeled as a single-phase isotropic elastic material model similar to other existing models[159,160]. This assumption is based around the elastic response of cartilage under short-term loading response and helps simplify the model. The orientation of collagen fibers within the menisci allow for the transfer of vertical compressive loads into hoop stresses[145,161]. For this reason, they are

modeled using a transversely isotropic material property. Ligaments were modeled using 1D elements with tensile stiffness and no compressive stiffness. The values used have been derived from literature and are similar to those used in other finite element models of the knee [67,136,159,162–165] (**Table 3**).

Table 3 Material properties applied to the finite element model.

Structure	Element Type	Material Description	Material Properties (MPa)
Femur	Shell	Rigid body and Linear elastic, isotropic	E = 12,000 ν = 0.38
Tibia Fibula			E = 6,900 ν = 0.49
Femoral cartilage Tibial cartilage	Hexahedral	Linear elastic, isotropic	E = 25 ν = 0.475
Meniscus Meniscal horns		Linear elastic, transversely isotropic	E1 =20, E2 = 120, E3 = 20 ν12 = 0.3, ν13 = 0.45, ν23 = 0.3
ACL	Truss	Neo Hookean Hyperelastic, isotropic	C10 = 1.95 D1 = 0.00683
PCL			C10 = 3.25 D1 = 0.0041
MCL			C10 = 1.44 D1 = 0.00126
LCL			C10 = 1.44 D1 = 0.00126

*Young's Modulus = E, Poisson's Ratio = ν, Strain energy potential equation coefficients = C10 and D1

While a base understanding of the material properties of the biological tissues found in the body exists, exact models still elude us. Adding to this complexity, material properties vary between subjects. In vitro studies can be used to implement these subject-specific material properties; however, this is not feasible for in vivo studies. Varying levels of complexity exist for cartilage models, with more complex

models allowing for depth and time dependent analysis of the tissue behavior. However, these more complex material models result in longer run times and convergence issues may occur [73,166]. For the current model we are interested in how changes in loading and kinematics change stress distribution over the gait cycle and at different time points after surgery. We will be comparing the same model to each other with different subject-specific motions and loads. For this reason, we have chosen a simplified linear elastic constitutive model for the cartilage. Future work could implement increasing levels of material model complexity, such as a fibril reinforced poroviscoelastic material model of cartilage[74,167,168], which might give further insight into the relationship between changes in kinematics and kinetics after ACLR and their impact on knee cartilage.

Contact Interactions

A default frictionless finite sliding surface-to-surface contact was assigned to all interaction pairs. This contact definition has been utilized in past FE models [139,169–171], and is based on cartilage's low friction coefficient of 0.002, resulting in negligible friction during gait [172]. Six discrete contact pairs were assigned as follows (main to secondary):

1. Lateral femoral cartilage to lateral tibial cartilage
2. Lateral femoral cartilage to lateral meniscus (proximal surface)
3. Lateral meniscus (distal surface) to lateral tibial cartilage
4. Medial femoral cartilage to medial tibial cartilage
5. Medial femoral cartilage to medial meniscus (proximal surface)
6. Medial meniscus (distal surface) to medial tibial cartilage

Model Assembly and Boundary Conditions

A reference point was placed at the center of the transepicondylar axis of the femur [173]. This reference point (RP-F) was defined as the center of the global axis with the x-axis aligned in the medial/lateral direction, the y-axis aligned in the anterior posterior direction, and the z-axis in the proximal/distal direction. The transepicondylar axis was found by using the apex of the medial and lateral femoral epicondyles [174], and has been shown to be a fixed axis that defines flexion and extension in the femur. Knee flexion rotations were applied about the y-axis at RP-F. Compartmental joint loads were obtained from a validated EMG driven musculoskeletal model and were applied as point loads within their respective compartment through reference points that were placed in the middle of the medial (RP-M) and lateral (RP-L) joint compartments along the transepicondylar axis[71] (**Figure 14).** The medial compartment and lateral compartment reference points were kinematically coupled to RP-F in all 6 degrees of freedom.

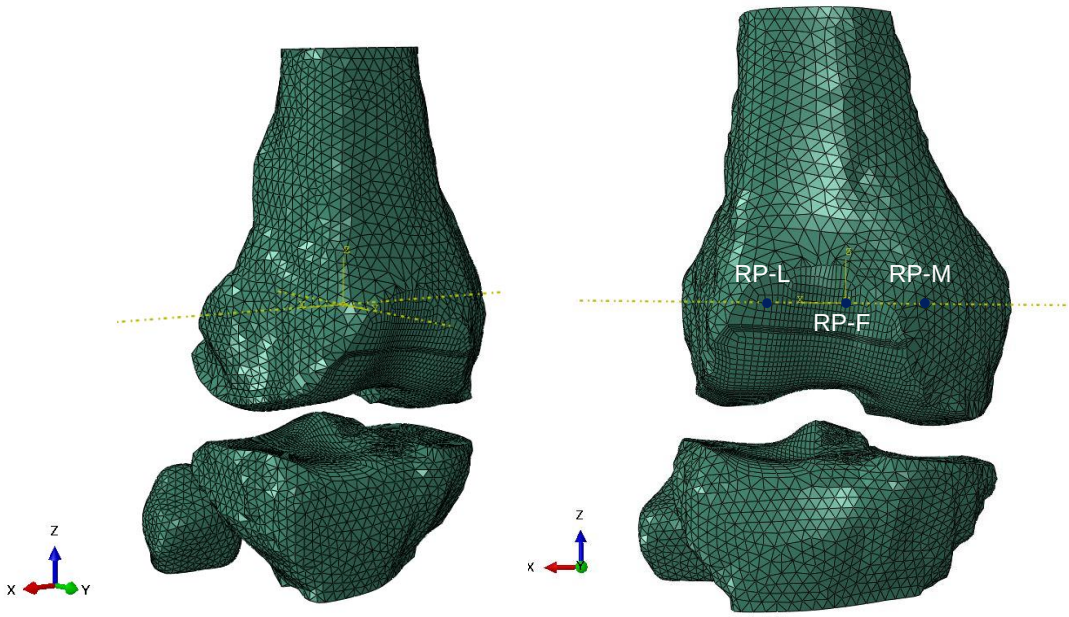

Figure 14 The local axis for the model was placed at the center of the transepicondylar axis. A reference point (RP-F) was placed at the center of the local axis. Compartmental reference points were place in the center of the lateral (RP-L) and medial (RP-M) compartments. RP-L and RP-M were tied to RP-F. Joint rotations were applied around the x-axis at RP-F and joint loads were applied to their respective compartmental reference point in the z direction.

Additional reference points were created for the tibia (RP-T) and fibula (RP-Fib) at the center of the global axis. The rigid body portions of the bones described earlier were tied to their respective reference points in all 6 degrees of freedom. All loads and rotations were applied to the femoral reference points, and boundary conditions were modified depending on the model step and will be described in detail later. The RP-T and RP-Fib were constrained in all 6 degrees of freedom. Cartilage

and meniscal horns were constrained at their bone cartilage interface through surface-to-surface tie constraints, with the bone surface acting as the main surface and the soft tissue defined as the secondary surface. Ligament insertion points were determined through the subjects' MRI scans and literature and were connected to their respective bones through pin type MPC (multi-point constraints).

Model input variables and simulation

The model runs in three distinct steps. All steps were defined as static general simulations and nonlinear geometries (nlgeom) were turned on due to the large rotations occurring during the simulation. The first two steps allowed for the model to stabilize by establishing contact between the femur and the tibia and applying the starting position and load. Both steps had a time duration of one second. Step three applied the subject's joint loads and knee flexion angle throughout stance. Gait variables were normalized to 100% of stance and the step had a hundred-second time duration (i.e. 1% of stance = 1 second time increment). Medial and lateral joint loads were applied as a continuous amplitude to their respective reference points as concentrated point loads in Newtons. Knee flexion angle was applied to RP-F as an angular velocity (rad/s) and varied by an amplitude of the difference in joint angle from the previous percent of stance (**Figure 3, left**). Joint loads and kinematics were acquired from the process described in the previous section. Simulation run time on an average CPU took an average of 8 ± 1.5 hours. The model output of interest for this study was Von Mises stress throughout gait (**Figure 15**). Von Mises stress gives a

measure of the combined magnitude of all components of stress at a given point and can be compared with material strength.

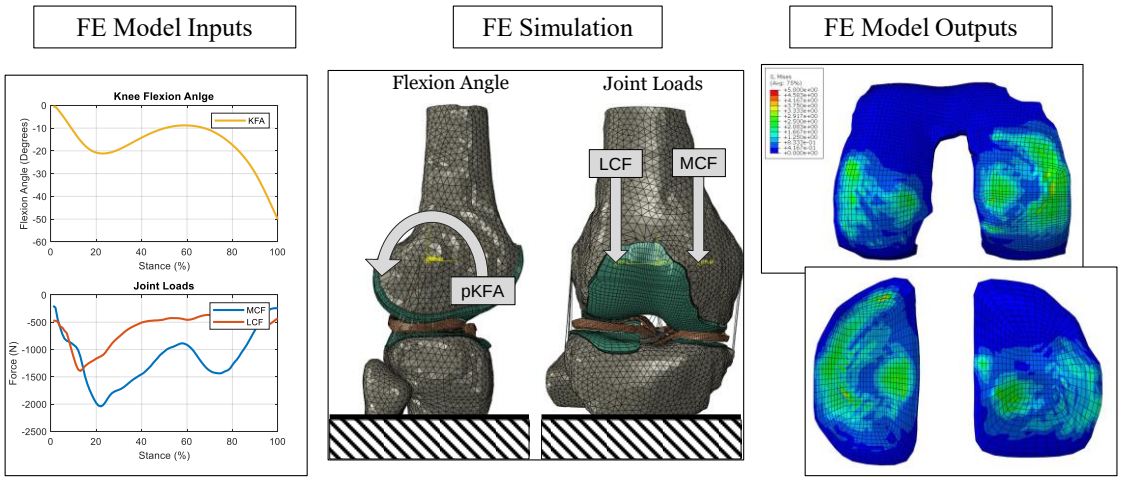

Figure 15 Workflow for simulating knee joint mechanics during walking using an FE model. FE model inputs include KFA (°), MCF (N), and LCF (N) throughout gait are applied to the model using amplitudes. Model outputs were von Mises stress maps of the femoral and tibial cartilage.

Mesh Scaling

A mesh scaling protocol was developed based on an atlas-based modeling approach established by Esrafilian et al. [168]. The use of this protocol reduced the amount of time needed for subject-specific model development and to maintain consistency between meshes. The meshed geometry developed in the previous section was used as a base template and scaled according to a ratio of morphological dimensions obtained from sagittal MRI scans of the subjects' knee. Measurements were taken in ITK-SNAP[175] from a sagittal and frontal view for both the template

subject and the test subject, the ratio of these values was then applied to the template model using MATLAB. The sagittal plane MRI images with the maximum anteroposterior lengths of the medial and lateral femoral condyles were identified (one slice for each compartment) and then used to perform the sagittal plane measurements. Measurements taken included the maximum anteroposterior lengths of the femoral condyle, the tibia, and the menisci. The joint space was also measured at the thickest spot where the tibia and femoral cartilages interacted. The frontal plane measurements included femoral and tibial bone and cartilage widths, tibiofemoral joint space, and meniscal thickness for the medial and lateral compartments. These measurements were performed on the image where the maximum femoral width occurred in the medial and lateral compartments (**Figure 16**). The sagittal plane measurements from the medial and lateral compartments were averaged to obtain one set of scaling factors.

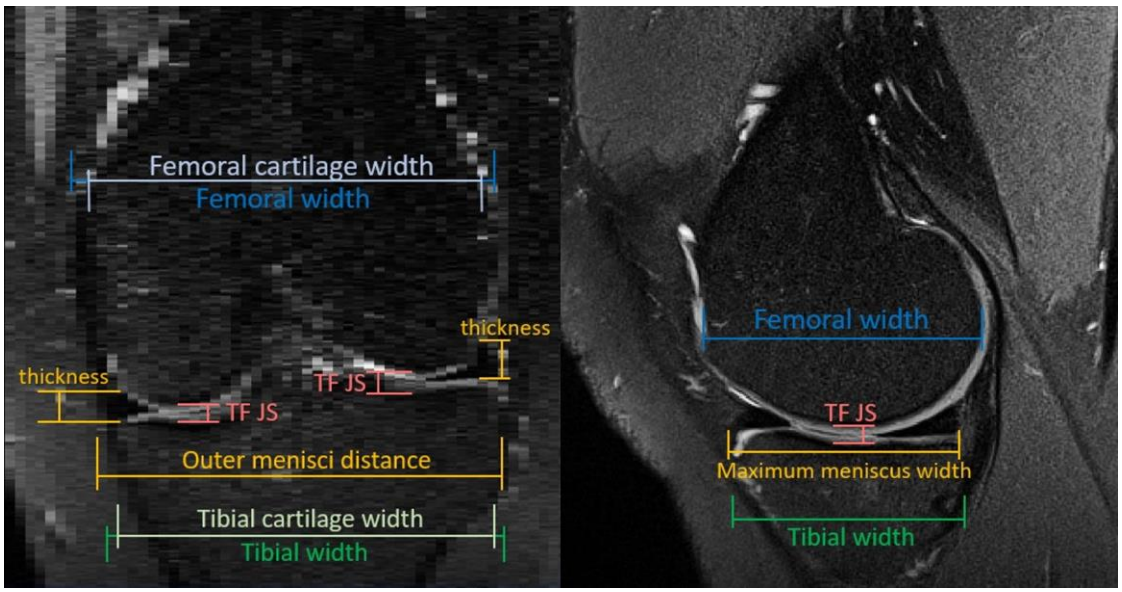

Figure 16 (A) Measurements from frontal plane: mediolateral (ML) femoral bone and cartilage width, medial (M) and lateral (L) tibiofemoral joint space, thickness of M and L menisci, and ML tibial bone and cartilage width. (B) Measurements from sagittal plane: anteroposterior (AP) width of M and L femoral condyles, AP width of M and L menisci, AP tibial bone width.

Within MATLAB the 2D meshes were scaled in the x- y- and z-direction as needed by modifying the nodal coordinates for each mesh. 3D nodal coordinates were first scaled in the x- and y-direction based on the corresponding scale factors (**Figure 17 A**). Cartilage and meniscal thickness were scaled by creating a vector map from the layers of the mesh and scaling each vector by the thickness scale (**Figure 17 B**).

The meshes are then translated relative to each other to assemble the model (**Figure 17 C**). After the scaling is complete, the scaled mesh is checked for any failed elements and fine-tuned in Hypermesh. These scaled meshes were then used as inputs along with subject-specific joint kinematics and kinetics into a python script for the development of the Abaqus input file. All other aspects of the Abaqus input files remained identical for all subjects. After scaling all meshes within the model, we found that the runtime of the MATLAB code averaged to 18.3 minutes (**Table 4**), which is significantly less than the time necessary to manually create these subject specific models. Using the scaling protocol we developed to create these models provides more personalized analysis and aids to study the mechanisms of OA development after ACLR.

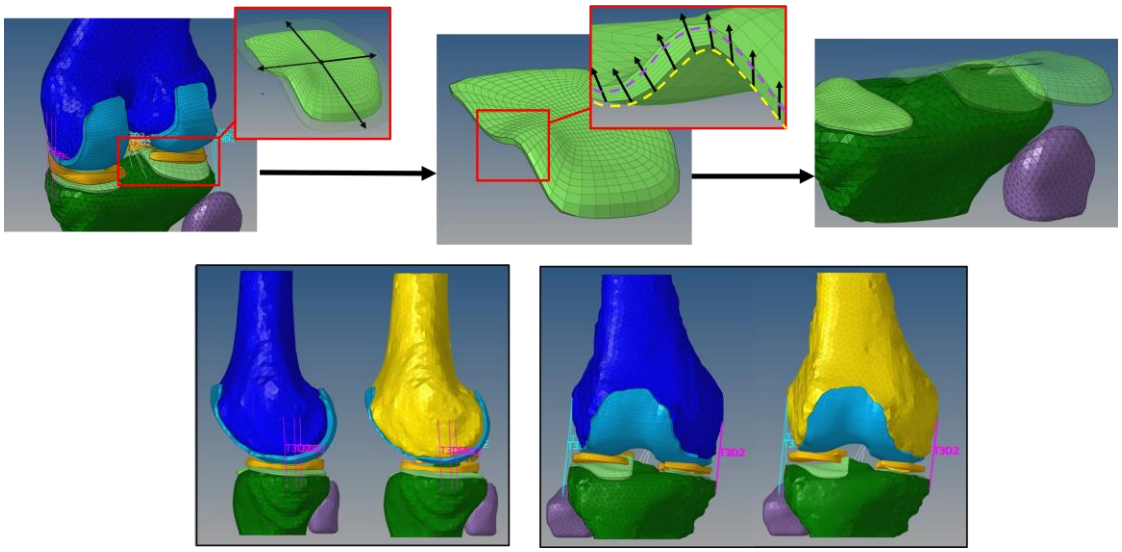

Figure 17 Top: example of scaling the lateral tibial cartilage mesh and translating it to align with the scaled tibia bone. Bottom: sagittal and frontal views of the original model (left) and a scaled model (right).

Table 4 Scaling run times by parts and total run times.

Model Components .inp File	Time Trials				Avg. Component Runtime
	Trial 1 (s)	Trial 2 (s)	Trial 3 (s)	Trial 4 (s)	
Tibial Cartilage	82.2	91.9	90.4	91.0	88.8
Menisci	450.8	452.3	458.3	434.5	449.0
Femoral Cartilage	562.2	507.6	548.1	502.0	530.0
Bone/Ligament	28.7	29.0	30.5	28.6	29.2
Total Time (s)	1123.9	1080.8	1127.3	1056.0	
Total Time (min)	18.7	18.0	18.8	17.6	
Avg. Total Time (min)	18.3				

Model Validation Analysis

Validation was performed by comparing our model results to the results of two previously validated and published models [156,159]. Model inputs mimicked those of

Mootanah[156] and Peña[159]. Both Mootanah and Peña model's applied total joint loads through a centralized reference point, however our model inputs require an input for both the medial and lateral compartments. For this reason, half of the total joint load was applied to the medial and lateral compartment reference points instead of applying the total load to a center reference point (**Table 5**).

Table 5 Model inputs for validation simulations

Reference Point	Initial Boundary Conditions	Compression (N)	Anterior/Posterior Loading (N)	Varus/Valgus Moment (Nm)
Mootanah 2014				
Femur Bone (Tibia held fixed)	Fixed at 20 degrees flexion; free to rotate about the y-axis and translate across z-axis	-374 z-axis	N/A	(+/-) 0-15 y-axis valgus/varus rotation
Peña 2006				
Femur Bone (Tibia held fixed)	Fixed at 0 degrees flexion; free to rotate about the y-axis and translate across z-axis	-1150 z-axis	+134 x-axis (1) anterior -134 x-axis (2) posterior (x-axis free)	+10 y-axis valgus rotation (3) *with anterior load* (4)

Validation Results

Mootanah et. al.[164] reported both experimental and FE model data as normalized pressure. Comparing normalized pressure using our model to both their model and experimental data we found RMSE values of 0.081 and 0.076 for medial and lateral tibial cartilage, respectively. Typically, a RMSE value of less than 0.5 is considered a good fit for the model, thus our results indicate that there is good agreement between our model and theirs. Similar RMSE values were observed when comparing our model to their experimental data (**Figure 18, Table 6**).

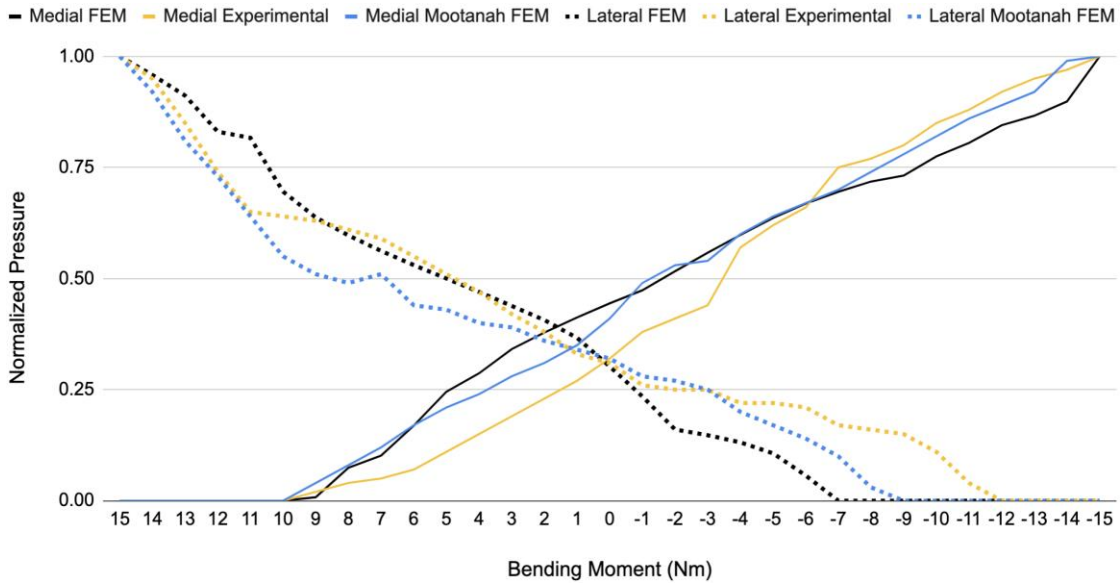

Figure 18 Medial and lateral tibial cartilage pressure over the valgus (0 to 15 Nm) and varus (0 to -15 Nm) y-axis rotation. Model validation comparing experimental data and FEM results from Mootanah et al. and our FE model.

Table 6 Statistical results for validation between our model (FE) and the experimental and FE model results from Mootanah et al.

		Absolute Peak Pressure (MPa)			Normalized Peak Pressure		
Location	Statistic	Moot. Exp. vs. ***FE***	Moot. FE vs. ***FE***	Moot. Exp. vs Moot. FE	Moot. Exp. vs. ***FE***	Moot. FE vs. ***FE***	Moot. Exp vs Moot. FE
Lateral Tibial Cartilage	RMSE	2.57	2.66	0.16	0.08	0.08	0.07
	FSE (%)	1.14	0.35	0.07	7.61	8.05	6.67
Medial Tibial Cartilage	RMSE	0.69	0.88	1.49	0.08	0.04	0.06
	FSE (%)	0.15	0.19	0.31	8.15	3.60	5.04

When validating against Pena, similar stress distributions for each of the 3 main loading conditions across the menisci, tibial cartilage, and femoral cartilage were found (**Figure 19**). Similar load distributions were seen between models, however larger stresses are present in the menisci of our model. Peak contact pressure across the medial tibial cartilage for our model was 2.01 MPa while Pena reported a peak contact pressure of 2.19 MPa, showing a low percent error of 8.2%.

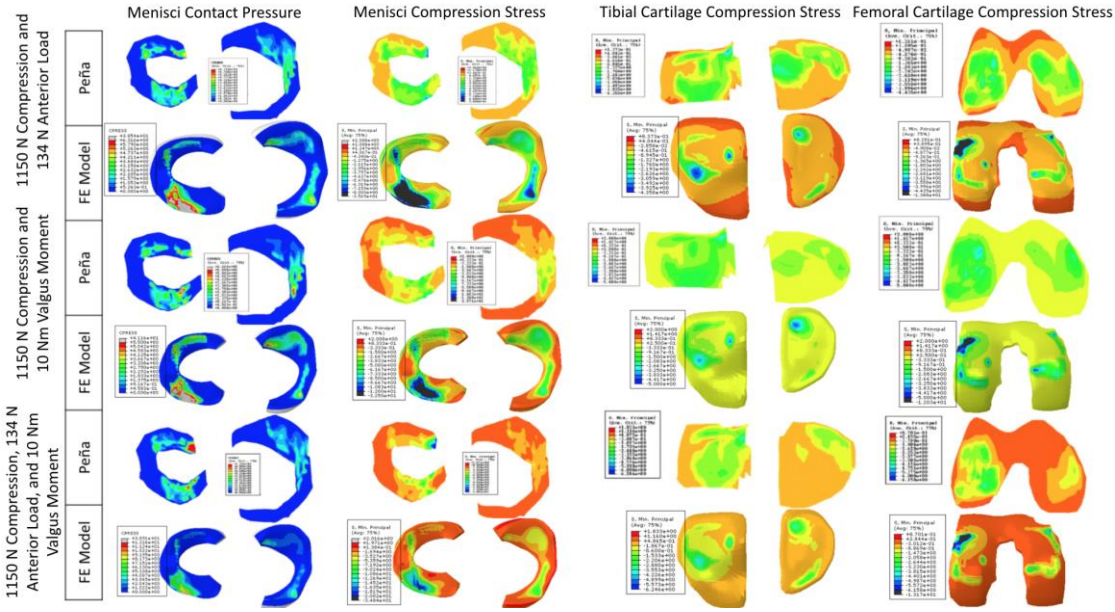

Figure 19 Peña contact pressure (top) compared to our FE Model (bottom) for each loading condition displayed on left.

Discussion

A protocol for the development and scaling of subject-specific FE models of the tibiofemoral compartment of the knee joint is presented in this chapter. These models were developed for the intended use of evaluating medial compartment cartilage stress after ACLR. We hope that reporting the stepwise process for model

development, and providing the codes needed to develop models and scale them, helps with model transparency and will allow for replication of the modeling process and results.

The current model was partially validated using previously reported experimental data and the results of previous validated FE models. Future work could be done to automate this pipeline which would make it more efficient in creating these models for different subjects. For our purposes we chose to simplify constitutive models and ligament geometries, future work could include more realistic constitutive models as well as 3D representations of the ligaments. Many existing models are unable to converge when applying physiologically reasonable loads, a unique aspect our model is its ability to converge while applying physiological loads throughout the stance phase. However, this model is still limited and starts to have trouble converging when the individual compartmental loads exceed 3000 N of force due to excessive distortion of the meniscal edge. Future work should investigate modifying this area of the mesh to prevent edge overlap. Overall, for the proposed use of this model we are confident that this model accurately represents the stresses within the tibiofemoral cartilage. The following chapters will use this model to report cartilage stress withing the tibiofemoral cartilage at three time points after ACLR.

Chapter 4

LONGITUDINAL CHANGES IN MEDIAL TIBIOFEMORAL CARTILAGE STRESSES AFTER ACLR AND THEIR ASSOCIATION TO CHANGES IN KNEE FLEXION ANGLE

Introduction

Altered gait mechanics after ACL reconstruction (ACLR) are thought to be a leading mechanism for the development of post traumatic osteoarthritis (OA). However, OA is a complex disease that develops over time due to the combination of factors such as changes in mechanics, structure, and biology. A theory developed by Chu and Andriacchi[176] predicts a framework of how these three components normally exist in a homeostatic range allowing for small changes (dynamic interplay) to occur within the joints natural environment and cartilage to remain healthy. However, concern arises when some or all these factors are pushed out of what Chu coined the "homeostasis envelope" shifting cartilage into a state referred to as a Pre-OA state making the tissue more susceptible to damage over time. Pre-OA occurs before irreversible damage is done to the cartilage and a better understanding of the interplay between these three categories could help with clinical approaches to shift the knee back into the Homeostasis envelope and out of the pre-OA state. A majority of ACL injuries occur in young active populations, suggesting that prior to injury their joint environment fell within a healthy range. While ACL injuries see some bruising of the cartilage and swelling, the cartilage structure is normally left intact. Assuming that

swelling is managed the main concern within this populations seems to be biomechanical alterations.

Commonly reported alterations include asymmetries between limbs in joint loading, knee flexion angle (KFA), and knee flexion moment (KFM). Asymmetries have been found to resolve by 2 years after ACLR however it is unclear how these alterations during this early time period impact the way cartilage is stressed. Underloading of the involved limb's medial tibiofemoral compartment of the knee (vs. uninvolved), as assessed by medial compartment force, is present 3 months after ACLR but is found to become more symmetric by 6 months[177]. Additionally, many individuals develop a stiff gait during this early time period resulting in less range of motion within the involved limb compared to the uninvolved[39,177]. Based on the Pre-OA theory these alterations in biomechanics maybe enough to move the location of contact that is repetitively stressed to new regions of cartilage that have not been adequately conditioned for this new loading environment. While alterations in gait mechanics are well documented, it is unknown how these changes impact load distribution and the stress environment at the tissue level within the joint. By combining the gait mechanics of subjects after ACLR and the use of finite element models of the knee to assess these changes in stress location and alterations between limbs and over time, we can provide a deeper insight into how the tissue level loading environment is changing after injury. This work has the potential to provide deeper insights into the mechanisms for longer term OA development, and to investigate Chu and Andriacchi's theory that changes in mechanics are in fact shifting the region of cartilage that is repetitively stressed.

In the previous chapter we established an approach using subject-specific motion analysis, a validated musculoskeletal model to estimate subject specific joint loads, and a finite element model of the knee joint that utilized subject specific loads to study cartilage stresses. The goals of this Aim were to (1) examine involve and uninvolved limb medial knee stresses at 3, 6, and 24 months after ACLR and (2) assess how altered gait mechanics are related to stress distribution. We hypothesize that the involved limb will experience lower stresses than the uninvolved limb, and that this asymmetry between limbs will decrease over time mostly due to the involved limb increasing to match the stresses in the uninvolved limb. We also hypothesize that stress location will be correlated with KFA in the femoral cartilage, with smaller knee flexion angles resulting in an anterior shift in stress.

Methods

Participants

Fifteen participants (**Table 7**) from a larger longitudinal cohort study were included in this study. All data were collected at the University of Delaware following approval from an Institutional Review Board. Participants were considered eligible if the following enrollment criteria were met: primary unilateral ACLR with no history of lower leg injury or surgery, no concomitant grade III ligament tears, no repairable meniscal injuries, no contraindications for MRI, and between 16-45 years old. Prior to participation all participants signed an informed consent. For individuals under the age of 18 both parental consent and minor assent were obtained. Eligibility criteria specific to this study included completion of motion analysis at 3, 6, and 24 months after ACLR and usable joint load data for both time points.

Table 7 Demographic Characteristics of Participants 3 Months after ACLR (n = 15)

Variable	Mean ± Standard Deviation or Number (%)
Age (years)	23 ± 6
Sex	7 Female (47%), 8 Male (53%)
Mass (kg)	73.2 ± 13.3
Height (m)	1.7 ± 0.1
BMI (kg/m^2)	24.5 ± 3.4
Graft Type	8 BPTB (53%), 5 Hamstring (33%), 2 Allograft (13%)
Meniscal Status	6 Meniscectomy (40%), 9 None (60%)
Walking Speed (m/s)	1.55 ± 0.18

Motion Analysis

Participants underwent gait analysis at 3, 6, and 24 months after ACLR. Walking trials were performed over a six-meter walkway at a self-selected speed (± 5%) that was set at the 3-month time point and replicated for the following sessions. Prior to data collection the participants skin was cleaned and prepped for the placement of EMG electrodes (MA-300 EMG System, Motion Lab Systems, Baton Rouge, LA) and retroreflective markers.

EMG electrodes were placed bilaterally on the muscle bellies of the rectus femoris, medial and lateral vasti, semimembranosus, long head of biceps femoris, and the medial and lateral gastrocnemii. Participants were then asked to performed maximum isometric contractions (MVICs) that would be used for the normalization of EMG signals obtained during overground walking. Retroreflective markers were then placed bilaterally on bony landmarks (1st and 5th metatarsals heads malleoli, femoral epicondyles, greater trochanters, and iliac crests) and rigid tracking shells were fixed

to the shanks, thighs, and pelvis. Motion data were then collected using an eight camera Vicon system (Oxford Metrics Limited) with a 120 Hz sampling rate, while ground reaction force data were collected using a single embedded force plate (600 x 900 mm^2, Bertec Corporation) with a 1080 Hz sampling rate.

EMG data were collected at 1080 Hz and subsequently high-pass filtered (30 Hz), rectified, and then low-pass filtered (6 Hz) using a second order Butterworth filter to create linear envelopes for the seven muscles. Linear envelopes were then transformed into muscle activations using a methodology previously described by Buchanan et al. 2006[101]. These muscle activations were used as inputs into a validated subject-specific neuromusculoskeletal model to calculate muscle forces. Medial and lateral joint compartment forces were then determined by balancing the internal and external frontal plane moments. Each participant's knee flexion angles and medial and lateral compartment loads throughout stance were then used as the inputs for the FE knee joint model.

Finite Element Analysis

A single finite element model of the healthy knee of a 19-year-old female, from the current study, was developed and used as the base model for all simulations. Model geometry including bones, cartilage, and the menisci were obtained from a sagittal proton density weighted sequence (Repetition time/echo time = 5100/30 ms, slice thickness = 2 mm with no gap, field of view = 14 cm, matrix = 800 x 800) MRI scans taken during their 6-month data collection. Geometries were then meshed using a combination of open-source software developed by Rodriguez-Vila et al 2017 [153] and meshing tools available in Hypermesh (HyperWorks, Altair Engineering, Inc, Troy,

MI). Cartilage and menisci were meshed using 3D hexahedral elements, bones were modeled as triangular shell elements, and ligaments were modeled using 1D truss elements. Model components were assembled in Abaqus CAE and boundary conditions were applied to allow for natural knee motion during normal walking. The development of this model and validation process is described in detail in Chapter 3.

Model inputs included medial (MCF) and lateral (LCF) compartment forces and knee flexion angles (KFA) throughout gait. Instead of scaling the geometry of the model to each individual, joint forces were normalized to the body weight (BW) of the model's primary subject allowing us to create a scale factor for the load of each individual. This allowed for direct comparison of mesh results and drastically reduced model development time and validation. Simulations were executed in three steps for each subject's involved and uninvolved limbs in Abaqus CAE (Dassault Systems Simulia Corp., Providence, USA). Step 1 initialized contact between all contact surfaces (1 second), Step 2 applied the initial conditions (1 second), and Step 3 simulated the gait cycle (100 seconds). KFA was applied to a reference point placed at the center of the transepicondylar axis, while compartment forces were applied quasi-statically to reference points placed at the center of the medial and lateral compartments along the transepicondylar axis. Cartilage stress was tracked throughout the entirety of the stance phase of walking gait (step three) for both the medial tibial and femoral cartilage (**Figure 20**). For this study we were interested in understanding stresses within the medial compartment for both the tibial and femoral cartilage, specifically during the percent of stance that peak medial compartment force occurred.

The weight bearing region of cartilage in the medial tibial and femoral cartilage were grouped into three regions: anterior, central, and posterior. These

regions were determined based off meniscal boundaries when the knee model was in full extension. The average stress for each region was identified by averaging the Von-Mises stress of each element within that region at pMCF.

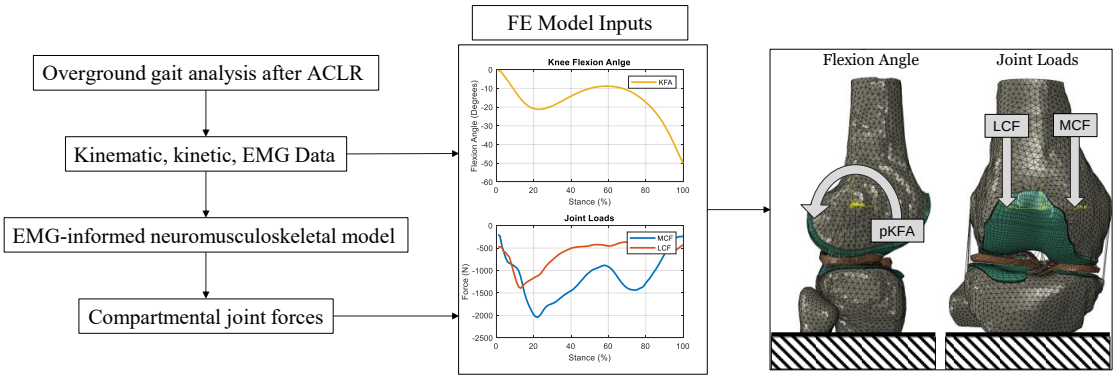

Figure 20 Flow chart depicting steps involved in obtaining model inputs for the FE model and how model inputs are applied to simulations gait.

Statistical Analyses

Statistical analyses were performed in MATLAB (MathWorks, Natick, MA, USA). A 2x3 (limb x time) repeated measures ANOVA was performed with statistical significance defined as $\alpha < 0.05$. Post-hoc 2-tailed paired t-tests were performed to compare stresses between limbs (involved vs. uninvolved) at individual time points and post-hoc 1x3 (limb x time) repeated measures ANOVAs were performed to analyze how stress within each limb changed with time. To account for multiple comparisons, Bonferroni corrections were used for all post-hoc tests. To assess the association between KFA at pMCF and average region stress at all three-time points Pearson correlations and simple linear regressions were used. Correlations were described using R^2 values of the following ranges: small ($R^2 > 0.02$), medium ($R^2 >$

0.13), or large ($R^2 > 0.26$)[178]. Similar statistical tests were run to assess the model inputs as well.

Results

Model Inputs: Gait Mechanics

At 3 and 6 months the involved limb had lower pMCFs compared to the uninvolved limb; these differences, however, were not significant. KFA at pMCF showed a main effect of time, while post-hoc t-tests found significantly lower KFAs in the involved limb at 3 and 6 months after ACLR. By 24 months these asymmetries are no longer present (**Figure 21)**.

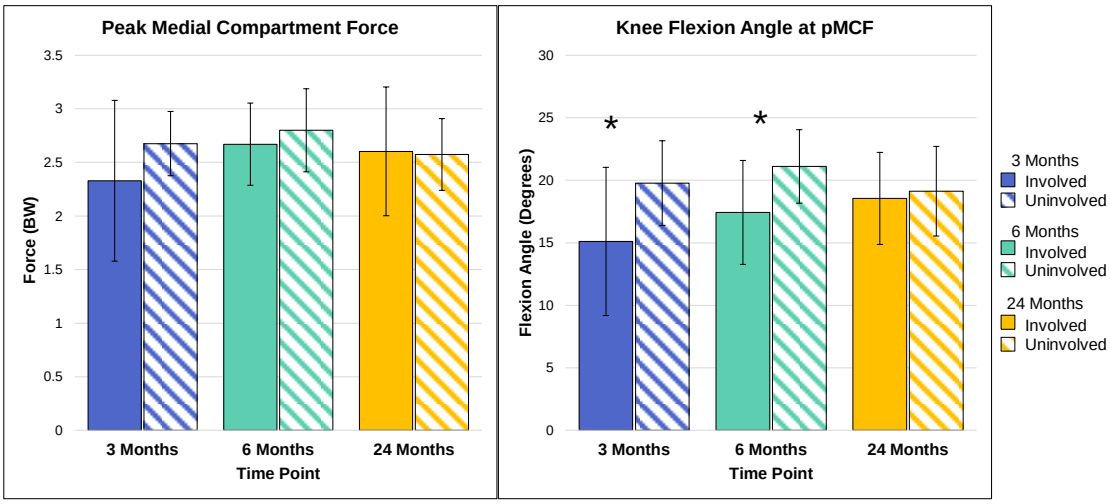

Figure 21 Mean involved (solid) and uninvolved (striped) model input data at 3 (Blue), 6 (green), and 24 months (yellow). (* = significantly different $p<0.05$)

Tibial Cartilage Stress

A limb-by-time interaction was present in the anterior region ($p = 0.046$) and central region ($p = 0.022$) of the tibial cartilage. No limb x time interaction was found in the posterior region (**Table 8**). The highest average stresses were present in the anterior region of cartilage regardless of time point. During the 3-month time point the involved limb experienced lower average stress in all three regions of cartilage with

significant differences in the central region ($p = 0.002$). The stress within the involved limb increased in all three regions by 6 months and surpassed the uninvolved limb in both the anterior and posterior regions, with the involved limb experiencing significantly higher stress in the posterior region ($p = 0.016$) during this time point. At 24 months the involved limb and the uninvolved limb are no longer significantly different in any region of interest (**Figure 22)**. The involved limb showed differences over time in the central region of cartilage ($p = 0.015$), while no significant differences were seen over time when evaluating the uninvolved limb.

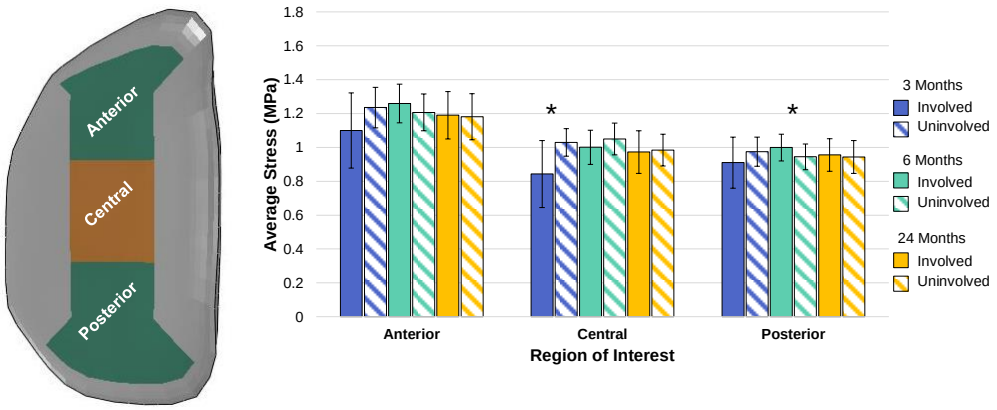

Figure 22 Medial tibial cartilage regions of interest for mean stress values. Mean stresses for the involved (solid) and uninvolved (striped) taken at pMCF in the anterior, central, and posterior regions of the medial tibial cartilage. Data is shown for the 3 (Blue), 6 (green), and 24 months (yellow). (* = significantly different p<0.016)

Table 8 Medial tibial stress at pMCF by region at 3, 6, and 24 months after ACLR statistical analysis. Significant results are bolded.

	3Months		Post-Hoc T-test	6 Months		Post-Hoc T-test	24 Months		Post-Hoc T-test	ANOVA interaction P-Value
Region	IN	UN	P-Value	IN	UN	P-Value	IN	UN	P-Value	Limb x Time
Anterior	1.10	1.26	0.036	1.26	1.21	0.068	1.19	1.18	0.838	**0.046**
Central	0.84	1.00	**0.002**	1.00	1.05	0.059	0.97	0.98	0.735	**0.022**
Posterior	0.91	1.00	0.126	1.00	0.95	**0.016**	0.96	0.94	0.674	0.085

Femoral Cartilage Stress

There were significant limb x time interactions in the central (p = 0.043) and posterior (p = 0.041) regions of the femoral cartilage. The highest stresses were

present in the central region of cartilage regardless of time point (**Table 9)**. At three months the involved limb displayed significantly lower average stress in the central (p = 0.005) and posterior (p = 0.001) regions of cartilage. At the 6-month time point the differences in the central and posterior regions are no longer statistically different due to an increase in the involved limbs stress. Within the anterior region of cartilage, we see a significant difference between limbs at 6 months (p = 0.001) that is driven by an increase in the involved limbs stress while the uninvolved limbs stress decreases. By 24 months there are no significant differences between limbs in any region of interest suggesting a return to a more symmetric gait pattern. When looking at the involved limb over time the central (p = 0.029) and posterior (p = 0.029) regions approached significant differences in stress. No differences due to time occurred in the anterior region of the involved limb or any of the regions of the uninvolved limb (**Figure 23)**.

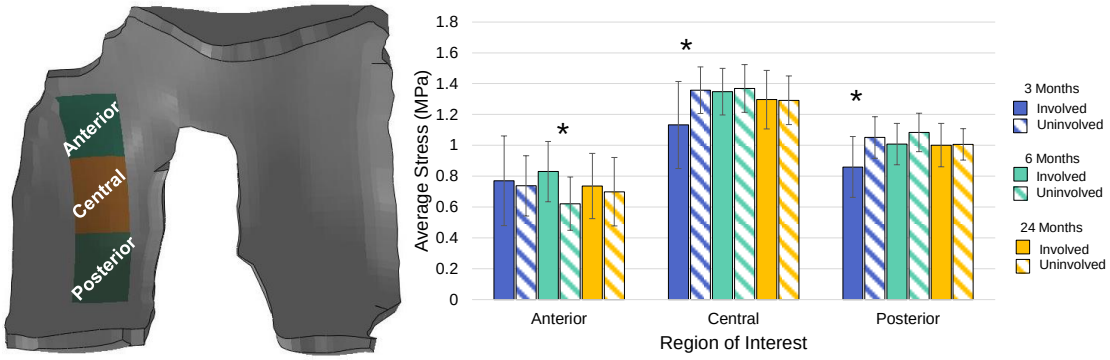

Figure 23 Medial Femoral cartilage regions of interest for mean stress values. Mean stresses for the involved (solid) and uninvolved (striped) taken at pMCF in the anterior, central, and posterior regions of the medial tibial cartilage. Data is shown for the 3 (Blue), 6 (green), and 24 months (yellow). (* = significantly different p<0.016)

Table 9 Medial femoral cartilage stress at pMCF by region at 3, 6, and 24 months after ACLR statistical analysis. Significant results are bolded.

	3Months		Post-Hoc T-test	6 Months		Post-Hoc T-test	24 Months		Post-Hoc T-test	ANOVA interaction P-Value
Region	IN	UN	P-Value	IN	UN	P-Value	IN	UN	P-Value	Limb x Time
Anterior	0.77	0.73	0.707	0.83	0.62	**0.001**	0.74	0.70	0.428	0.245
Central	1.13	1.35	**0.005**	1.35	1.37	0.521	1.30	1.29	0.943	**0.043**
Posterior	0.86	1.01	**0.001**	1.01	1.08	0.039	1.00	1.01	0.905	**0.041**

Knee Flexion Angle vs. Tibial Cartilage Stress

Stresses within the central region of the involved limb showed a positive correlation with KFA at all three time points with large correlations at 6 and 24 months and a medium correlation at 3 months. The anterior and posterior regions in the involved limb did not show strong correlations between stress and KFA. The uninvolved limb showed strong correlations between stress and KFA in all three regions, however these occurred at different time points. At 3 months significant negative correlations existed in the anterior and posterior regions of cartilage. This correlation was not seen in the anterior or posterior region during the 6-month time point, but was present again in the posterior region by 24 months. The central region showed a positive correlation at 6 months, but not at 3 or 24 months (**Figure 24, Table 10**).

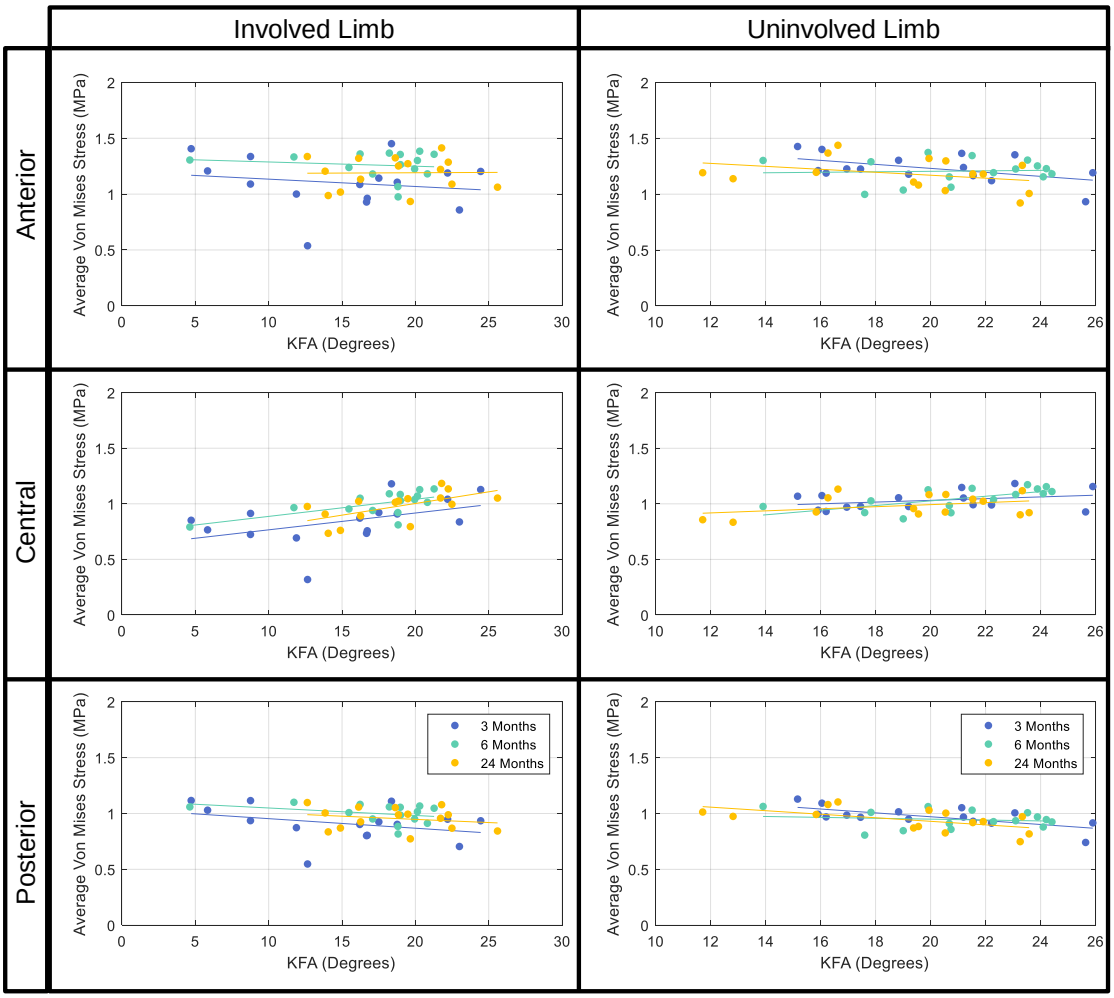

Figure 24 Association between KFA and average Von Mises Stress in the anterior, central, and posterior regions of the medial tibial cartilage at the 3 (Blue), 6 (green), and 24 months (yellow) for the involved and uninvolved limbs.

Table 10 Involved and uninvolved limbs association between KFA and average regional stress for all three time points. Significant associations are bolded.

		Involved Limb			Uninvolved Limb		
Region	Time Point	r	Effect Size (R^2)	p Value	r	Effect Size (R^2)	p Value
Anterior	3 Months	-0.175	0.031	0.531	**-0.506**	**0.256**	**0.055**
	6 Months	-0.138	0.019	0.623	-0.063	0.004	0.835
	24 Months	-0.014	0.000	0.958	-0.349	0.122	0.202
Central	3 Months	0.454	0.206	0.090	0.107	0.107	0.235
	6 Months	**0.637**	**0.406**	**0.011**	**0.428**	**0.428**	**0.008**
	24 Months	**0.611**	**0.373**	**0.016**	0.127	0.127	0.193
Posterior	3 Months	-0.337	0.114	0.219	**-0.683**	**0.467**	**0.005**
	6 Months	-0.352	0.124	0.198	-0.155	0.024	0.583
	24 Months	-0.219	0.048	0.433	**-0.586**	**0.343**	**0.022**

Femoral Cartilage Stress vs. Knee Flexion Angle

The anterior region of cartilage experienced strong negative correlations at all three time points for both the involved and uninvolved limbs, while the posterior region showed strong negative correlations at all three time points for the involved limb and at 6 months in the uninvolved limb. No large correlations were seen in the central region of cartilage. (**Figure 25, Table 11**)

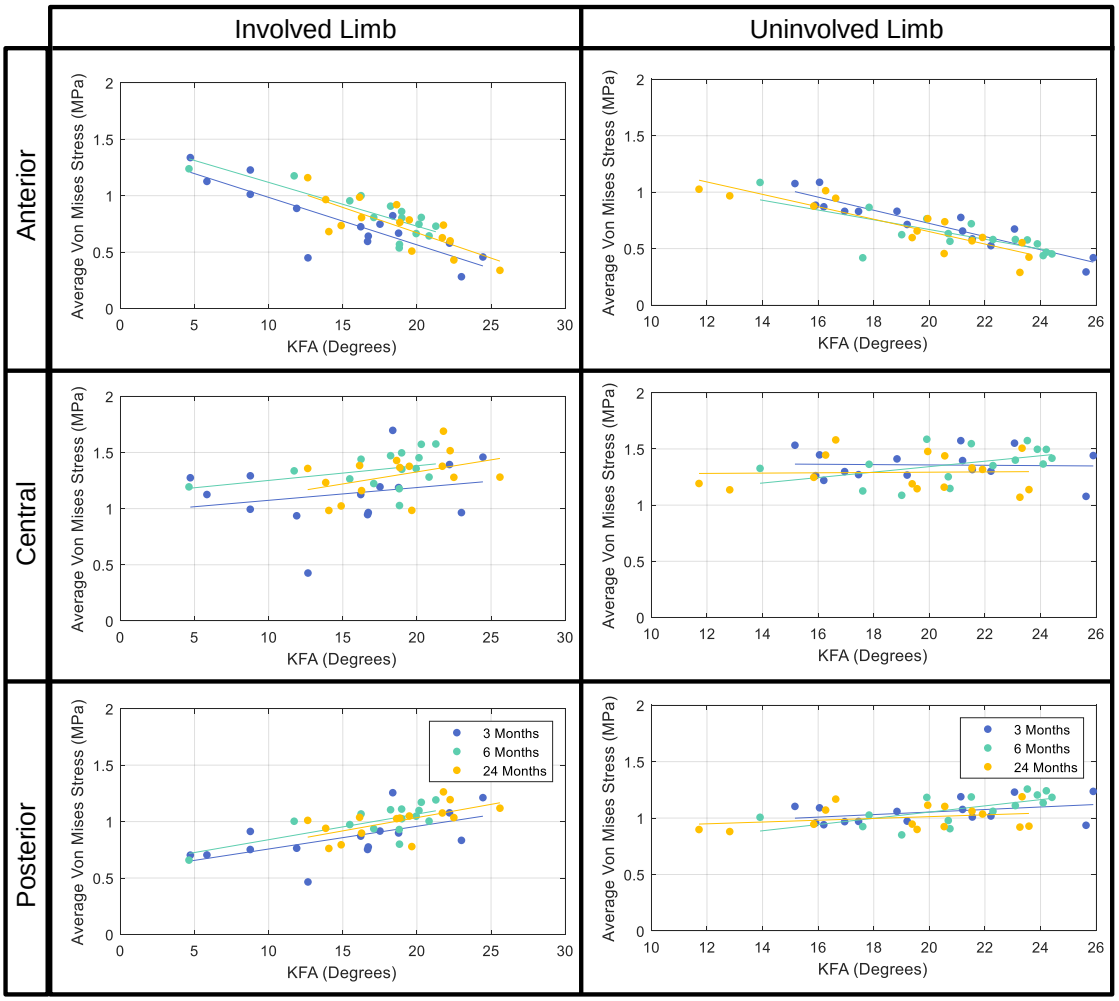

Figure 25 Association between KFA and average Von Mises Stress in the anterior, central, and posterior regions of the medial femoral cartilage at the 3 (Blue), 6 (green), and 24 months (yellow) for the involved and uninvolved limbs.

Table 11 Involved and uninvolved limbs association between KFA and average regional stress for all three time points. Significant associations are bolded.

		Involved Limb			Uninvolved Limb		
Region	Time Point	r	Effect Size (R^2)	p Value	r	Effect Size (R^2)	p Value
Anterior	3 Months	**-0.857**	**0.734**	**<0.001**	**-0.927**	**0.86**	**<0.001**
	6 Months	**-0.826**	**0.683**	**<0.001**	**-0.735**	**0.54**	**0.002**
	24 Months	**-0.780**	**0.609**	**0.001**	**-0.889**	**0.79**	**<0.001**
Central	3 Months	0.239	0.057	0.390	0.039	0.0015	0.890
	6 Months	0.359	0.129	0.188	0.461	0.2122	0.084
	24 Months	0.415	0.172	0.124	0.032	0.001	0.913
Posterior	3 Months	**0.606**	**0.368**	**0.017**	0.385	0.148	0.156
	6 Months	**0.702**	**0.493**	**0.004**	**0.647**	**0.418**	**0.009**
	24 Months	**0.617**	**0.380**	**0.014**	0.281	0.079	0.312

Discussion

This study is one of the first to assess cartilage stress over time after ACLR and to determine if alterations in KFA are associated with changes in stress location within the medial tibiofemoral cartilage. We hypothesized that (1) lower stresses would be present in the involved limb (vs. uninvolved) with differences most pronounced early after surgery and resolving over time and (2) joint mechanics, specifically KFA, would be related to location of stress. Both of our hypotheses were partially supported by our findings. When assessing the medial tibial cartilage, we found that stresses in the central region may be the most susceptible to changes in biomechanics, while all three regions of the femoral cartilage seem to be highly influenced by these variables.

While certain areas of cartilage may see overall higher stress, we were interested in the differences in stress patterns between limbs and over time since multiple studies of healthy individuals have observed a relationship between the

mechanical environment and the cartilage structure[119,179–182]. For instance, it was found that cartilage subjected to higher stresses was significantly stiffer than cartilage in lower stress environments, and that these differences in stiffness occur in different locations within the same joint [179,180]. These findings indicate that cartilage may be mechanically conditioned to a specific stress environment, and it is unknown how changes in these environments impact the cartilage over time. Our findings show that stress patterns within the medial tibiofemoral cartilage not only differ between limbs but also over time in the involved limb. At 3 months the involved limb experienced lower stresses compared to the uninvolved limb in all three regions of the tibial and in the central and posterior regions of the femoral cartilage. At 6 months we see an increase in these stresses compared to three months and in certain regions the involved limb's stresses surpassed those of the uninvolved. It remains unknown if these alterations in stress magnitude impact cartilage composition. It is known that individuals who underload their medial compartment 6 months after ACLR are more likely to develop OA by 5 years post-surgery than those who do not underload[42]. While significant underloading was not seen in this cohort at any time point, significantly lower stresses were present in the central region of the tibial cartilage at 3 months and in the central and posterior regions of the femoral cartilage at 3 months. It is unknown how these altered stress patterns during the early time points after ACLR are playing a role in cartilage remodeling. Future work should be done to assess which subjects develop OA from this cohort to help with answering this question.

Symmetric stress patterns between limbs were present at 24 months after surgery. This aligns well with our previous investigations in medial compartment loading which found that participants generally display symmetric loading patterns at

this time point[35,42]. It is not clear if the time it takes to regain symmetry and the way symmetry is achieved is playing a role in the eventual deconditioning of cartilage. Studies describing healthy tibiofemoral contact relative to flexion angle found that as knee flexion moves from 0° to 30° the centroid moves posteriorly on the tibia [183–185], and becomes even more pronounced in the ACL deficient knee[186.] This was depicted in our results as the central region of cartilage was the only region in the tibia cartilage to see a correlation with knee flexion angle. While the point of contact moves posteriorly on the medial tibial cartilage, the medial femoral condyle experiences minimal posterior translation[183]. The anterior and posterior regions of the femoral cartilage showed stress was highly correlated with KFA. A negative association was present in the anterior region of cartilage showing that individuals with less knee flexion saw higher stresses than those with larger knee flexion angles. The opposite association was present in the posterior region of cartilage. These associations can be explained through the shape of the curved shape of the femoral condyle and its interaction with the menisci. Increases in knee flexion angle increases the anterior region of cartilage may no longer interact with the meniscus and the load is applied to the more posterior regions of cartilage[130,187,188]. The subjects in this cohort displayed stiff gait patterns in their involved limbs at both 3 and 6 months after surgery but had relatively symmetric knee flexion by 24 months. This could suggest that these individuals experience a shift in stress back to regions that were experiencing higher stresses before injury. If the framework set out by Chu and Andriacchi [24,176] is accurate, these findings may indicate that the spatial shifts seen in contact location and load bearing regions after ACLR may be shifting anteriorly and relatively over stressing this new region of cartilage. This combined with other factors such as

swelling and trauma due to the initial injury could place these regions in the initiation phase of this framework eventually leading to OA.

When interpreting the results of this study it is important to be aware of several limitations. The current model was validated against previously published models and experimental data, however since we were working with a clinical population it was not possible to test patient-specific parameters. A major limitation is that subject specific geometry or scaling of geometry was not used in this study. Segmentations of MRIs have been shown to vary widely between individuals and even within a single segmentor[189]. This combined with smoothing that must be done to geometries and small modifications to geometry to develop quality meshes could modify results between subjects due to modeling error[73,86]. The process of developing a model is also one that takes even a skilled modeler multiple weeks to complete. For this reason, we chose to scale the model inputs (joint loads) to those of the original models subject.

While none of the subjects had meniscal repairs a subset had meniscectomies, this was not taken into account by our model's geometry and is a limitation to the current study. Another limitation is the simplified constitutive models used. Modeling cartilage as a single-phase isotropic elastic material limits the ways this specific model can be applied to other questions. This assumption, however, is based around the elastic response of cartilage under short term loading responses, since we were assessing a single time point throughout stance and were not interested in fluid pressure or how stresses change over time when in compression, for the purposes of this study we found this an acceptable assumption, however future work could implement a more complex and accurate material model. The addition of a visco-

elastic material property would allow us to gain insight into how the cartilage reacts to rate dependent and cyclic loading conditions.

Only fifteen subjects were evaluated in this study, future work should look at increasing the sample size, as well as assess if regions of lower stress after ACLR are associated with long-term cartilage degeneration. Future work should look to assess if the structural and biological variations are also occurring in regions of cartilage that are seeing altered stresses. The next chapter will do this by assessing cartilage stress by region to quantitative MRI values.

In conclusion using a combination of gait analysis, EMG driven musculoskeletal modeling, and finite element modeling we are one of the first to report stress patterns in the tibiofemoral joint after ACLR. We found lower stresses in the involved limb (vs. uninvolved) early after surgery, and that the involved limb changes over time and that alterations in biomechanics may play a role in these altered stress patterns. This work helps support Chu and Andriachi's framework of pre-OA verifying that changes in gait mechanics are in fact causing shifts in stress patterns early after ACLR.

Chapter 5

MEDIAL TIBIOFEMORAL CARTILAGE STRESSES 3 AND 6 MONTHS AFTER ACLR AND THEIR ASSOCIATION WITH QUANTITATIVE MRI

Introduction

Anterior cruciate ligament (ACL) injuries are one of the most common joint injuries in young active populations, with over 200,000 injuries occurring in the United States each year[190]. After injury and subsequent reconstruction (ACLR), individuals are at an elevated risk of developing post-traumatic osteoarthritis (OA) far earlier than their uninjured peers [6,53,191,192]. A better understanding of the relationship between ACLR and the early development of OA may be essential to helping slow or prevent disease onset. Identifying individuals who are at high risk of OA development could help illuminate the mechanisms of OA development and help with the develop rehabilitation strategies to delay the onset of this debilitating disease.

OA is often identified using radiographs, which can only detect morphological changes to the tissue that occur during the later stages of the disease. Recently, however, researchers have started investigating new techniques that could identify early signs of OA prior to late-stage morphological alterations. One approach to early detection is through a technique called quantitative magnetic resonance imaging (qMRI), which can identify early signs of OA such as the loss of proteoglycans and the breakdown of the collagen matrix [17]. This approach can be used to assess small biological changes in cartilage composition long before morphological damage occurs. This provides a means for earlier identification of individuals who are at risk of OA

and a better understanding of how the disease progresses. Transverse relaxation time (T_2) is one such qMRI tool that indirectly measures the health of the collagen matrix, where a prolonged (higher) T_2 value is indicative of collagen matrix degeneration [193].

Changes in gait mechanics early after ACLR is one mechanism that is thought to play a role in the development of OA[42,53,54]. Alterations to the involved limb's joint loads, knee flexion angles, knee flexion moments, and knee abduction moments (compared to healthy controls and the uninjured limb) are commonly reported after ACLR[35,47,54,150,177]. Through the addition of qMRI, some have found associations linking these changes in biomechanics to a break down on the collogen matrix within the joint cartilage[30,31,42,122]. We found a connection between altered gait mechanics and alterations in the stress distribution within the knee (Aim 3); however, it is unknown if these changes in the stress environment impact cartilage at a biochemical level.

Cartilage is known to be a mechanosensitive tissue that adapts to withstand the stress environment of our normal, pre-injury, mechanics. However, it is relatively unknown how changes in stress environment after injury impact the biochemical composition of cartilage and how fast these changes in cartilage composition occur. The initial injury and subsequent surgery may also put the cartilage in a sensitive state through a combination of bruising to the tissue and increased inflamation. The combination of these factors plus changes in gait mechanics and loading may make cartilage less adaptable, meaning that changes in stress environment, whether it be relatively higher or lower stresses, may push the tissue environment further past homeostasis making even slight changes in stress detrimental. One commonly accepted theory, proposed by Chu and Andriachi[176], views knee cartilage through the lens of three systems: biological, mechanical, and structural all of which are in balance

in the healthy knee. In their theory, they explain that “Pre-OA” is when the cartilage is placed in a high-risk state due to one or more of these systems being knocked out of their typical operating range. In this case, when one system skews from homeostasis, the knee is now at risk for further OA development if nothing is done (hence the term Pre-OA) as disruption to one system is thought to lead to changes in other systems that can build upon each other to accelerate the progression towards disease development. For traumatic injuries like ACLR, it is thought that alterations in biomechanics are playing a major role to push cartilage into the Pre-OA state. This raises the question of how changes in biomechanics impact the way cartilage is stressed, and how these changes are impacting the biochemical composition of the cartilage over time.

To our knowledge, no study has evaluated whether or not there is any association between cartilage stress, as assessed via an FE model, and the biochemical composition of the tissue, as assessed via qMRI. Thus, the goal of this aim is to assess if alterations in cartilage stress after ACLR are associated with changes to cartilage’s biochemical composition. We hypothesize that regions of cartilage with asymmetries in stresses at peak medial compartment force (pMCF) will also asymmetries in T_2 relaxation times. Our second hypothesis is that regions of cartilage within the involved limb that experience larger changes in stress between 3 months and 6 months will experience larger changes in T_2 from 3 to 6 months and higher T_2 values at 24 months.

Methods

Participants

The participant information for this chapter is identical to those found in chapter 4 (**Table 7**).

Quantitative Magnetic Resonance Imaging (qMRI)

Each subject underwent supine bilateral knee MRIs (15 channel knee coil, 3 Tesla, Siemens) using a sagittal 2-dimentional T_2 mapping sequence (TR = 3090 ms, TE = 10, 20, 30, 40, 50, 60, 70 ms, slice thickness = 3 mm, FOV = 150 mm). Images were analyzed in 3D Slicer (https://www.slicer.org/)[147] using a mono-exponential fit to a two-parameter model to calculate T_2 maps. To reduce stimulated echo artifacts the first echo in each sequence was skipped. For each subject, images from the involved limb were registered to those of the uninvolved limb. Segmentations were performed on 3 slices that corresponded to the center of the medial tibiofemoral compartment, which is referred to in literature as the load bearing region[193]. For each image, both femoral and tibial cartilage were segmented into anterior, central, and posterior regions of interest (ROI) based on meniscal boundaries. All voxels with a T_2 relaxation time greater than 100 ms were removed to reduce artifacts caused by synovial fluid [194], the remaining T_2 relaxation time for each voxel in a region were then averaged. The T_2 relaxation time were then averaged across all 3 slices to find the average T_2 relaxation for each ROI in the medial compartment.

Finite Element Analysis

Stress maps of the medial tibiofemoral compartment were calculated using a finite element model of the knee joint using the protocol reported in Aims 2 and 3. Model geometry was based off a single subject's MRI scans and simulations were run in Abaqus CAE. Model inputs included knee flexion angle (KFA) and medial (MCF) and lateral compartment forces (LCF) throughout the stance phase of gait and were acquired from a larger cohort study through motion analysis data and a validated EMG musculoskeletal model[177]. All simulations were run in Abaqus Standard CAE where loads were applied quasi-statically through reference points placed at the center of the medial and lateral compartment on the transepicondylar axis in the z direction. KFA was applied to a reference point at the center of the transepicondylar axis about the x-axis. Three ROIs for the tibial and femoral cartilage, matching those from our quantitative MRI images, were identified based on meniscal boundaries when the knee was in full extension and unloaded (**Figure 26)**. Average Von Mises stress values were calculated for each region of interest at the percent of stance that peak MCF was applied.

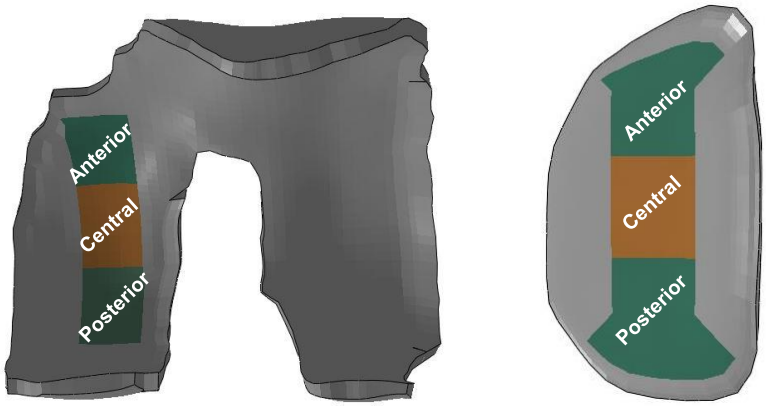

Figure 26 Medial femoral and tibial cartilage regions of interest for FE model results.

The mean stress data and mean T_2 relaxation times at 3, 6, and 24 months for the involved and uninvolved limbs were assessed. Changes in cartilage stress over time were then compared to changes in biochemical composition over time from 3 to 6 months (6 months -3 months) and to 24-month data (**Figure 27)**.

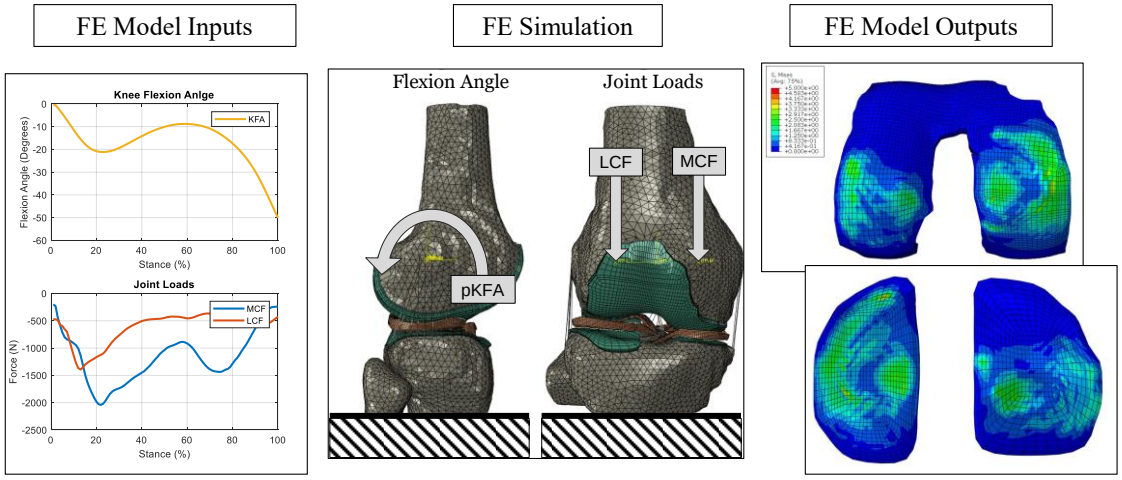

Figure 27 Workflow for simulating gait during walking using an FE model. FE model inputs include KFA (°), MCF (N), and LCF (N) throughout gait are applied to the model. Model outputs were von Mises stress maps of the femoral and tibial cartilage.

Statistical Analyses

Statistical analyses were performed in MATLAB (MathWorks, Natick, MA, USA). A 2x3 [limb x time] repeated measures ANVOA was performed with statistical significance defined as $\alpha < 0.05$. Post-hoc 2-tailed paired t-tests were performed to compare stresses between limbs (involved vs. uninvolved) at individual time points and post-hoc 1x3 (limb x time) repeated measures ANOVAs were performed to analyze how stress within each limb changed with time. This same analysis was done for T_2 relaxation times. To account for multiple comparisons, Bonferroni corrections were used for all post-hoc tests. Changes in cartilage stress over time (3 to 6 months) were compared to changes in biochemical composition over time (3 to 6 months) and the biochemical composition only at the 24-month time point using Pearson correlations and simple linear regressions. Correlations were described using R^2 values of the following ranges: small ($R^2 > 0.02$), medium ($R^2 > 0.13$), or large ($R^2 > 0.26$)[178].

Results

Tibial Cartilage

A limb-by-time interaction was present in the anterior region ($p = 0.046$) and central region ($p = 0.022$) when assessing stress at pMCF. The central region of cartilage experienced significantly lower stresses in the involved limb (vs. the uninvolved limb) at 3 months ($p = 0.002$), while the posterior region saw significant differences at 6 months ($p = 0.016$). The involved limb showed significant difference over time in the central region ($p = 0.015$), while the uninvolved limb did not. By 24 months both the involved and uninvolved limbs experienced similar joint stresses. No

statistically significant differences were found when assessing T_2 relaxation times regardless of limb or timepoint assessed (**Figure 28)**.

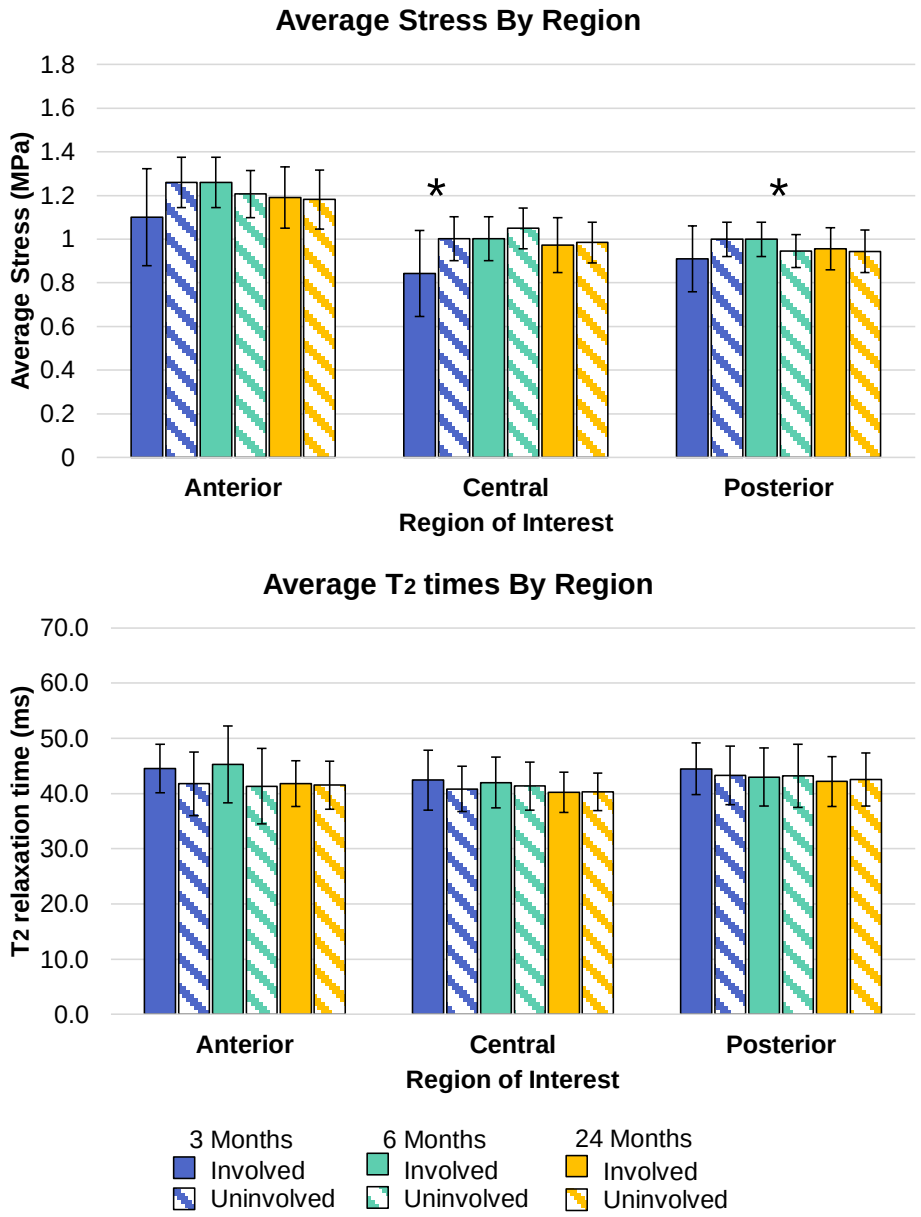

Figure 28 Medial tibial cartilage mean stress values taken at pMCF (top) and mean T_2 (bottom) for the involved (solid) and uninvolved (striped) in the anterior, central, and posterior regions of the medial tibial cartilage. Data is shown for the 3 (Blue), 6 (green), and 24 months (yellow). (* = significantly different $p<0.016$)

When comparing changes in stress from 3 to 6 months to changes in T_2 relaxation times from 3-6 months in the involved limb, negative correlations were present in the anterior (R^2 = 0.325) and posterior (R^2 = 0.219) regions of cartilage, while a small correlation was present in the central region (R^2 =0.047). A negative correlation indicates that increases in stress from 3 to 6 months are associated with improved T_2 relaxation times over time (**Figure 29)**. No correlations were present when comparing changes in stress from 3 to 6 months to T_2 relaxation times at 24 months.

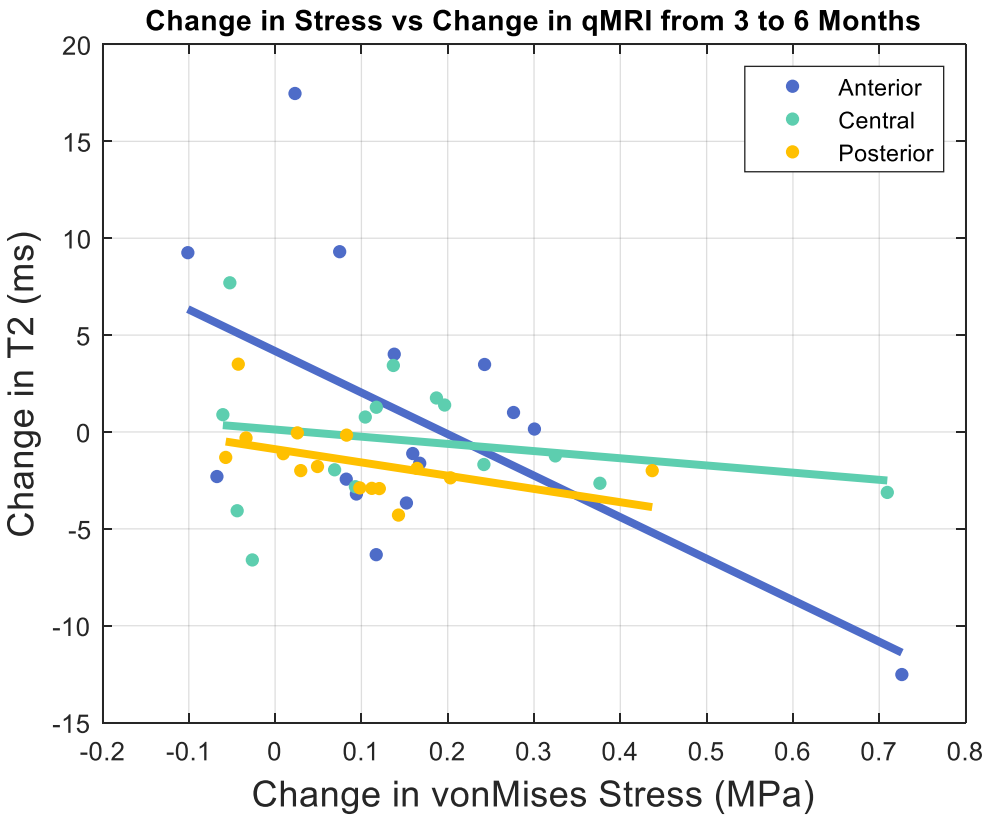

Figure 29 Changes in the involved limbs stress from 3 to 6 months compared to changes in T_2 relaxation time from values 3 to 6 months after ACLR for the anterior (blue), central (green), and posterior (yellow) regions of the medial tibial cartilage

Femoral Cartilage

When assessing cartilage stress, limb-by-time interactions were present in the central ($p = 0.043$) and posterior ($p = 0.041$) regions. The anterior region experienced significantly higher stresses in the involved limb compared to the uninvolved limb at 6 months. While the central and posterior regions experienced significantly lower stresses in the involved limb at 3 months. By 24 months no significant differences were present between limbs. When looking at the involved limb over time the central ($p = 0.029$) and posterior ($p = 0.029$) regions approached significant differences in stress. There were no differences between limbs or across time when assessing T2 relaxation times (**Figure 30)**.

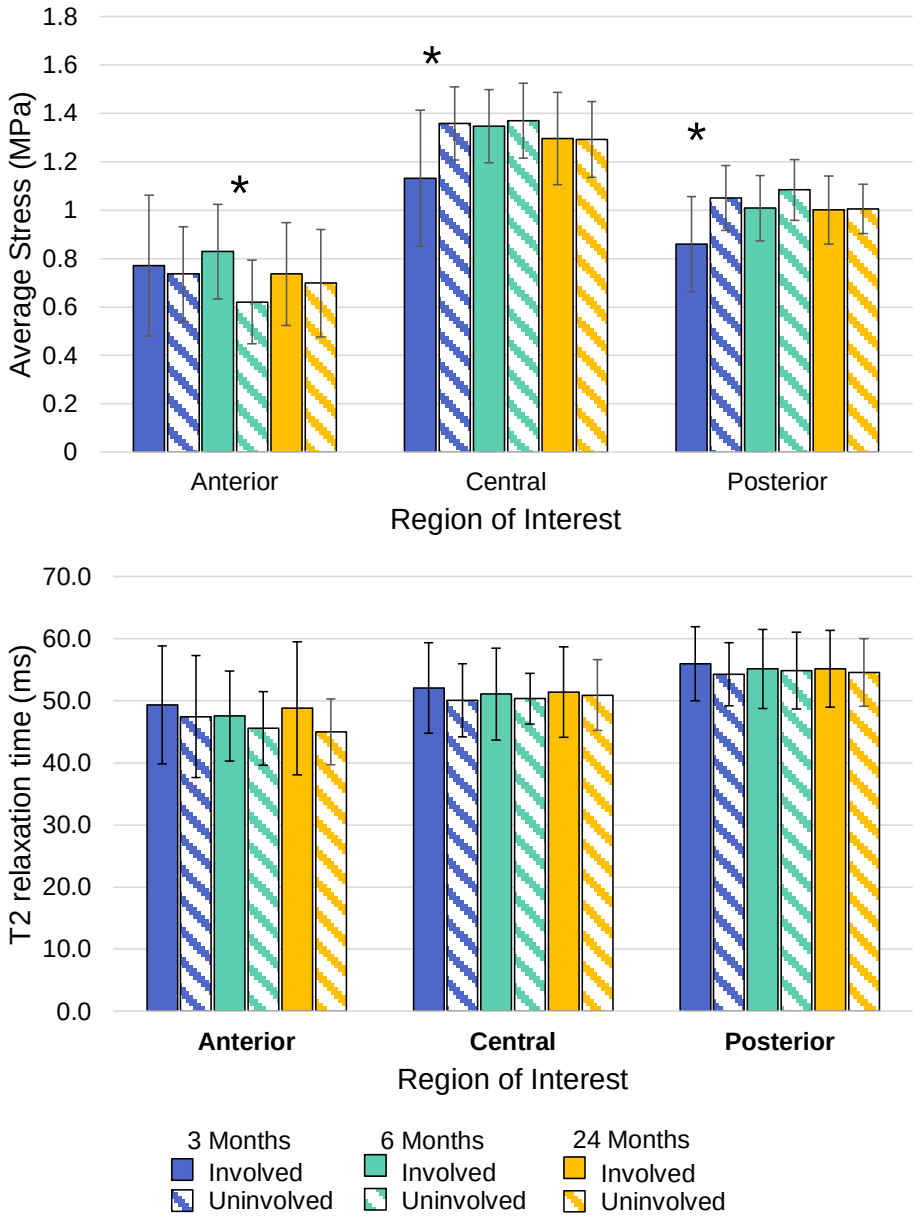

Figure 30 Medial Femoral cartilage mean stress values taken at pMCF (top) and mean T_2 (bottom) for the involved (solid) and uninvolved (striped) in the anterior, central, and posterior regions of the medial tibial cartilage. Data is shown for the 3 (Blue), 6 (green), and 24 months (yellow). (* = significantly different $p<0.016$)

Changes in stress from 3 to 6 months were negatively associated with changes in T_2 values from 3 to 6 months in the anterior (R^2 =0.233) and central (R^2 =0.163) regions of cartilage (**Figure 31)**. No correlations were seen when comparing changes in stress to T_2 relaxation times at 24 months (not shown).

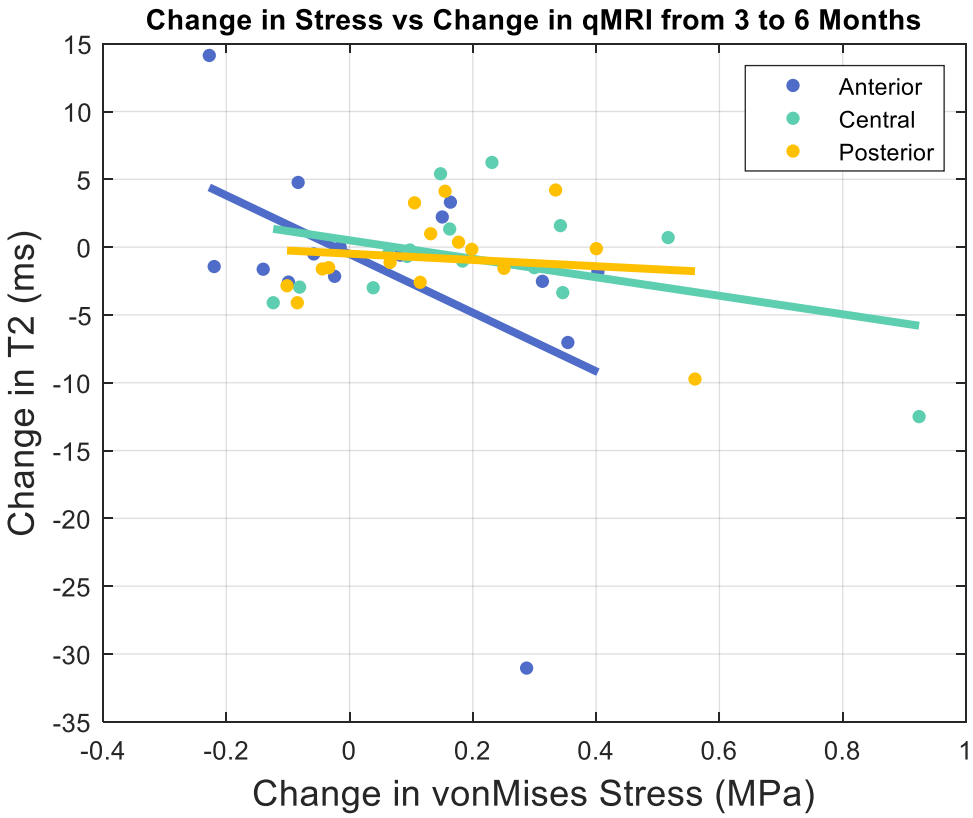

Figure 31 Changes in the involved limbs stress from 3 to 6 months compared to changes in T_2 relaxation time from values 3 to 6 months after ACLR for the anterior (blue), central (green), and posterior (yellow) regions of the medial femoral cartilage

Discussion

This study was the first to examine if knee cartilage stress was associated with the biochemical composition of cartilage across multiple timepoints after ACLR. Our

first hypothesis, that cartilage regions with limb-by-time interaction in stress would also have limb-by-time interactions for T_2 relaxation times in those regions, was not supported. While the central and posterior regions of tibial cartilage and all three regions in the femoral cartilage experienced significant differences in stress between limbs, no differences were present between limbs at any timepoint when comparing T_2 relaxation times. For our second hypothesis, we predicted that regions of cartilage that experienced larger changes in stress from 3 months to 6 months would see larger changes in T_2 relaxation times from 3 to 6 months and show prolonged (worse) T_2 values at 24 months. This hypothesis was partially supported, while there were no correlations between changes in stress from 3 to 6 months when comparing the involved limbs T_2 values at 24 months, we did see associations in the tibial and femoral cartilage when comparing changes in stress to changes in T_2 relaxation times from 3 to 6 months. Interestingly an increase in stress from 3 to 6 months showed a decrease in T_2 relaxation times within the involved limb. Since this is an exploratory study, no direct conclusions can be made, however, these findings suggest that an increase in stress over time could improve/protect biochemical composition during the early stages of recovery. Since no associations were seen when examining changes in stress vs. 24-month T2 data it is unclear if these associations are maintained overtime. One possible explanation for this lack of association could be the limited sample size of this study (15). Having such a small sample may have limited the power of the sample. Additionally, it is possible that the small sample from which we analyzed were full of individuals who could end up not getting long-term OA. Future work should examine these associations among a larger cohort to minimize these possible other explanations.

In Chu and Andriacchi's theory on the development of OA, "Pre-OA" is thought to develop into OA after ACLR due to alterations in gait and resultant shifts in stress patterns. However, it is possible that those who saw large changes in stress early after ACLR are in fact returning to a more symmetric stress patterns over time which could represent a return of the mechanics-based system to a normal operating range, potentially allowing cartilage to move from a state of Pre-OA to typical healthiness (represented by a decrease in T2). This, however, cannot be proven with the current study due to the lack of long-term follow up as well as the limited number of subjects.

The combination of qMRI and finite element modeling has the potential to help identify how changes in stress relate to biochemical cartilage health and is just now starting to gain footing in the ACLR research community. A recent study performed by Bolcos et al.[166] compared knee joint cartilage stress to biochemical composition after ACLR by utilizing subject-specific models of the knee and qMRI measures. To our knowledge, this is the only other study after ACLR to examine associations between stress and knee cartilage biochemical health. In this study they assessed stress in tibia cartilage at 1 year after ACLR and changes in T_2 from 1 to 3 years after ACLR. Their analysis was focused on peak principal stresses throughout gait and used a threshold of 7 MPa to identify volumes of cartilage that they predicted would be most at risk of showing signs of early degeneration (called volumes of interest (VOI)). Similarly, VOIs were identified from the T_2 images at 1 year and 3 years using a threshold of 60ms. The percent volume difference between the 1- and 3-year data was then calculated to represent the degenerated volume of cartilage. This study showed strong correlations between the percent degenerated volumes predicted by the FE model and the degenerated volume measured by T_2 maps. However, they

did not report if these volumes of degeneration were occurring in the same location. They also compared peak principal stress at one year with change in T_2 at the same location and found higher stresses at 1 year relate to an increase in T_2 values over time. Their study only assessed stresses at one time point, so they were unable to assess how alterations in stress patterns influence knee cartilage biochemical composition. Another limitation to this study, that our study addresses, is that they could not analyze how stresses differ between limbs, as they only compared the involved limb of ACLR individuals to healthy controls. The lack of contralateral limb data and only one time point after ACLR for stress data made it difficult to also assess if lower stresses after ACLR were playing a role in changes in cartilage composition. Like our study, their study was limited to 13 subjects, six of which were healthy controls, which could limit the generalizability of their results. Future work could perform a similar analysis as theirs using our subject's data to see we obtain similar results at earlier time points. Given that they assessed later time points after surgery, it could be that increases in stress early after ACLR seen here are representative of a mechanical improvement post-surgery which may be beneficial for long-term cartilage health. The larger stresses in their study could be representative of negative stress-adaptions in the longer-term after surgery.

A recent study from our lab found that individuals that experienced interlimb differences in joint loading from 3 to 6 months after surgery showed worse T_2 relaxation times at 24 months compared to individuals who remained symmetric over this early time period. Future work could examine if these trends are also seen when looking at cartilage stresses and if consistently symmetric stress patterns is related to better cartilage composition.

There are several limitations to this study that should be considered. In the current analysis, we found average values for three relatively large regions of cartilage. Future work should look at employing a more sophisticated analysis approach such as voxel based relaxometry[195,196] which would allow T_2 relaxation times to be evaluated over the entirety of the cartilage, this along with an overlay of FE stress maps, could give a more holistic view of specific locations that are seeing altered stresses, and the T_2 values for those specific cartilage locations. These, in turn, could provide much deeper insights into the potential mechanisms for long-term OA development.

The deep and superficial layers of cartilage differ in structure, which is typically reflected in qMRI variables[193]. The use of the same material model for cartilage throughout limits our ability to assess stress differences within different zones of cartilage. Future work, using a more complex model, could examine layer dependent stress distributions and evaluate whether or not these relate to differences in T2 relaxation times between layers.

Another limitation to this study is that only one FE model was used throughout. The lack of subject-specific geometry may have influenced the accuracy of the comparison to T_2. With the development of AI based protocols and automatic segmentation and meshing software this could soon become a viable option.

While the results of this study are limited, this technique shows great promise in furthering our understanding of how alterations in gait are impacting how knee joint cartilage stress is change over time, and how these alterations are impacting the cartilage on a biochemical level. The next steps to this project would include expanding the sample size, improving the model so that it can handle higher loads,

incorporate subject-specific geometry into each model, and developing more advanced analysis techniques to compare stress distribution with cartilage qMRI maps. With further development and tuning of this process, researchers may be able to better understand the development of OA after ACLR, which could eventually help inform the development of targeted interventions aimed at mitigating these damaging biomechanical patterns.

Chapter 6

CONCLUSIONS AND FUTURE WORK

Aim 1

Conclusions

This aim assessed gait mechanics 3 and 6 months after ACLR using SPM, giving us a holistic view of the gait cycle that may provide insights into alterations that others may have missed. We hypothesized that 1) interlimb asymmetries in knee gait variables would be present at 3 and 6 months after ACLR and 2) these asymmetries would be greater at 3 months than at 6 months, with the involved limb changing over time. Both of our hypotheses were partially supported.

We found significant asymmetries between limbs in KFA, KFM, KEF and MCF 3 months after ACLR but by 6 months KEF and MCF were no longer significantly different. While differences between limbs were still present for KFA and KFM, these asymmetries had significantly decreased by 6 months. Gait mechanics in the uninvolved limb stayed relatively consistent between 3 and 6 months, while the involved limb's mechanics trended towards that of the uninvolved limb over time. Given that asymmetrical gait patterns as early as 6 months after ACLR are linked to the development of long-term post-traumatic OA, these early time periods may be the ideal time to implement rehabilitative interventions. This study expands upon the existing literature which has focused on discrete values to understand aberrations in

gait mechanics and is among the first to assess timepoints prior to six months after surgery. Altogether, this work adds to our understanding of how biomechanical alterations are changing over stance phase during the early months after surgery and may have important implications for the design of future rehabilitation interventions.

Future Work

For this study no strength measures were performed, limiting the conclusions that can be made about how muscular strength is progressing after ACLR and its impact of gait mechanics over these time periods. The additional collection of strength measurements in future studies may help distinguish between changes in strength and one's ability to exert force throughout gait. Future work should focus on helping to understand if these early changes are associated with longer-term OA. Having subjects return at 24 months for gait analysis will allow further understanding of how gait biomechanics are changing over the first two years of recovery as well as assess if discrete data at these time points shows a similar story. In addition, quantitative MRI (qMRI) measures will be obtained to assess the biochemical composition of the cartilage. By comparing gait alterations early after surgery to qMRI results, we may be able to identify alterations that are associated with worsening cartilage health. Another avenue would be to have subjects return 5 years after ACLR to obtain radiographs of the knee to identify if radiographic OA is present. From these findings an OA group and non-OA group could be identified, and the current data could be compared. These finding can then be used by clinicians and researchers in the development of rehabilitation interventions that could help ameliorate gait alterations early after surgery that are related to eventual OA development.

Aim 2

Conclusions

This aim reported the process of developing subject-specific finite element models of the knee joint, a scaling protocol for a generic use model, and the validation of a generic model. The use of these models can help to better understand subject-specific alterations in joint stresses. This aim provides research groups that wish to develop FE models of the knee joint a step-by-step framework to either modify the existing model or create their own from their own subjects' geometries. The "art" of modeling requires the developer to make many decisions that can play a role in the model's results, which can lead to inconsistencies in reproducing results and hesitation surrounding model findings[73,86]. Through transparency regarding how our model was made, the assumptions made, and limitations of the current model design, we hope to mitigate these common modeling issues and allow others to build upon our work.

Future Work

Limitations exist for this modeling protocol. A linear elastic isotropic material model was used as the cartilage constitutive model. This simplified material model helped reduce simulation run time and helped with model convergence. Our model was able to produce general information on how changes in gait mechanics impact stress magnitude and location, however the use of a more complex model may allow for a more in-depth analysis. Future work could implement a fibril reinforced poro-viscoelastic material model[74] of cartilage to assess how these changes impact fluid flow within the cartilage and the impact of long-term loading on the tissue.

The geometry of the knee is very complex, and choices were made to simplify certain components including ligaments. Future work could include 3D geometries of ligament meshes. Modifications also had to be made to some components to allow for valid meshing of the geometry. Specifically, we had to modify the edges of the cartilage and menisci to generate a valid mesh. For the interface of cartilage to meniscus this caused an issue with the inside edge of the crescent, causing penetration errors in compartment loads over 3000N and certain angles. This limited the number of subject's that would converge and may have limited the results of the study by excluding those who had higher joint loads.

The current workflow requires model geometry to be segmented by hand. This process is a lengthy procedure and, combined with mesh development process, makes application of this method impractical for larger cohorts. This led us to develop a scaling protocol, decreasing the amount of time needed to develop individual models as well as removing potential inconsistencies with segmentation quality. Future work should explore the implementation of semi-automated segmentation tools and artificial intelligence to reduce the amount of time needed to obtain subject-specific geometries and to ensure consistent segmentation methods across subjects. Another limitation to the meshing protocol is that the user must manually realign different meshes, further increasing model development time and leaving room for unnecessary error. Future work should focus on the design of an automatic realignment procedure.

The current model was validated against published model results and experimental data against contact stresses and pressures. Further verification should be performed for joint translations, if needed tuning should be performed for ligament pre-strains which were not included in the current version of the model.

Aim 3

Conclusions

Little is known about how altered movement patterns after ACLR impact the way cartilage is stressed within the knee joint. This aim assessed how changes in knee flexion angles after ACLR influenced knee cartilage stress patterns across multiple time points. For this aim we had two hypotheses 1) that the involved limb will experience lower stresses than the uninvolved limb, and that this asymmetry between limbs will decrease over time mostly due to the involved limb increasing to match the stresses in the uninvolved limb and 2) that stress location will be correlated with KFA in the femoral cartilage, with smaller knee flexion angles resulting in an anterior shift in stress. Both hypotheses were partially supported.

We found that in some regions of interest altered stress patterns were present in the involved limb (vs. uninvolved) at 3- and 6-months after ACLR but that these alterations were largely resolved by 24 months after surgery. Interestingly, while the involved limb experienced lower stresses compared to the uninvolved limb at 3 months, by 6 months some regions saw higher involved limb stresses than the uninvolved limb. The femoral cartilage seemed to be the most impacted by changes in knee flexion angle, with increases in knee flexion angle correlating with increases in the posterior region's stresses, while the opposite trend was seen in the anterior region. These findings suggest that a return to symmetry is not a straightforward path from lower stress to symmetric stress, but that the cartilage may see a fluctuation in stress patterns early after surgery until ultimately achieving symmetry by two years.

Future Work

One of the largest limitations to this work is the lack of knowledge about cartilage stresses in a healthy population. Future work aimed at quantifying meaningful interlimb differences would help clarify if the changes in stress reported here are meaningful, or if these alterations are within normal walking limits. Another limitation to this study was the sample size. The current model starts to have trouble converging with medial compartment loads over 3000 N limiting the total number of subjects that could be included in this study. Future work should refine the model development cycle to allow for model convergence over this maximum load limit.

For this study only one generic model was used, limiting our understanding of how subject specific geometry impacts cartilage stress. We were able to scale subject loads to that of the original model, to help limit the impact that smaller or larger geometry would have on model outputs. Future work could focus on building a limited number of subject-specific models to assess the influence of subject-specific geometries. However, by not changing the models we were able to isolate changes in stress that are a result of alterations in biomechanics rather than being a function of both mechanics and model geometry/quality.

This study did not include subjects who had undergone a meniscal repair however there was a subset of subjects who did have a meniscectomy. This is a limitation to this study as we did not change the geometry based on meniscal shape which is known to alter joint stresses[197,198]. Future work should focus on modifying the current menisci to examine the impact of a meniscectomy on cartilage stresses.

Finally, the current model did not change ligament properties based on subject-specific joint laxity, subject-specific material properties, or model differences between

the native ACL and the reconstructed ACL. Obtaining joint laxity measurements and subject-specific material properties are difficult measurements to acquire on human subjects; thus, most models base these measurements on cadaveric knees. Future models using qMRI techniques to help determine cartilage material properties[199,200] may address this limitation.

Only select regions of the medial compartment were examined. Future work should examine the remaining areas of medial compartment cartilage that were not assessed here. Particularly, it may be interesting to examine stresses near the medial edge of the tibial compartment as this is where osteophytes typically form during OA development following ACLR. Additionally, the current approach analyzed data by taking the average stress values within pre-defined regions of interest. Future work needs to explore and develop more sophisticated means to analyzing this data such as 3D SPM which could provide more holistic insights into the stress alterations present among this population. Finally, only the medial compartment was analyzed. Future work should examine stress patterns within the lateral and patellofemoral compartments which also have high incidence rates of OA development.

Aim 4

Conclusions

This aim used a combination of FE modeling and qMRI to assess how stress in different regions of the medial tibial and femoral cartilage relates to the biochemical composition of the cartilage over time. We hypothesized that regions of cartilage with asymmetries in stresses at peak medial compartment force (pMCF) will also

asymmetries in T_2 relaxation times. Our second hypothesis was that regions of cartilage within the involved limb that experience larger changes in stress between 3 months and 6 months will experience larger changes in T_2 from 3 to 6 months and prolonged T_2 values at 24 months.

Our first hypothesis was not supported while our second hypothesis was partially supported. We found that stresses in the involved limb significantly increased over time compared to the uninvolved limb for some regions in the medial tibial and femoral cartilage. However, no differences were present between limbs or across time when looking at T_2 relaxation times. When assessing how the biochemical composition of the involved limb's cartilage related to changes in cartilage stress over time, we found associations between changes in stress and changes in T_2 relaxation time from 3 to 6 months. Individuals who saw an increase in stress from 3 to 6 months saw a decrease in T_2 relaxation times (improvement in cartilage health). These associations were not seen when assessing changes in stress over time to T_2 relaxation times at 24 months in the involved limb.

Future Work

Further work should be done to help transition this aim from an exploratory study to a full research study. The next steps to this project would include expanding the sample size, improving the model so that it can handle higher loads, incorporate subject-specific geometry into each model, and developing more advanced analysis techniques to compare stress distribution with cartilage qMRI maps. The use of voxel-based relaxometry, which allows us to analyze T_2 relaxation times for each voxel within an image rather than for specific regions of interest, could help fully capture the

varying biochemical alterations seen in qMRI maps. Using this approach, we could then overlay the T_2 maps and stress maps which would allow us to both quantitatively and qualitatively assess if regions of cartilage that are seeing altered stresses also see alterations in their biochemical composition. Additionally, it would be interesting to implement a constitutive model for the cartilage that accounts for the varying material properties of cartilage as this would allow for an analysis that assesses how stress changes throughout the depth of the cartilage. This could be particularly enlightening as previous work has demonstrated layer-specific findings when investigating T_2 relaxation times after ACLR. To fully assess if alterations in stress are associated with the development of OA, long term follow up would need to be done to identify who from the cohort has developed the disease. With the identification of an OA and a non-OA group we would be better able to review the data and identify what types of alterations in stress are detrimental to the health of cartilage. These findings could help us further understand the pathogenesis of this debilitating disease and help inform clinicians who are actively working to develop rehabilitation protocols to reduce the likelihood of long-term disease development.

REFERENCES

1. Kiapour AM, Murray MM. 2014. Basic science of anterior cruciate ligament injury and repair. British Editorial Society of Bone and Joint Surgery.
2. Di Stasi SL, Logerstedt D, Gardinier ES, Snyder-Mackler L. 2013. Gait patterns differ between ACL-reconstructed athletes who pass return-to-sport criteria and those who fail. American Journal of Sports Medicine 41(6):1310–1318.
3. Chandra A, Kar O, Wu K-C, et al. 2015. Prognosis of anterior cruciate ligament reconstruction: a data-driven approach. Proceedings of the Royal Society A: Mathematical, Physical and Engineering Sciences 471(2176):20140526–20140526.
4. Andriacchi TP, Favre J, Erhart-Hledik JC, Chu CR. 2015. A Systems View of Risk Factors for Knee Osteoarthritis Reveals Insights into the Pathogenesis of the Disease. Ann Biomed Eng 43(2):376–387.
5. Hasler EM, Herzog W, Leonard TR, et al. 1997. In vivo knee joint loading and kinematics before and after ACL transection in an animal model. J Biomech .
6. Lohmander LS, Englund PM, Dahl LL, Roos EM. 2007. The Long-term Consequence of Anterior Cruciate Ligament and Meniscus Injuries. Am J Sports Med 35(10):1756–1769 [cited 2018 Oct 8] Available from: http://journals.sagepub.com/doi/10.1177/0363546507307396.
7. Bolcos PO, Mononen ME, Mohammadi A, et al. 2018. Comparison between kinetic and kinetic-kinematic driven knee joint finite element models OPEN. Scientific REpoRTS | 8:17351.
8. Titchenal MR, Williams AA, Chehab EF, et al. 2018. Cartilage Subsurface Changes to Magnetic Resonance Imaging UTE-T2* 2 Years After Anterior Cruciate Ligament Reconstruction Correlate With Walking Mechanics Associated With Knee Osteoarthritis. American Journal of Sports Medicine 46(3):565–572.
9. Capin JJ, Williams JR, Neal K, et al. 2020. Slower Walking Speed Is Related to Early Femoral Trochlear Cartilage Degradation After ACL Reconstruction. Journal of Orthopaedic Research 38(3):645–652.
10. Wellsandt E, Khandha A, Capin J, et al. 2020. Operative and nonoperative management of anterior cruciate ligament injury: Differences in gait biomechanics at 5 years. Journal of Orthopaedic Research 38(12):2675–2684.
11. Abulhasan JF, Grey MJ. 2017. Anatomy and Physiology of Knee Stability. Journal of Functional Morphology and Kinesiology 2017, Vol. 2, Page 34 2(4):34.

12. Brody LT. 2015. Knee osteoarthritis: Clinical connections to articular cartilage structure and function. Physical Therapy in Sport 16(4):301–316.
13. Sophia Fox AJ, Bedi A, Rodeo SA. 2009. The Basic Science of Articular Cartilage: Structure, Composition, and Function. Sports Health 1(6):461.
14. Matzat SJ, van Tiel J, Gold GE, Oei EHG. 2013. Quantitative MRI techniques of cartilage composition. Quant Imaging Med Surg 3(3):162–16274.
15. Messner K, Gao J. 1998. The menisci of the knee joint. Anatomical and functional characteristics, and a rationale for clinical treatment. J Anat 193(2):161–178.
16. Fox AJS, Wanivenhaus F, Burge AJ, et al. 2015. The human meniscus: A review of anatomy, function, injury, and advances in treatment. Clinical Anatomy 28(2):269–287.
17. Li X, Majumdar S. 2013. Quantitative MRI of Articular Cartilage and Its Clinical Applications.1008:991–1008.
18. Petersson IF, Boegård T, Saxne T, et al. 1997. Radiographic osteoarthritis of the knee classified by the Ahlbäck and Kellgren & Lawrence systems for the tibiofemoral joint in people aged 35-54 years with chronic knee pain. Ann Rheum Dis 56(8):493–6 [cited 2018 Oct 13] Available from: http://www.ncbi.nlm.nih.gov/pubmed/9306873.
19. Karas V, Calkins TE, Bryan AJ, et al. 2019. Total Knee Arthroplasty in Patients Less Than 50 Years of Age: Results at a Mean of 13 Years. Journal of Arthroplasty 34(10):2392–2397 [cited 2023 May 3] Available from: http://www.arthroplastyjournal.org/article/S0883540319304929/fulltext.
20. Evans JT, Walker RW, Evans JP, et al. 2019. How long does a knee replacement last? A systematic review and meta-analysis of case series and national registry reports with more than 15 years of follow-up. Lancet 393(10172):655 [cited 2023 May 3] Available from: /pmc/articles/PMC6381229/.
21. Granan LP, Forssblad M, Lind M, Engebretsen L. 2009. The scandinavian ACL registries 2004-2007: Baseline epidemiology. Acta Orthop 80(5):563–567.
22. Castagnini F, Sudanese A, Bordini B, et al. 2017. Total Knee Replacement in Young Patients: Survival and Causes of Revision in a Registry Population. Journal of Arthroplasty 32(11):3368–3372 [cited 2019 Dec 14].
23. Thambyah A. 2005. A hypothesis matrix for studying biomechanical factors associated with the initiation and progression of posttraumatic osteoarthritis. Med Hypotheses 64(6):1157–1161 [cited 2023 May 1].
24. Andriacchi TP, Mündermann A, Smith RL, et al. 2004. A framework for the in vivo pathomechanics of osteoarthritis at the knee. Ann Biomed Eng 32(3):447–457 [cited 2019 Dec 21].
25. Buckwalter JA. 1998. Articular cartilage: injuries and potential for healing. J Orthop Sports Phys Ther 28(4):192–202 [cited 2023 May 1] Available from: https://pubmed.ncbi.nlm.nih.gov/9785255/.

26. Anderson DD, Chubinskaya S, Guilak F, et al. 2011. Post-Traumatic Osteoarthritis : Improved Understanding and Opportunities for Early Intervention.(June):802–809.
27. Mosher TJ, Dardzinski BJ. 2004. Cartilage MRI T2 relaxation time mapping: Overview and applications. Semin Musculoskelet Radiol 8(4):355–368 [cited 2023 May 1] Available from: http://www.thieme-connect.com/products/ejournals/html/10.1055/s-2004-861764.
28. Gardinier ES, Manal K, Buchanan TS, et al. 2013. Gait and Neuromuscular Asymmetries after Acute ACL Rupture. Med Sci Sports Exerc 44(8):1490–1496 [cited 2021 Sep 6] Available from: https://journals.lww.com/acsm-msse/Fulltext/2012/08000/Gait_and_Neuromuscular_Asymmetries_after_Acute.10.aspx.
29. Butler RJ, Minick KI, Ferber R, Underwood F. 2009. Gait mechanics after ACL reconstruction: Implications for the early onset of knee osteoarthritis. Br J Sports Med 43(5):366–370.
30. PFEIFFER SJ, SPANG J, NISSMAN D, et al. 2019. Gait Mechanics and T1ρ MRI of Tibiofemoral Cartilage 6 Months after ACL Reconstruction. Med Sci Sports Exerc 51(4):630–639 [cited 2019 Dec 22] Available from: http://Insights.ovid.com/crossref?an=00005768-201904000-00004.
31. Williams JR, Neal K, Alfayyadh A, et al. 2021. Knee cartilage T2 relaxation times 3 months after ACL reconstruction are associated with knee gait variables linked to knee osteoarthritis. Journal of Orthopaedic Research :1–8 Available from: www.slicer.org/.
32. White K, Logerstedt D, Snyder-Mackler L. 2013. Gait asymmetries persist 1 year after anterior cruciate ligament reconstruction. Orthop J Sports Med 1(2).
33. Capin JJ, Zarzycki R, Ito N, et al. 2019. Gait Mechanics in Women of the ACL-SPORTS Randomized Control Trial: Interlimb Symmetry Improves Over Time Regardless of Treatment Group. Journal of Orthopaedic Research 37(8):1743–1753.
34. Capin JJ, Khandha A, Zarzycki R, et al. 2018. Gait mechanics and tibiofemoral loading in men of the ACL-SPORTS randomized control trial. Journal of Orthopaedic Research 36(9):2364–2372.
35. Hart HF, Culvenor AG, Collins NJ, et al. 2016. Knee kinematics and joint moments during gait following anterior cruciate ligament reconstruction: A systematic review and meta-analysis. Br J Sports Med 50(10):597–612 [cited 2021 Feb 6] Available from: https://pubmed.ncbi.nlm.nih.gov/26265562/.
36. Sigward SM, Lin P, Pratt K. 2016. Knee loading asymmetries during gait and running in early rehabilitation following anterior cruciate ligament reconstruction: A longitudinal study. Clinical Biomechanics 32:249–254.
37. Lin PE, Sigward SM. 2018. Contributors to knee loading deficits during gait in individuals following anterior cruciate ligament reconstruction. Gait Posture 66:83–87.

38. Ektas N, Scholes C, Kulaga S, et al. 2019. Recovery of knee extension and incidence of extension deficits following anterior cruciate ligament injury and treatment: A systematic review protocol. J Orthop Surg Res 14(1):1–7.
39. Shabani B, Bytyqi D, Lustig S, et al. 2015. Gait knee kinematics after ACL reconstruction: 3D assessment. Int Orthop 39(6):1187–1193 [cited 2021 Sep 15] Available from: https://link.springer.com/article/10.1007/s00264-014-2643-0.
40. Hughes-Oliver CN, Harrison KA, Williams DSSBB, Queen RM. 2019. Statistical parametric mapping as a measure of differences between limbs: Applications to clinical populations. J Appl Biomech 35(6):377–387.
41. Hooper DM, Morrissey MC, Drechsler WI, et al. 2002. Gait analysis 6 and 12 months after anterior cruciate ligament reconstruction surgery. Clin Orthop Relat Res (403):168–178.
42. Wellsandt E, Gardinier ES, Manal K, et al. 2016. Decreased knee joint loading associated with early knee osteoarthritis after anterior cruciate ligament injury. American Journal Sports Medicine 44(1):143–151.
43. Zabala ME, Favre J, Scanlan SF, et al. 2013. Three-dimensional knee moments of ACL reconstructed and control subjects during gait, stair ascent, and stair descent. J Biomech 46(3):515–520.
44. Roewer BD, Di Stasi SL, Snyder-Mackler L. 2011. Quadriceps strength and weight acceptance strategies continue to improve two years after anterior cruciate ligament reconstruction. J Biomech 44(10):1948–1953.
45. Webster KE, Feller JA. 2012. The knee adduction moment in hamstring and patellar tendon anterior cruciate ligament reconstructed knees. Knee Surgery, Sports Traumatology, Arthroscopy 20(11):2214–2219.
46. Webster KE, Wittwer JE, O'Brien J, Feller JA. 2005. Gait patterns after anterior cruciate ligament reconstruction are related to graft type. American Journal of Sports Medicine 33(2):247–254.
47. Davis-Wilson HC, Pfeiffer SJ, Johnston CD, et al. 2020. Bilateral Gait 6 and 12 Months Post-Anterior Cruciate Ligament Reconstruction Compared with Controls. Med Sci Sports Exerc 52(4):785–794 [cited 2021 Sep 16] Available from: /pmc/articles/PMC7078064/.
48. Patterson MR, Delahunt E, Caulfield B. 2014. Peak knee adduction moment during gait in anterior cruciate ligament reconstructed females. Clinical Biomechanics 29(2):138–142.
49. Varma RK, Duffell LD, Nathwani D, McGregor AH. 2014. Knee moments of anterior cruciate ligament reconstructed and control participants during normal and inclined walking. BMJ Open 4(6):e004753.
50. Shi H, Huang H, Ren S, et al. 2019. The relationship between quadriceps strength asymmetry and knee biomechanics asymmetry during walking in individuals with anterior cruciate ligament reconstruction. Gait Posture 73:74–79.

51. Lewek M, Rudolph K, Axe M, Snyder-Mackler L. 2002. The effect of insufficient quadriceps strength on gait after anterior cruciate ligament reconstruction. Clinical Biomechanics 17(1):56–63.
52. MV P, LC S, KR F, et al. 2010. Biomechanical measures during landing and postural stability predict second anterior cruciate ligament injury after anterior cruciate ligament reconstruction and return to sport. Am J Sports Med 38(10):1968–1978.
53. Khandha A, Manal K, Wellsandt E, et al. 2017. Gait mechanics in those with/without medial compartment knee osteoarthritis 5 years after anterior cruciate ligament reconstruction. J Orthop Res 35(3):625–633 [cited 2018 Oct 13] Available from: http://www.ncbi.nlm.nih.gov/pubmed/27082166.
54. Slater L V., Hart JM, Kelly AR, Kuenze CM. 2017. Progressive changes in walking kinematics and kinetics after anterior cruciate ligament injury and reconstruction: A review and meta-Analysis. J Athl Train 52(9):847–860.
55. Andriacchi TP, Mundermann A, Smith RL, et al. 2004. A Framework for the in Vivo Pathomechanics of Osteoarthritis at the Knee: 2nd Special Edition on Musculoskeletal Bioengineering. Ann Biomed Eng 51(1):31–39.
56. Andriacchi TP, Koo S, Scanlan SF. 2009. Gait mechanics influence healthy cartilage morphology and osteoarthritis of the knee. Journal of Bone and Joint Surgery - Series A 91(SUPPL. 1):95–101.
57. Shimizu T, Samaan MA, Tanaka MS, et al. 2019. Abnormal Biomechanics at 6 Months Are Associated With Cartilage Degeneration at 3 Years After Anterior Cruciate Ligament Reconstruction. Arthroscopy - Journal of Arthroscopic and Related Surgery 35(2):511–520.
58. Koo S, Andriacchi TP. 2007. A comparison of the influence of global functional loads vs. local contact anatomy on articular cartilage thickness at the knee. J Biomech .
59. Chu CR, Andriacchi TP. 2015. Dance between biology, mechanics, and structure: A systems-based approach to developing osteoarthritis prevention strategies. Journal of Orthopaedic Research 33(7):939–947.
60. Andriacchi TP, Koo S, Scanlan SF. 2009. Gait Mechanics Influence Healthy Cartilage Morphology and Osteoarthritis of the Knee. J Bone Joint Surg Am 91(Suppl 1):95 [cited 2023 May 3] Available from: /pmc/articles/PMC2663350/.
61. Bingham JT, Papannagari R, Van de velde SK, et al. 2008. In vivo cartilage contact deformation in the healthy human tibiofemoral joint. Rheumatology 47(11):1622–1627.
62. Wei L, Svensson O, Hjerpe A. 1997. Correlation of morphologic and biochemical changes in the natural history of spontaneous osteoarthrosis in guinea pigs. Arthritis Rheum 40(11):2075–2083.
63. Simon WH. 1970. Scale effects in animal joints. I. articular cartilage thickness and compressive stress. Arthritis Rheum 13(3):244–255.

64. Liu C, Wang Y, Li Z, et al. 2018. Tibiofemoral joint contact area and stress after single-bundle anterior cruciate ligament reconstruction with transtibial versus anteromedial portal drilling techniques. J Orthop Surg Res 13(1):1–9.
65. Brown TD, Shaw DT. 1984. In vitro contact stress distribution on the femoral condyles. Journal of Orthopaedic Research 2(2):190–199.
66. Brown TD. 2004. Finite element modeling in musculoskeletal biomechanics. J Appl Biomech 20(4):336–366.
67. Kazemi M, Dabiri Y, Li LP. 2013. Recent Advances in Computational Mechanics of the Human Knee Joint Article in Computational and Mathematical Methods in Medicine · February 2013 Recent Advances in Computational Mechanics of the Human Knee Joint.2013(June 2017).
68. Linka K, Itskov M, Truhn D, et al. 2017. T2 MR imaging vs. computational modeling of human articular cartilage tissue functionality. J Mech Behav Biomed Mater 74(May):477–487.
69. Peters AE, Akhtar R, Comerford EJ, Bates KT. 2017. Tissue material properties and computational modelling of the human knee: A critical review. PeerJ Prepr :1–48 Available from: https://peerj.com/preprints/3050/%0Apapers3://publication/uuid/6159A28D-B43A-45FB-A2F5-68187B11EF7F.
70. Harris MD, Cyr AJ, Ali AA, et al. 2016. A Combined Experimental and Computational Approach to Subject-Specific Analysis of Knee Joint Laxity. [cited 2019 Jun 16] Available from: https://biomechanical.asmedigitalcollection.asme.org.
71. Manal K, Buchanan TS. 2013. An electromyogram-driven musculoskeletal model of the knee to predict in vivo joint contact forces during normal and novel gait patterns. J Biomech Eng 135(2):021014 [cited 2019 Sep 3] Available from: http://www.ncbi.nlm.nih.gov/pubmed/23445059.
72. Sole G, Pataky T, Tengman E, Häger C. 2017. Analysis of three-dimensional knee kinematics during stair descent two decades post-ACL rupture – Data revisited using statistical parametric mapping. Journal of Electromyography and Kinesiology 32:44–50.
73. Erdemir A, Besier TF, Halloran JP, et al. 2019. Deciphering the “Art” in Modeling and Simulation of the Knee Joint: Overall Strategy. J Biomech Eng 141(7):0710021 [cited 2023 May 3] Available from: /pmc/articles/PMC6611350/.
74. Esrafilian A, Stenroth L, Mononen ME, et al. 2021. 2 Degrees of Freedom Muscle Force Driven Fibril-Reinforced Poroviscoelastic Finite Element Model of the Knee Joint Index Terms-Multiscale modeling, Musculoskeletal modeling, finite element analysis, knee joint, electromyog-raphy (EMG), elastic foundation. IEEE TRANSACTIONS ON NEURAL SYSTEMS AND REHABILITATION ENGINEERING 29:123 Available from: https://doi.org/10.1109/TNSRE.2020.3037411,.

75. Honegger JD, Actis JA, Gates DH, et al. 2020. Development of a multiscale model of the human lumbar spine for investigation of tissue loads in people with and without a transtibial amputation during sit-to-stand. Biomechanics and Modeling in Mechanobiology 2020 20:1 20(1):339–358 [cited 2023 May 3] Available from: https://link.springer.com/article/10.1007/s10237-020-01389-2.
76. Sun D, Song Y, Cen X, et al. [date unknown]. Workflow assessing the effect of Achilles tendon rupture on gait function and metatarsal stress: Combined musculoskeletal modeling and finite element analysis. J Engineering in Medicine 2022(5):676–685 [cited 2023 May 3].
77. Wang M, Li S, Teo EC, et al. 2021. The Influence of Heel Height on Strain Variation of Plantar Fascia During High Heel Shoes Walking-Combined Musculoskeletal Modeling and Finite Element Analysis. Front Bioeng Biotechnol 9:1301 [cited 2023 May 3].
78. Damsgaard M, Rasmussen J, Christensen ST, et al. 2006. Analysis of musculoskeletal systems in the AnyBody Modeling System. Simul Model Pract Theory 14(8):1100–1111 [cited 2023 May 3].
79. Loan P, Delp S, Smith K, et al. 2004. SIMM 4.0 for Windows ® User's Manual Trademarks Cover Illustration. Available from: http://www.musculographics.comandhttp://www.motionanalysis.com.
80. Seth A, Sherman M, Reinbolt JA, Delp SL. 2011. OpenSim: a musculoskeletal modeling and simulation framework for in silico investigations and exchange. Procedia IUTAM 2:212 [cited 2023 May 3] Available from: /pmc/articles/PMC4397580/.
81. Maas SA, Ellis BJ, Ateshian GA, Weiss JA. 2012. FEBio: Finite elements for biomechanics. J Biomech Eng 134(1) [cited 2023 May 3] Available from: https://asmedigitalcollection.asme.org/biomechanical/article/134/1/011005/455684/FEBio-Finite-Elements-for-Biomechanics.
82. 1991. ABAQUS/CAE User's Manual.
83. 'DeSalvo G 'Swanson, J. 1985. ANSYS Engineering Analysis System User's Manual. Houston, Pa. :Swanson Analysis Systems, .
84. Murray YD, APTEK Inc. 2007. Users Manual for LS-DYNA Concrete Material Model 159. [cited 2023 May 3] Available from: https://rosap.ntl.bts.gov/view/dot/38730.
85. Galbusera F, Freutel M, Dürselen L, et al. 2014. Material models and properties in the finite element analysis of knee ligaments: A literature review. Front Bioeng Biotechnol 2(NOV):1–11.
86. Erdemir A, Guess TM, Halloran J, et al. 2012. Considerations for reporting finite element analysis studies in biomechanics. J Biomech 45(4):625–633 [cited 2023 Apr 18].
87. Halloran JP, Abdollahi Nohouji N, Hafez MA, et al. 2023. Assessment of reporting practices and reproducibility potential of a cohort of published studies in computational knee biomechanics.41(2):325–334 [cited 2023 Apr 18] Available from: https://onlinelibrary.wiley.com/doi/full/10.1002/jor.25358.

88. Kiapour AAM, Kiapour AAM, Kaul V, et al. 2014. Finite Element Model of the Knee for Investigation of Injury Mechanisms : Development and Validation. J Biomech Eng 136(1):011002.
89. Mall NA, Chalmers PN, Moric M, et al. 2014. Incidence and trends of anterior cruciate ligament reconstruction in the United States. American Journal of Sports Medicine 42(10):2363–2370.
90. Herzog MM, Marshall SW, Lund JL, et al. 2018. Trends in Incidence of ACL Reconstruction and Concomitant Procedures Among Commercially Insured Individuals in the United States, 2002-2014. Sports Health 10(6):523–531.
91. Paterno M V., Ford KR, Myer GD, et al. 2007. Limb asymmetries in landing and jumping 2 years following anterior cruciate ligament reconstruction. Clinical Journal of Sport Medicine 17(4):258–262.
92. Arhos EK, Capin JJ, Buchanan TS, Snyder-Mackler L. 2021. Quadriceps Strength Symmetry Does Not Modify Gait Mechanics After Anterior Cruciate Ligament Reconstruction, Rehabilitation, and Return-to-Sport Training. American Journal of Sports Medicine 49(2):417–425.
93. Pietrosimone B, Blackburn JT, Harkey MS, et al. 2016. Greater Mechanical Loading during Walking Is Associated with Less Collagen Turnover in Individuals with Anterior Cruciate Ligament Reconstruction. American Journal of Sports Medicine 44(2):425–432.
94. Zhao D, Banks SA, Mitchell KH, et al. 2007. Correlation between the knee adduction torque and medical contact force for a variety of gait patterns. Journal of Orthopaedic Research 25(6):789–797.
95. Duffell LD, Southgate DFL, Gulati V, McGregor AH. 2014. Balance and gait adaptations in patients with early knee osteoarthritis. Gait Posture 39(4):1057–1061.
96. Lewek MD, Rudolph KS, Snyder-Mackler L. 2004. Control of frontal plane knee laxity during gait in patients with medial compartment knee osteoarthritis. Osteoarthritis Cartilage 12(9):745–751.
97. Mündermann A, Dyrby CO, Andriacchi TP. 2005. Secondary gait changes in patients with medial compartment knee osteoarthritis: Increased load at the ankle, knee, and hip during walking. Arthritis Rheum 52(9):2835–2844.
98. Foroughi N, Smith R, Vanwanseele B. 2009. The association of external knee adduction moment with biomechanical variables in osteoarthritis: A systematic review. Knee 16(5):303–309.
99. Khandha A, Manal K, Capin J, et al. 2019. High muscle co-contraction does not result in high joint forces during gait in anterior cruciate ligament deficient knees. Journal of Orthopaedic Research 37(1):104–112.
100. Blackburn T, Pietrosimone B, Goodwin JS, et al. 2019. Co-activation during gait following anterior cruciate ligament reconstruction. Clinical Biomechanics 67:153–159.

101. Buchanan TS, Lloyd DG, Manal K, Besier TF. 2006. Neuromusculoskeletal modeling: estimation of forces and joint moments and movements from mrasuerments of nueral command. J Appl Biomech 20(4):367–395.
102. Winby CR, Lloyd DG, Besier TF, Kirk TB. 2009. Muscle and external load contribution to knee joint contact loads during normal gait. J Biomech 42(14):2294–2300.
103. Pataky TC, Vanrenterghem J, Robinson MA. 2016. The probability of false positives in zero-dimensional analyses of one-dimensional kinematic, force and EMG trajectories. J Biomech 49(9):1468–1476.
104. Pataky TC, Robinson MA, Vanrenterghem J. 2013. Vector field statistical analysis of kinematic and force trajectories. J Biomech 46(14):2394–2401.
105. Pataky TC. 2010. Generalized n-dimensional biomechanical field analysis using statistical parametric mapping. J Biomech 43(10):1976–1982.
106. Hasofer AM. 1978. Upcrossings of Random Fields. Adv Appl Probab 10:14.
107. Adler RJ, Hasofer AM. 1976. Level Crossings for Random Fields. https://doi.org/10.1214/aop/1176996176 4(1):1–12.
108. Friston KJ, Holmes AP, Poline JB, et al. 1995. Analysis of fMRI time-series revisited. Neuroimage 2(1):45–53.
109. Friston KarlJ, Ashburner J, Frith CD, et al. 1995. Spatial registration and normalization of images. Hum Brain Mapp 3(3):165–189.
110. Li W, Kornak J, Harris T, et al. 2009. Identify fracture-critical regions inside the proximal femur using statistical parametric mapping. Bone 44(4):596–602.
111. Pataky TC, Goulermas JY. 2008. Pedobarographic statistical parametric mapping (pSPM): A pixel-level approach to foot pressure image analysis. J Biomech 41(10):2136–2143.
112. Gardinier ES, Manal K, Buchanan TS, et al. 2013. Gait and Neuromuscular Asymmetries after Acute ACL Rupture. Med Sci Sports Exerc 44(8):1490–1496.
113. Pataky TC. 2012. One-dimensional statistical parametric mapping in Python. Comput Methods Biomech Biomed Engin 15(3):295–301.
114. D'agostino RB, Belanger A. 1990. A Suggestion for Using Powerful and Informative Tests of Normality.44(4):316–321.
115. Pataky TC, Vanrenterghem J, Robinson MA. 2015. Zero- vs. one-dimensional, parametric vs. non-parametric, and confidence interval vs. hypothesis testing procedures in one-dimensional biomechanical trajectory analysis. J Biomech 48(7):1277–1285.
116. Wretenberg P, Ramsey DK, Németh G. 2002. Tibiofemoral contact points relative to flexion angle measured with MRI. Clinical Biomechanics 17(6):477–485.
117. Masouros SD, Bull AMJJ, Amis AA. 2010. (i) Biomechanics of the knee joint. Orthop Trauma 24(2):84–91.
118. Scanlan SF, Favre J, Andriacchi TP. 2013. The relationship between peak knee extension at heel-strike of walking and the location of thickest femoral cartilage

in ACL reconstructed and healthy contralateral knees. J Biomech 46(5):849–854.
119. Koo S, Gold GE, Andriacchi TP. 2005. Considerations in measuring cartilage thickness using MRI: Factors influencing reproducibility and accuracy. Osteoarthritis Cartilage 13(9):782–789 [cited 2021 Feb 6] Available from: https://pubmed.ncbi.nlm.nih.gov/15961328/.
120. Capin JJ, Zarzycki R, Arundale A, et al. 2017. Report of the Primary Outcomes for Gait Mechanics in Men of the ACL-SPORTS Trial: Secondary Prevention With and Without Perturbation Training Does Not Restore Gait Symmetry in Men 1 or 2 Years After ACL Reconstruction. Clin Orthop Relat Res 475(10):2513–2522.
121. Perraton LG, Hall M, Clark RA, et al. 2018. Poor knee function after ACL reconstruction is associated with attenuated landing force and knee flexion moment during running. Knee Surgery, Sports Traumatology, Arthroscopy 26(2):391–398.
122. Schmitz RJ, Harrison D, Wang HM, Shultz SJ. 2017. Sagittal-plane knee moment during gait and knee cartilage thickness. J Athl Train 52(6):560–566 [cited 2021 Feb 24] Available from: www.natajournals.org.
123. Teng HL, Wu D, Su F, et al. 2017. Gait Characteristics Associated With a Greater Increase in Medial Knee Cartilage T1ρ and T2 Relaxation Times in Patients Undergoing Anterior Cruciate Ligament Reconstruction. American Journal of Sports Medicine 45(14):3262–3271.
124. Webster KE, Feller JA, Wittwer JE. 2012. Longitudinal changes in knee joint biomechanics during level walking following anterior cruciate ligament reconstruction surgery. Gait Posture 36(2):167–171.
125. Chehab EF, Favre J, Erhart-Hledik JC, Andriacchi TP. 2014. Baseline knee adduction and flexion moments during walking are both associated with 5year cartilage changes in patients with medial knee osteoarthritis. Osteoarthritis Cartilage 22(11):1833–1839.
126. Buckthorpe M, La Rosa G, Villa F Della. 2019. RESTORING KNEE EXTENSOR STRENGTH AFTER ANTERIOR CRUCIATE LIGAMENT RECONSTRUCTION: A CLINICAL COMMENTARY. Int J Sports Phys Ther 14(1):159–172.
127. Hurley M V. 1999. The role of muscle weakness in the pathogenesis of osteoarthritis. Rheumatic Disease Clinics of North America 25(2):283–298.
128. Hart JMJA, Turman KA, Diduch DR, et al. 2011. Quadriceps muscle activation and radiographic osteoarthritis following ACL revision. Knee Surgery, Sports Traumatology, Arthroscopy 19(4):634–640.
129. Gardinier ES, Stasi S Di, Pt §, et al. [date unknown]. Knee Contact Force Asymmetries in Patients Who Failed Return-to-Sport Readiness Criteria 6 Months After Anterior Cruciate Ligament Reconstruction.

130. D'Lima DD, Patil S, Steklov N, et al. 2006. Tibial forces measured in vivo after total knee arthroplasty. Journal of Arthroplasty 21(2):255–262 [cited 2021 Sep 15].
131. Kaiser J, Vignos MF, Liu F, et al. 2016. American Society of Biomechanics Clinical Biomechanics Award 2015: MRI assessments of cartilage mechanics, morphology and composition following reconstruction of the anterior cruciate ligament. Clinical Biomechanics 34:38–44.
132. Di Stasi SL, Snyder-Mackler L. 2012. THE EFFECTS OF NEUROMUSCULAR TRAINING ON THE GAIT PATTERNS OF ACL-DEFICIENT MEN AND WOMEN. Clin Biomech (Bristol, Avon) 27(4):360.
133. Zumbo BD, Hubley AM. 1998. A note on misconceptions concerning prospective and retrospective power. Journal of the Royal Statistical Society Series D: The Statistician 47(2):385–388.
134. Hoenig JM, Heisey DM. 2001. The abuse of power: The pervasive fallacy of power calculations for data analysis. American Statistician 55(1):19–24.
135. Saxby DJ, Bryant AL, Van Ginckel A, et al. 2019. Greater magnitude tibiofemoral contact forces are associated with reduced prevalence of osteochondral pathologies 2–3 years following anterior cruciate ligament reconstruction. Knee Surgery, Sports Traumatology, Arthroscopy 27(3):707–715.
136. Erdemir A. 2014. Open Knee: Open Source Modeling and Simulation in Knee Biomechanics. Journal of Knee Surgery 29(2):107–116.
137. Erdemir A. 2013. Open knee: A pathway to community driven modeling and simulation in joint biomechanics. Journal of Medical Devices, Transactions of the ASME 7(4):1 [cited 2019 Dec 14].
138. Shelburne KB, Torry MR, Pandy MG. 2006. Contributions of muscles, ligaments, and the ground-reaction force to tibiofemoral joint loading during normal gait. Journal of Orthopaedic Research 24(10):1983–1990 [cited 2018 Oct 18] Available from: http://doi.wiley.com/10.1002/jor.20255.
139. Ali AA, Harris MD, Shalhoub S, et al. 2017. Combined measurement and modeling of specimen-specific knee mechanics for healthy and ACL-deficient conditions. J Biomech 57:117–124.
140. Buchanan TS, Lloyd DG, Manal K, Besier TF. [date unknown]. Neuromusculoskeletal Modeling: Estimation of Muscle Forces and Joint Moments and Movements From Measurements of Neural Command.
141. Manal K, Buchanan TS. 2013. An electromyogram-driven musculoskeletal model of the knee to predict in vivo joint contact forces during normal and novel gait patterns. J Biomech Eng 135(2):021014.
142. Manal K, Gardinier E, Buchanan TS, Snyder-Mackler L. 2015. A more informed evaluation of medial compartment loading: the combined use of the knee adduction and flexor moments. Osteoarthritis Cartilage 23(7):1107–1111.
143. Gardinier ES, Manal K, Buchanan TS, Snyder-Mackler L. 2013. Altered loading in the injured knee after ACL rupture. J Orthop Res 31(3):458–64.

144. Yamaguchi GT, Sawa A, Moran DW, et al. 1990. A survey of human musculotendon actuator parameters.
145. Fox AJS, Wanivenhaus F, Burge AJ, et al. 2015. The human meniscus: A review of anatomy, function, injury, and advances in treatment. Clinical Anatomy 28(2):269–287.
146. Esrafilian A, Stenroth L, Mononen ME, et al. 2020. EMG-Assisted Muscle Force Driven Finite Element Model of the Knee Joint with Fibril-Reinforced Poroelastic Cartilages and Menisci. Sci Rep 10(1):1–16 [cited 2022 Jan 26] Available from: https://www.nature.com/articles/s41598-020-59602-2.
147. Fedorov A, Beichel R, Kalpathy-Cramer J, et al. 2012. 3D Slicer as an image computing platform for the Quantitative Imaging Network. Magn Reson Imaging 30(9):1323–1341 [cited 2019 Dec 22].
148. Yushkevich PA, Gao Y, Gerig G. 2016. ITK-SNAP: an interactive tool for semi-automatic segmentation of multi-modality biomedical images. Conf Proc IEEE Eng Med Biol Soc 2016:3342 [cited 2023 May 28] Available from: /pmc/articles/PMC5493443/.
149. Rahman MM, Dürselen L, Seitz AM. 2020. Automatic segmentation of knee menisci – A systematic review. Artif Intell Med 105:101849 [cited 2023 May 13].
150. Ridhma, Kaur M, Sofat S, Chouhan DK. 2021. Review of automated segmentation approaches for knee images. IET Image Process 15(2):302–324 [cited 2023 May 13] Available from: https://onlinelibrary.wiley.com/doi/full/10.1049/ipr2.12045.
151. Adeola EO. 2020. Knee Bone Segmentation from MRI Images Using a Deep Learning Model. [cited 2023 May 13].
152. Awan MJ, Rahim, Salim N, et al. 2022. Automated Knee MR Images Segmentation of Anterior Cruciate Ligament Tears. Sensors (Basel) 22(4) [cited 2023 May 13] Available from: /pmc/articles/PMC8876207/.
153. Rodriguez-Vila B, Sánchez-González P, Oropesa I, et al. 2017. Automated hexahedral meshing of knee cartilage structures – application to data from the osteoarthritis initiative. Comput Methods Biomech Biomed Engin 20(14):1543–1553 [cited 2019 Dec 14] Available from: http://im.engr.uconn.edu/downloads.php.ARTICLEHISTORY.
154. Tadepalli SC, Erdemir A, Cavanagh PR. 2011. Comparison of hexahedral and tetrahedral elements in finite element analysis of the foot and footwear. J Biomech 44(12):2337–2343 Available from: http://dx.doi.org/10.1016/j.jbiomech.2011.05.006.
155. Grosland NM, Bafna R, Magnotta VA. 2009. Automated hexahedral meshing of anatomic structures using deformable registration. Comput Methods Biomech Biomed Engin 12(1):35–43 [cited 2019 Feb 26] Available from: http://www.tandfonline.com/doi/abs/10.1080/10255840802136143.
156. Mootanah R, Imhauser CW, Reisse F, et al. 2014. Computer Methods in Biomechanics and Biomedical Engineering Development and validation of a

computational model of the knee joint for the evaluation of surgical treatments for osteoarthritis Development and validation of a computational model of the knee joint for the evaluation of surgical treatments for osteoarthritis. Comput Methods Biomech Biomed Engin 17(13):1502–1517 Available from: https://www.tandfonline.com/action/journalInformation?journalCode=gcmb20.

157. Abulhasan JF, Grey MJ. 2017. Anatomy and Physiology of Knee Stability. Journal of Functional Morphology and Kinesiology 2017, Vol. 2, Page 34 2(4):34 [cited 2023 Apr 30] Available from: https://www.mdpi.com/2411-5142/2/4/34/htm.
158. Kiapour A, Kiapour AM, Kaul V, et al. 2013. Finite Element Model of the Knee for Investigation of Injury Mechanisms: Development and Validation. J Biomech Eng 136(1):011002 Available from: http://biomechanical.asmedigitalcollection.asme.org/article.aspx?doi=10.1115/1.4025692.
159. Peña E, Calvo B, Martínez MA, Doblaré M. 2006. A three-dimensional finite element analysis of the combined behavior of ligaments and menisci in the healthy human knee joint. J Biomech 39(9):1686–1701 [cited 2023 May 1].
160. Haut Donahue TL, Hull ML, Rashid MM, et al. 2002. A finite element model of the human knee joint for the study of tibio-femoral contact. J Biomech Eng 124(3):273–280 [cited 2019 Sep 12] Available from: https://asmedigitalcollection.asme.org/biomechanical/article/124/3/273/450137/A-Finite-Element-Model-of-the-Human-Knee-Joint-for.
161. Fox AJS, Bedi A, Rodeo SA. 2012. The Basic Science of Human Knee Menisci: Structure, Composition, and Function. Sports Health 4(4):340–351.
162. Kiapour A, Hewett TE. 2014. Finite Element Model of the Knee for Investigation of Injury Mechanisms : Development and Validation.136(January):1–14.
163. Wangerin S. 2013. Development and Validation of a Human Knee Joint Finite Element Model for Tissue Stress and Strian Predictions During Exercise.(December):85.
164. Mootanah R, Imhauser CW, Reisse F, et al. 2014. Development and validation of a computational model of the knee joint for the evaluation of surgical treatments for osteoarthritis. Comput Methods Biomech Biomed Engin 17(13):1502–1517 [cited 2019 Nov 12].
165. Du G, Zhan H, Ding D, et al. 2016. Abnormal Mechanical Loading Induces Cartilage Degeneration by Accelerating Meniscus Hypertrophy and Mineralization after ACL Injuries in Vivo. American Journal of Sports Medicine 44(3):652–663.
166. Bolcos PO, Mononen ME, Roach KE, et al. 2022. Subject-specific biomechanical analysis to estimate locations susceptible to osteoarthritis—Finite element modeling and MRI follow-up of ACL reconstructed patients. Journal of Orthopaedic Research® 40(8):1744–1755 [cited 2023 May 25] Available from: https://onlinelibrary.wiley.com/doi/full/10.1002/jor.25218.

167. Mononen ME, Mikkola MT, Julkunen P, et al. 2012. Effect of superficial collagen patterns and fibrillation of femoral articular cartilage on knee joint mechanics-A 3D finite element analysis. J Biomech 45(3):579–587.
168. Esrafilian A, Stenroth L, Mononen ME, et al. 2022. An EMG-Assisted Muscle-Force Driven Finite Element Analysis Pipeline to Investigate Joint- and Tissue-Level Mechanical Responses in Functional Activities: Towards a Rapid Assessment Toolbox. IEEE Trans Biomed Eng 69(9):2860–2871.
169. Donahue TLH, Hull ML, Rashid MM, Jacobs CR. 2002. A finite element model of the human knee joint for the study of tibio-femoral contact. J Biomech Eng 124(3):273–280.
170. Peña E, Calvo B, Martínez MA, Doblaré M. 2006. A three-dimensional finite element analysis of the combined behavior of ligaments and menisci in the healthy human knee joint. J Biomech .
171. Adouni M, Shirazi-Adl A. 2009. Knee joint biomechanics in closed-kinetic-chain exercises. Comput Methods Biomech Biomed Engin 12(6):661–670.
172. Guilak F. 2005. The slippery slope of arthritis. Arthritis Rheum 52(6):1632–1633.
173. DM Daniel WA. 1990. Knee ligaments: structure, function, injury and repair. [cited 2019 Dec 15] Available from: https://scholar.google.com/scholar_lookup?title=Knee Ligaments%3A Structure%2C Function%2C Injury and Repair&publication_year=1990&author=D.M. Daniels.
174. Churchill D, Incavo S, Johnson C, Beynnon B. 1998. The transepicondylar axis approximates the optimal flexion axis of the knee. Clin Orthop Relat Res 356:111–118.
175. Yushkevich PA, Gao Y, Gerig G. 2016. ITK-SNAP: an interactive tool for semi-automatic segmentation of multi-modality biomedical images. Conf Proc IEEE Eng Med Biol Soc 2016:3342 [cited 2023 May 13] Available from: /pmc/articles/PMC5493443/.
176. Chu CR, Andriacchi TP. 2015. Dance Between Biology, Mechanics, and Structure: A Systems-Based Approach to Developing Osteoarthritis Prevention Strategies. J Orthop Res 33(7):939 [cited 2023 May 20] Available from: /pmc/articles/PMC5823013/.
177. Neal K, Williams JR, Alfayyadh A, et al. 2022. Knee joint biomechanics during gait improve from 3 to 6 months after anterior cruciate ligament reconstruction. Journal of Orthopaedic Research 40(9):2025–2038 [cited 2022 May 5] Available from: https://onlinelibrary.wiley.com/doi/full/10.1002/jor.25250.
178. Cohen J. 2013. Statistical power analysis for the behavioral sciences. [cited 2023 May 20] Available from: https://books.google.com/books?hl=en&lr=&id=rEe0BQAAQBAJ&oi=fnd&pg=PP1&dq=Cohen+J.+1988.+Statistical+Power+Analysis+for+the+Behavioral+Sciences,+2nd+ed.+New+York:+Routledge.+567+p.&ots=sw-UPpQUp7&sig=STWKSX7x6Ds_9c8zweJKEfc8yb8.

179. Swann AC, Seedhom BB. 1993. The stiffness of normal articular cartilage and the predominant acting stress levels: Implications for the aetiology of osteoarthrosis. Rheumatology 32(1):16–25 [cited 2023 May 15].
180. Yao JQ, Seedhom BB. 1993. Mechanical conditioning of articular cartilage to prevalent stresses. Br J Rheumatol 32(11):956–965 [cited 2023 May 15] Available from: https://pubmed.ncbi.nlm.nih.gov/8220934/.
181. Faber SC, Eckstein F, Lukasz S, et al. 2001. Gender differences in knee joint cartilage thickness, volume and articular surface areas: assessment with quantitative three-dimensional MR imaging. Skeletal Radiol 30(3):144–150 [cited 2023 May 15] Available from: https://pubmed.ncbi.nlm.nih.gov/11357452/.
182. Eckstein F, Winzheimer M, Westhoff J, et al. 1998. Quantitative relationships of normal cartilage volumes of the human knee joint - Assessment by magnetic resonance imaging. Anat Embryol (Berl) 197(5):383–390 [cited 2023 May 15].
183. Wretenberg P, Ramsey DK, Németh G. 2002. Tibiofemoral contact points relative to flexion angle measured with MRI. Clinical Biomechanics 17(6):477–485 [cited 2023 May 22].
184. Freeman MARAR, Pinskerova V. 2005. The movement of the normal tibio-femoral joint. J Biomech 38(2):197–208 [cited 2019 Aug 21] Available from: https://linkinghub.elsevier.com/retrieve/pii/S0021929004000788.
185. Johal P, Williams A, Wragg P, et al. 2005. Tibio-femoral movement in the living knee. A study of weight bearing and non-weight bearing knee kinematics using “interventional” MRI. J Biomech 38(2):269–276 [cited 2023 May 22] Available from: https://pubmed.ncbi.nlm.nih.gov/15598453/.
186. Li G, Moses JM, Papannagari R, et al. 2006. Anterior cruciate ligament deficiency alters the in vivo motion of the tibiofemoral cartilage contact points in both the anteroposterior and mediolateral directions. J Bone Joint Surg Am 88(8):1826–1834 [cited 2023 May 22] Available from: https://pubmed.ncbi.nlm.nih.gov/16882908/.
187. Li G, Zhou C, Zhang Z, et al. 2022. Articulation of the Femoral Condyle during Knee Flexion. J Biomech 131:110906 [cited 2023 May 22] Available from: /pmc/articles/PMC8760888/.
188. Liu F, Kozanek M, Hosseini A, et al. 2010. In vivo tibiofemoral cartilage deformation during the stance phase of gait. J Biomech 43(4):658–665 [cited 2023 May 22].
189. Mohammadi A, Myller KAH, Tanska P, et al. 2020. Rapid CT-based Estimation of Articular Cartilage Biomechanics in the Knee Joint Without Cartilage Segmentation. Ann Biomed Eng 48(12):2965 [cited 2023 May 18] Available from: /pmc/articles/PMC7723937/.
190. Cho Y, Lee S, Lee YS, Lee MC. 2014. Gender disparity in anterior cruciate ligament injuries. Arthroscopy and Orthopedic Sports Medicine 1(2):65–74 Available from: http://www.e-aosm.org/journal/DOIx.php?id=10.14517/aosm14004.

191. Simon D, Mascarenhas R, Saltzman BM, et al. 2015. The Relationship between Anterior Cruciate Ligament Injury and Osteoarthritis of the Knee. Adv Orthop 2015 [cited 2023 May 19].
192. Barenius B, Ponzer S, Shalabi A, et al. 2014. Increased Risk of Osteoarthritis After Anterior Cruciate Ligament Reconstruction A 14-Year Follow-up Study of a Randomized Controlled Trial. Am J Sports Med 42(5):1049–1057 [cited 2019 Dec 14] Available from: http://www.ncbi.nlm.nih.gov/pubmed/24644301.
193. Argentieri EC, Burge AJ, Potter HG. 2018. Magnetic Resonance Imaging of Articular Cartilage within the Knee. Journal of Knee Surgery 31(2):155–165.
194. Su F, Hilton JF, Nardo L, et al. 2013. Cartilage morphology and T1ρ and T2 quantification in ACL-reconstructed knees: a 2-year follow-up. Osteoarthritis Cartilage 21(8):1058–1067 [cited 2023 May 19].
195. Pedoia V, Gallo MC, Souza RB, Majumdar S. 2017. A longitudinal Study using voxel-based relaxometry: association between cartilage T1ρ and T2 and patient reported outcome changes in hip osteoarthritis. J Magn Reson Imaging 45(5):1523 [cited 2023 May 25] Available from: /pmc/articles/PMC5350069/.
196. Pedoia V, Li X, Su F, et al. 2016. Fully Automatic Analysis of the Knee Articular Cartilage T1ρ relaxation time using Voxel Based Relaxometry. J Magn Reson Imaging 43(4):970 [cited 2023 May 25] Available from: /pmc/articles/PMC5018211/.
197. Haut Donahue TL, Hull ML, Rashid MM, Jacobs CR. 2003. How the stiffness of meniscal attachments and meniscal material properties affect tibio-femoral contact pressure computed using a validated finite element model of the human knee joint. J Biomech 36(1):19–34 [cited 2023 Apr 17].
198. Peña E, Calvo B, Martínez MA, et al. 2005. Finite element analysis of the effect of meniscal tears and meniscectomies on human knee biomechanics. Clinical Biomechanics .
199. Orozco GA, Bolcos P, Mohammadi A, et al. 2021. Prediction of local fixed charge density loss in cartilage following ACL injury and reconstruction: A computational proof-of-concept study with MRI follow-up. Journal of Orthopaedic Research 39(5):1064–1081.
200. Bolcos PO, Mononen ME, Roach KE, et al. 2022. Subject-specific biomechanical analysis to estimate locations susceptible to osteoarthritis—Finite element modeling and MRI follow-up of ACL reconstructed patients. Journal of Orthopaedic Research 40(8):1744–1755 [cited 2023 Apr 26].

Appendix A

INSTITUTIONAL REVIEW BOARD APPROVAL LETTER

Institutional Review Board
210H Hullihen Hall
Newark, DE 19716
Phone: 302-831-2137
Fax: 302-831-2828

DATE:	March 15, 2021
TO:	Thomas Buchanan, PhD
FROM:	University of Delaware IRB
STUDY TITLE:	[868724-15] Understanding the role of unloading in the knee in osteoarthritis (OA) following anterior cruciate ligament reconstruction (ACLR).
SUBMISSION TYPE:	Continuing Review/Progress Report
ACTION:	APPROVED
APPROVAL DATE:	March 15, 2021
EXPIRATION DATE:	March 15, 2022
REVIEW TYPE:	Expedited Review
REVIEW CATEGORY:	Expedited review category # *(9)*

Thank you for your Continuing Review/Progress Report submission to the University of Delaware Institutional Review Board (UD IRB). The UD IRB has reviewed and APPROVED the proposed research and submitted documents via Expedited Review in compliance with the pertinent federal regulations.

As the Principal Investigator for this study, you are responsible for and agree that:

- All research must be conducted in accordance with the protocol and all other study forms as approved in this submission. Any revisions to the approved study procedures or documents must be reviewed and approved by the IRB prior to their implementation. Please use the UD amendment form to request the review of any changes to approved study procedures or documents.
- Informed consent is a process that must allow prospective participants sufficient opportunity to discuss and consider whether to participate. IRB-approved and stamped consent documents must be used when enrolling participants and a written copy shall be given to the person signing the informed consent form.
- Unanticipated problems, serious adverse events involving risk to participants, and all non-compliance issues must be reported to this office in a timely fashion according with the UD requirements for reportable events. All sponsor reporting requirements must also be followed.

Oversight of this study by the UD IRB REQUIRES the submission of a CONTINUING REVIEW seeking the renewal of this IRB approval, which will expire on March 15, 2022. A continuing review/progress report form and up-to-date copies of the protocol form and all other approved study materials must be submitted to the UD IRB at least 45 days prior to the expiration date to allow for the required IRB review of that report.

If you have any questions, please contact the UD IRB Office at (302) 831-2137 or via email at hsrb-research@udel.edu. Please include the study title and reference number in all correspondence with this office.

Appendix B

INSTITUTIONAL REVIEW BOARD INFORMED CONSENT

INFORMED CONSENT/ASSENT/PARENTAL PERMISSION TO PARTICIPATE IN RESEARCH

Title of Project: Understanding the role of unloading in the knee in osteoarthritis (OA) following anterior cruciate ligament reconstruction (ACLR)

Principal Investigator(s): Dr. Thomas S. Buchanan

You or your child are being invited to participate in a research study. This consent form tells you about the study including its purpose, what you will be asked to do if you decide to take part, and the risks and benefits of being in the study. Please read the information below and ask us any questions you may have before you decide whether or not you want to participate as a volunteer or parent.

Participation is voluntary for your or your child and you can refuse to participate or withdraw at any time without penalty or loss of benefits to which you are otherwise entitled. If you decide to participate, you will be asked to sign this form and a copy will be given to you to keep for your reference.

WHAT IS THE PURPOSE OF THIS STUDY?

The purpose of this research study is understand the role of unloading in the knee in osteoarthritis (OA) following anterior cruciate ligament reconstruction (ACLR) surgery.

Though ACLR restores knee stability, it does not fully address abnormal knee movement and knee loading patterns, i.e. abnormal walking patterns where the ACLR knee is unloaded compared to the other non-surgical knee. Abnormal walking patterns are believed to be a mechanism leading to knee osteoarthritis (OA). Knee OA is a condition wherein the load bearing region of the knee, the cartilage, undergoes degradation. Reliable identification of knee OA requires the use of radiographs, commonly known as X-rays.

Motion analysis testing is the most common method used to analyze walking patterns. Motion analysis testing comprises of non-invasive walking experiments, often including surface electromyography (non-invasive muscle signal recording) to estimate muscle coordination patterns and force production.

In addition to walking patterns, biological and chemical changes (biochemical changes) in knee cartilage are also believed to affect the progression of OA. An imaging method, known as quantitative magnetic resonance imaging (MRI) allows for non-invasive estimation of these changes in knee cartilage. Quantitative MRI is being increasingly used over the past two decades. However, estimates of biochemical changes in knee cartilage, specific to an ACLR population, are not yet readily available in literature. It is also not known how these changes are related to walking patterns. Finally, changes in knee geometry, which can be studied using standard MRI, are also known to affect the progression of knee OA.

With that background, the purpose of this research project is to study changes in walking patterns and biochemical properties of knee cartilage after ACLR. Knee geometry measurements and OA related changes will also be evaluated. 75 subjects will be recruited 3 months after ACLR. Testing will be conducted for each subject at the following time points after ACLR:

Participant's Initials _____

- 3, 6, and 24 months

Motion analysis testing will be used to assess walking patterns. Quantitative MRI will be used to estimate biochemical changes in knee cartilage, while standard MRI will be used to construct a geometric representation of the knee. Finally, the presence/absence of knee OA and progression of OA will be verified using radiographs.

In addition, 30 subjects, in the same age groups as ACLR subjects, but with no history of knee injury will also be recruited, to allow for comparison against subjects with ACLR. Control subjects will only be required to complete motion analysis testing and imaging (quantitative and standard MRI), similar to subjects with ACLR, and at one time point only, i.e. immediately after recruitment.

The ultimate goal of this research project is to use a mathematical model to reveal conditions that can affect the knee cartilage negatively, and result in knee OA. We also hope that an improved understanding of these conditions will eventually contribute to preventative therapeutic protocols.

WHY ARE YOU OR YOUR CHILD BEING ASKED TO PARTICIPATE?

We are asking you or your child to be in the study because you or your child has undergone ACLR approximately three months ago, and can be part of the ACLR group, or because you have no history of knee injury, and can be part of the control group. The age range for participation, for both groups, is between 16 and 45 years.

Exclusion criteria for ACLR group:

You could be excluded from volunteering for the study if you have sustained major leg injury, have undergone major leg surgery that requires serious medical management (i.e. fracture or re-injury), or an ACL injury/repair prior to the most recent procedure in either knee. You could also be excluded if you sustained major tears to other knee ligaments, or repairable meniscus injuries.

Exclusion criteria for control group:

You could be excluded from volunteering for the study if you have sustained major leg injury, have undergone major leg surgery that requires serious medical management (i.e. fracture), knee ligament injuries or knee meniscus injuries.

Exclusion criteria common to both ACLR and control groups:

You could be excluded if you have any condition that prevents you from walking, or laying still on your back.

Additionally, the conditions listed below, if met, will be grounds for exclusion because of standard precautions for imaging. Pregnancy is not a contraindication to MRI of the knee, but our scans may be taken by community providers who screen for and do not perform MRI on pregnant women when it is not medically necessary.

Participant's Initials _____

- Joint replacement with metallic parts
- Surgical procedure that includes metallic components
- Extreme claustrophobia (fear of small, closed spaces)
- Pacemaker (a medical implant in the heart)
- Metal in the body (implants, screws, plates, shrapnel, etc.)
- Aneurysm clips (clips used to treat bulging blood vessels)
- Ear or Eye Implants

WHAT WILL YOU BE ASKED TO DO?

If you or your child want to participate, the information below lists the location and details about the study. All the procedures are non-invasive, i.e. nothing will be inserted in the body, and rather, components will be attached to the surface of the body, when required.

Motion analysis testing will be conducted at STAR campus at the University of Delaware (540 S College Avenue, Newark DE 19713).

MRI will be conducted at either of the following locations:

- University of Delaware's Center for Biomedical or Brain Imaging, located at 75 East Delaware Avenue, Newark DE 19716, OR
- Diagnostic Imaging Associates, located at L-6 Omega Drive, Newark DE 19713, OR
- Best Open MRI-Abby Medical Center, 1 Centurian Drive, Suite 107, Newark DE 19713

Finally, radiography (x-ray imaging) will take place at either of the following locations:

- Diagnostic Imaging Associates, located at L-6 Omega Drive, Newark DE 19713, OR
- Go-Care at Abby Medical Center, 1 Centurian Drive, Suite 106, Newark DE 19713, OR
- First State Orthopedics (4745 Ogletown Stanton Rd #225, Newark, DE 19713) OR

The information below provides a description of what the testing sessions will include.

Study questionnaire

Relevant time points: 3, 6 and 24 months

Participant's Initials _____

You or your child will fill out a survey form that will be used to capture information related to injury and functional capabilities. This will enable us to get information about the current status of the knee. It generally takes an average of 5 minutes for the survey form to be filled out.

Motion analysis testing

Relevant time points: 3, 6 and 24 months

Surface electrodes taped to your (or your child's) skin will be used to record the electrical activity of your muscles (electromyography). After all electrodes have been placed, you will perform a maximum contraction of each muscle (i.e. applying maximum effort that is comfortable), with straps applied to your ankles to provide resistance. Nine electrodes will be secured to each leg and then plugged into a small (6" x 4" x 3") transmitter box that will be attached to the back of a vest with Velcro. The transmitter sends the signal to the computer so we can determine when the muscles are contracting during the activities. These measurements will also be taken during the walking trials of motion analysis testing.

Markers will be attached to your skin and sneakers on both legs using adhesive skin tape. Shells with markers on them will be placed on your pelvis, thighs and calves and will be held in place with elastic wraps. These markers will allow the cameras to track your leg positions. You will be asked to perform several walking trials in our laboratory. Walking trials will give us information about the way your hips, knees, and ankles move while you walk. You will be asked to perform 7 trials of walking at a comfortable, self-selected speed, although additional trials may be required to obtain enough data. During the trials, you will also walk over a force plate that is embedded in the floor. The force plate enables collection of loading data during walking.

The electrodes and markers will be removed at the end of the testing session. Motion analysis testing is a safe, non-invasive process. The entire testing session will last approximately two (2) hours.

Quantitative and Standard MRI

Relevant time points: 3, 6 and 24 months

This study involves measuring anatomy and estimating biochemical properties of the knee using magnetic resonance imaging (MRI).

You (or your child) will be required to lie completely still on the scanner bed that will slide into the center (bore) of the MRI scanner. A knee coil will be placed around each leg, alternately, to measure the signal emitted from the knee. Pillows and other cushions may be used to make you more comfortable. Several scans will be taken and you will be required to remain still on the table for about 5-10 minutes at a time. You will be given periodic breaks in which they will be able to relax but will be asked to remain on the scanner bed for the duration of the session, which should last about 45-50 minutes. Another similar MRI session will also be conducted, which can be on the same day, or a different day, depending on your preference.

Participant's Initials _____

You (or your child) will be able to communicate with us via a built-in intercom. You will also be holding an emergency bulb that you can squeeze at any time to let us know you want to come out of the MRI scanner. If at any time you feel uncomfortable or unwilling to continue, no matter what the reason, you can request to immediately stop the study, and the operator will remove you from the scanner. All scans will be conducted by a certified MRI Technologist or other experienced personnel with relevant safety training.

These scans will provide information regarding biochemical and geometrical knee properties.

This is not a clinical evaluation

The images of the knee collected in this study are not intended to reveal illness, in part because this research protocol is not designed for clinical diagnosis. The images will not be routinely examined by a clinical radiologist. The personnel at the MRI Center are not qualified to medically evaluate these images. However, if, in the course of collecting images, we have any concerns, we may show scans to a clinical radiologist, who may suggest that you (or your child) obtain further diagnostic tests. Do not rely on this research MRI to detect or screen for abnormalities.

At our discretion, you may view their images and receive digital copies of them. These images will show the inside of the knee and you should be aware of the potential distress or discomfort that may occur by viewing these type of images.

Radiographs

Relevant time points: 3 and 24 months

Standing x-rays will be taken with the knee slightly bent. These x-rays will allow a radiologist to verify the presence or absence of OA, and to determine knee joint space width (JSW) measurements. This takes 5-10 minutes to be completed.

Radiographs at the 3 month time point will be useful for establishing a baseline, while radiographs at the 24 month time point will be useful to verify the presence/absence of knee OA, and OA progression. These x-rays will be locked in a cabinet for research purposes only.

If you (or your child) are part of the control group (i.e. no history of knee injury), you will only be required to complete motion analysis testing and imaging (quantitative and standard MRI), similar to subjects with ACLR, and at one time point only, i.e. immediately after recruitment.

WHAT ARE THE POSSIBLE RISKS AND DISCOMFORTS? (WHAT ARE THE POSSIBLE BAD THINGS ABOUT THIS RESEARCH?)

A few things about this study that could make a volunteer uncomfortable are listed below.

Motion analysis testing

Participant's Initials _____

All motion analysis testing procedures involve a simple walking task that has been standardized at the University of Delaware. The risk of re-injury for the ACL-reconstructed population within the first 5 years after ACLR is approximately 5%. Of the hundreds of tests performed on ACLR individuals at the University of Delaware, no one has torn their surgical graft during testing. At the end of motion analysis testing, you may experience discomfort from the removal of tape holding markers and electrodes in place.

Quantitative and Standard MRI

MRI is an imaging technique that uses radio waves and magnetic fields to produce images of internal structures in the body. It is commonly used in hospitals. Unlike X-rays, the MRI does not use any ionizing radiation, and it does not use radioactivity, so there are no radiation related risks from having an MRI scan. Below there is a description of MRI related risks and what is being done to reduce any possible risks associated with them:

Metal: The MRI scanner produces a constant strong magnetic field, which may cause any metal implants, clips, or implanted medical devices within the body to shift position or malfunction. You (or your child) will not be allowed to participate in this study if you have any implanted metal, clips or devices. You will be screened to make sure that it is safe for you to enter a strong magnetic field. Please provide us with as much information as you can, for example if you had surgery in the past, so that we may decide whether it is safe for you to be a participant. Metallic objects brought into the MRI environment can become hazardous projectiles and can also interfere with the data quality. To minimize this risk, metal earrings, other piercings, necklaces and any other metal in contact with your body will be removed prior to the study. You will also be asked to remove all items from your pockets, including coins, electronics (including cell phones and hearing aids) and wallets. You will also be asked to remove belts with metal buckles, and may be asked to change into a gown that we will provide if your clothing contains significant metal, including metal underwire bras.

Pregnancy: Exposure to MRI scanning might be harmful to an unborn child. Although there are no established guidelines at this time regarding MRI and pregnancy, you (or your child) should be informed that there is a possibility of a yet undiscovered pregnancy related risk. If you know or suspect you may be pregnant or if you do not want to expose yourself to this risk, you will be excluded from participating in this study.

Inner ear damage: MRI scanning produces loud noises that can cause damage to the inner ear if appropriate hearing protection is not used. Earplugs and/or headphones will be provided to protect your (or your child's) ears.

Claustrophobia: When you (or your child) is inside the MRI scanner, the "bore" of the scanner will surround the knee that is being scanned. You will be positioned so that their knee is centered in the bore of the scanner. If you feel anxious in confined, spaces, you may not want to participate. If you are unsure, you can try a "mock" scanner when available, to evaluate the comfort level with the enclosed space of the

Participant's Initials _____

magnet bore. If you decide to participate and begin to feel claustrophobic, you will be able to tell us via the intercom or the squeeze ball and we will discontinue the study immediately.

Burns: In rare cases, contact with the MRI transmitting and receiving coil, conductive materials such as wires or other metallic objects, or skin-to-skin contact that forms conductive loops may result in excessive heating and burns during the experiment. The operators of the MRI scanner will take steps, such as using foam pads when necessary, to minimize this risk. Tattoos with metallic inks can also potentially cause burns. In addition, you (or your child) are requested to let the MRI operator know immediately if you experience any heating or burning sensations during a scan. The scanning session will be stopped as soon as you tell the operator.

Nerve or muscle stimulation: While the scanner is operating, there is a small chance that the rapidly changing magnetic fields could cause a slight tingling sensation or a muscle twitch, usually felt in the upper arms or torso. While these sensations may be startling, they are not dangerous or a health risk, and they have no lasting consequences. The sensations should stop when the scan ends. Because these sensations may nevertheless be distracting or even possibly uncomfortable, you (or your child) will be able to squeeze the signal bulb to alert the scanner operator if you feel tingling or muscle twitching, and we will immediately stop the scan. You will then have the opportunity to choose to withdraw from the study or to continue.

Other Risks: Besides the risks listed above, there are no other known risks from the magnetic field or radio waves at this time. Although MRI scanning has been used for more than 20 years, long-term effects are unknown.

Radiographs

This research study involves exposure to radiation from a standard radiograph (x-ray). This radiation exposure is not necessary for your medical care and is for research purposes only. At each time point that the radiograph is obtained, the total amount of radiation that you will receive in this study is about 0.12 mSv (mili-Silvert) and is approximately equivalent to a uniform whole body exposure of 15 days of exposure to natural background radiation. This use involves minimal risk per National Institutes of Health guidelines, and is necessary to obtain the research information desired. To reduce exposure, you (or your child) will wear a lead apron to cover the rest of your body while the x-rays of your leg are captured.

WHAT IF YOU OR YOUR CHILD ARE INJURED DURING PARTICIPATION IN THE STUDY?

If you or your child are injured during research procedures, you will be offered first aid at no cost to you. If additional medical treatment is needed, the cost of this treatment will be your responsibility or that of your third-party payer (for example, your health insurance). By signing this document, you are not waiving any rights that you may have if injury was the result of negligence of the university or its investigators.

Participant's Initials _____

WHAT ARE THE POTENTIAL BENEFITS? (WHAT ARE THE POTENTIAL GOOD THINGS ABOUT THIS RESEARCH?)

The proposed motion analysis testing procedure aims to study walking patterns after ACLR, and the change in these patterns over time. The data collected will be used to propose a mechanism for OA, and distinguish between abnormal versus normal walking patterns. A link between abnormal patterns and OA has not yet been established and validated. Hence, the proposed motion analysis testing procedure, by itself, cannot identify OA, and as such, no direct benefit to you is expected.

Similarly, the proposed MRI imaging procedure only aims to estimate biochemical properties of the knee cartilage, which has not yet been shown to predict OA. These properties will be used in a mathematical model to reveal conditions that can affect the knee cartilage negatively, and may result in knee OA. The proposed MRI imaging procedure, by itself, cannot predict OA, and as such, no direct benefit to you is expected.

However, we do hope that an improved understanding of the effect of the study measurements will provide information about knee OA in an ACLR population, and contribute to preventative therapeutic protocols in the future.

NEW INFORMATION THAT COULD AFFECT YOUR PARTICIPATION:

During the course of this study, we may learn new information that could be important to you. This may include information that could cause you to change your mind about participating in the study. We will notify you as soon as possible if any new information becomes available.

HOW WILL CONFIDENTIALITY BE MAINTAINED? (WHO MAY KNOW WHO PARTICIPATED IN THIS RESEARCH?)

No one other than the investigators will know that you or your child were in this study. If we tell other people about the research, we will not use names.

More details for adult participants and for parents/guardians of adolescent participants are provided below.

All information obtained during the study will be held in strict confidence to the fullest extent possible by law. In no case will personal identifiable information be shared with any other individuals or groups without your expressed written consent. Your (or your child's) images will be stored on secured computer servers and will be archived indefinitely. Non-identifiable images of your scans may be used for teaching purposes, be presented at meetings, published, and also shared in databases accessible to other researchers for further research and educational purposes. Your names or other identifying information will not be used in any publication or teaching materials without your specific permission.

Identities will be kept confidential by coding them with a subject identification number stored on a password protected computer. Only the investigators and research coordinator will have access to that file on the secure server.

Participant's Initials _____

All data will be electronically encrypted and archived indefinitely for comparative analyses of scientific and clinical questions related to the ACL injury, surgery and knee OA. All research findings will be compared to knee cartilage properties, knee loading patterns and knee movement patterns reported via peer-reviewed academic journals and conferences that emphasize outcomes after ACLR.

While rare, an accidental breach of confidentiality is a risk. Should an accidental breach of confidentiality occur, the event will be reported to the institutional review board (IRB) immediately, and appropriate follow up steps will be taken based on IRB recommendations.

HIPAA AUTHORIZATION

State and federal privacy laws protect your PHI. These laws say that, in most cases, your health care provider can release your PHI for the purpose of conducting research only if you give permission by signing an Authorization.

The research team would like and appreciate access to your PHI, specifically regarding any knee injury and or surgery, to make the study as complete as possible; however, if you do not sign this Authorization, you may still participate in the research study.

Who May Disclose and Who may Use and/or Receive my PHI?

By signing this document, you are hereby permitting your physicians, medical care providers, and UD's physical therapy clinic to disclose the PHI described in this Authorization to the research team involved in this project; the study sponsor and its employees; the Institutional Review Board (IRB) and other regulatory agencies responsible for overseeing research.

Once your PHI is shared with these persons, you understand that the PHI may no longer be protected by federal or state privacy laws.

What PHI Will Be Disclosed and Used, and for What Purpose?

The following PHI may be disclosed to, collected by, used by, and shared with those listed above:

Operative report (about an operation) and Physical therapy records.

This only pertains to medical records related to your ACL injury and surgery.

This Authorization will expire at the conclusion of the research study. You may cancel this Authorization at any time before, during, or after your participation in this study by giving a written request with your signature on it to the Principal Investigator at buchanan@udel.edu. If you cancel this Authorization, your PHI obtained before that date may still be used for this research study.

Participant's Initials _____

I hereby authorize the disclosure and use of **my Personal Health Information**

_____ _____

Signature of Patient or Authorized Representative Date

Printed Name of Person Signing: _____

Relationship to Patient: _____

WILL THERE BE ANY COSTS TO YOU FOR PARTICIPATING IN THIS RESEARCH?

There are no costs associated with participating in the study.

WILL YOU RECEIVE ANY COMPENSATION FOR PARTICIPATION?

Participants will be compensated 50 USD for motion analysis testing, 50 USD for qMRI, and 50 USD for a radiograph (x-ray). Thus, there will be a total of 150 USD compensation associated with each time point, i.e. 3, 6 and 24 month time points.

DO YOU HAVE TO TAKE PART IN THIS STUDY? (CAN YOU CHANGE YOUR MIND ABOUT BEING IN THE STUDY?)

You do not have to say yes. Taking part in this research study is up to you or your child. If you choose to take part, you can change your mind and stop at any time. If, at any time, you decide to stop, please let us know by telling one of the researchers.

If you are a student volunteer and decide not to take part in this research, your choice will not affect your grades or your relationship with your classmates and your teachers.

We may ask you to stop participating if any leg injury that requires serious medical management (i.e. fracture or re-injury) has occurred before the testing session.

WHO SHOULD YOU CALL IF YOU HAVE QUESTIONS OR CONCERNS?

If you have any questions about this study, please contact the Principal Investigator, Dr. Thomas S Buchanan at buchanan@udel.edu or (302) 831-2410.

If you have any questions or concerns about your rights as a research participant, you may contact the University of Delaware Institutional Review Board at hsrb-research@udel.edu or (302) 831-2137.

Participant's Initials _____

Appendix C

AIM 1 (CHAPTER 2) PERMISSION

Journal of Orthopaedic Research®

ORS Orthopaedic Research Society

Author Guidelines

Editorial Office Information

If you wish to reuse your own article in a new publication of which you are the author, editor or co-editor, prior permission is not required. However, a formal grant of license can be downloaded free of charge from RightsLink© if required.

For a complete guide to seeking permission with Wiley, visit www.wiley.com/permissions.